

Spokesman: J. WHITMORE No. 394  
 Department of Physics  
 Michigan State University  
 East Lansing, Mich. 48824  
 517-353-5180

Spokesman: W. D. SHEPHARD No. 558  
 Department of Physics  
 University of Notre Dame  
 Notre Dame, Ind. 46446  
 219-283-7311

Spokesman: W. D. WALKER No. 304  
 Physics Department  
 Duke University  
 Durham, N. Carolina 27706  
 919-684-8228

PROPOSAL FOR A HIGH STATISTICS STUDY OF  $\bar{p}p$  ANNIHILATIONS  
AND A COMPARISON OF  $\bar{p}, p, \pi^-, \pi^+$ , and  $K^+$  INTERACTIONS ON HYDROGEN,  
MAGNESTUM AND GOLD AT 100-GeV/c UTILIZING THE FERMILAB 30-INCH HYDROGEN  
BUBBLE CHAMBER AND DOWNSTREAM PARTICLE IDENTIFIER

R. E. ANSORGE, J. R. CARTER, W. W. NEALE,  
 J. G. RUSHBROOKE, D. R. WARD and T. W. WHITE  
 Cavendish Laboratory, University of Cambridge, Cambridge CB3 0HE ENGLAND

L. R. FORTNEY, A. T. GOSHAU, P. LUCAS, W. J. ROBERTSON and W. D. WALKER  
 Physics Department  
 Duke University, Durham, North Carolina 27706, U.S.A.

L. VOYVODIC and R. J. WALKER  
 Fermi National Accelerator Laboratory, Batavia, Illinois 60510 U.S.A.

R. A. LEWIS, R. J. MILLER, B. Y. OH, M. PRATAP, G. A. SMITH and J. WHITMORE  
 Department of Physics  
 Michigan State University, East Lansing, Michigan 48824, U.S.A.

H. N. BISWAS, J. H. BISHOP, N. M. CASON, V. P. KENNEY, R. C. RUCHTI and W. D. SHEPHARD  
 Department of Physics  
 University of Notre Dame, Notre Dame, Indiana 46556, U.S.A.

G. EKSPONG, S. O. HOLMGREN, S. NILSSON and N. YAMDAGNI  
 Institute of Physics, University of Stockholm, S-113 46 Stockholm, SWEDEN

20 January 1978

106/1978

## TABLE OF CONTENTS

	Page
I. Summary . . . . .	1
II. Introduction. . . . .	3
III. Beam and Bubble Chamber . . . . .	6
IV. Downstream Particle Identifier (ISIS and OSIRIS). . . . .	7
V. Neutral Particle Calorimeter ( $\bar{n}, \gamma$ ). . . . .	12
VI. Physics Justification . . . . .	17
VII. Efficiency for Separating Annihilation and Nonannihilation Events. . . . .	32
VIII. Analysis of Experimental Data . . . . .	33
REFERENCES . . . . .	35
APPENDIX	
A. Summary of Publications from Experiments 2B, 163A, 281 and 311. . . . .	66
B. Particle Identifiers for Hadron Physics. . . . .	69
C. Preliminary Results of Tests on Components of the Proposed Multicelled Cerenkov Counter for the Fermilab DPI . . . . .	78
D. Revised Proposal for a Study of the Interaction of High Energy $\pi^\pm$ with Gold and Magnesium . . . . .	84

## I. Summary

### 1. Physics Objectives

A high statistics study of 100 GeV/c  $\bar{p}$ , p,  $K^+$  and  $\pi^\pm$  interactions with protons, Mg, and Au will be performed using the Fermilab 30-inch hydrogen bubble chamber hybrid system with downstream particle identification. We anticipate at least the following topics:

- (a) The  $\bar{p}p$  annihilation cross section at 100 GeV/c, and its relation to  $\Delta\sigma_T = \sigma_T(\bar{p}p) - \sigma_T(pp)$ ;
- (b) Studies of the properties of baryon annihilations and comparisons with  $e^+e^- \rightarrow$  hadrons;
- (c) Studies of the differences in multiparticle production in  $\bar{p}p$ -pp,  $\pi^-p$ - $\pi^+p$  interactions;
- (d) Studies of  $\pi\pi$  and  $K\pi$  interactions for masses  $\lesssim 5$  GeV;
- (e) Structure of the quark distributions in soft hadronic processes;
- (f) Central region physics, e.g.  $K\pi$  correlations, resonance production, locality of quantum number conservation; and
- (g) Studies of high energy interactions off Mg and Au.

### 2. Request:

$1.45 \times 10^6$  pictures of  $\bar{p}p/\pi^-p$  ( $10^6$  at 100 GeV/c),  $pp/K^+p/\pi^+p$  ( $4 \times 10^5$  at 100 GeV/c), and  $\pi^-p$  ( $5 \times 10^4$  at 360 GeV/c) interactions in the 30-inch hydrogen bubble chamber with downstream particle identifier and neutral calorimeter, taken in an untriggered, but tagged, mode. In addition, we request thin metallic foil targets in the hydrogen to study nuclear interactions.

### 3. Beams:

100 GeV/c  $\bar{p}$  enriched negative (30%  $\bar{p}$  /70%  $\pi^-$ ), 100 GeV/c positive (30% p/10%  $K^+$ /60%  $\pi^+$ ), and 360 GeV/c  $\pi^-$  beams to the 30-inch bubble chamber with the standard

octuple pulsing. The beam particles are to be tagged by Cerenkov counters and upstream proportional wire chambers.

4. Equipment:

- (a) 30-inch hydrogen bubble chamber with thin metal foils and Downstream Particle Identifier (ISIS/OSIRIS).
- (b) Neutral calorimeter, to be provided by these proposers for  $\bar{n}$  and photon detection.

5. Data Analysis:

- (a) Measurements will be done on 4 image-plane digitizers (MSU), 2 image-plane digitizers and 1 SWEEPNIK (Cambridge), SMM (Fermilab), 1 Spiral Reader (Stockholm), 1 RIPPLE (Duke) and 2 film-plane and 3 image-plane digitizers (Notre Dame).
- (b) Event reconstruction and analysis will be done on the MSU CDC6500/6400, Cambridge IBM370-165, Fermilab CDC6600, Duke IBM370/165, Notre Dame IBM370/158 and Stockholm computers.
- (c) We believe that all events ( $p^{\pm}p$ ,  $K^{\pm}p$ ,  $\pi^{\pm}p$ , heavy nucleus events) will be measured and analyzed in less than  $\sim 2$  years following film acquisition. Many results will be available much earlier.

## II. Introduction

Current theoretical ideas suggest that hadronic final states in both lepton-nucleon and hadron-nucleon collisions are produced via the interaction<sup>1</sup> between constituents (partons - quarks or gluons) which, after the elementary interaction, either fragment or recombine to form the hadronic final state. The latter process should involve only the parton fragmentation or recombination functions and should be independent of whether the initial state involves a lepton or only hadrons or whether the final state hadrons are observed at low or high transverse momentum. Data from  $e^+e^-$ , ep and  $\mu p$  interactions can be well described by the above ideas and, more recently, both low and high  $P_T$  data from hadronic interactions have also been shown to be in agreement with this quark-proton model. Since the  $\bar{p}p$  annihilation process exhibits no strong leading particle effects it is of obvious interest to compare the baryon annihilation process, where the three valence quarks in the proton interact pairwise with the three valence antiquarks in the antiproton, with the "single-jet"  $e^+e^-$  data. For this reason we propose to compare our  $\bar{p}p$  annihilation data both with existing data from SPEAR and DORIS (which correspond to data with similar energy per parton), as well as with future data from CESR, PEP and PETRA (at similar overall CM energies).

Previous lower-statistics experiments with the Fermilab 30-inch bubble chamber and hybrid systems have provided information on a number of interesting topics in strong interactions. Frequently, however, the statistics have been sufficient to indicate the existence of interesting features of the data but insufficient to allow an adequate study of these features. In other cases, the statistics or particle identification have been inadequate for the study of topics of potentially great interest.

The early bubble chamber studies have clearly shown the persistence at Fermilab energies of effects dependent on the nature of beam and target particles over the complete available range of rapidity. Such effects are most evident when beam and target particles are different. By comparing data for different beam particles the nature of these "leading particle" effects may be studied.

Another factor clearly revealed in previous studies has been the importance of having as complete information about all of the secondary particles in an event as possible. For example, our understanding of two-particle correlations was greatly advanced over early ISR studies when information about the charges of the secondary particles was obtained in Fermilab bubble chamber experiments. Further advances are expected when  $K^\pm$  can be distinguished from  $\pi^\pm$  among the secondaries and when better information about neutral secondaries is available. This experiment will yield information on  $K^\pm$  production and on neutral pion production over much of the forward hemisphere.

A subset of our collaboration (Cambridge, Fermilab, MSU) completed data taking for E-311 in January, 1975. This experiment was a survey experiment of  $10^5$  pictures of antiproton-proton interactions at 100 GeV/c using the Fermilab 30-inch bubble chamber-wide gap optical spark chamber hybrid system. The data analysis has progressed rapidly with all of the  $\sim 12,000$   $\bar{p}p$  events having been measured. Six papers on the multiplicity distributions and inclusive neutral particle and  $\pi^-$  production in  $\bar{p}p$  and  $pp$  interactions have already been published<sup>2-7</sup>, and additional analysis on annihilation and nonannihilation effects is in progress.

On the basis of the current analysis of E-311, as well as our other studies (see Appendix A for Bibliography of Publications) of multiparticle production in high energy interactions at Fermilab from E-2B, E-163A, and E-281, we are requesting  $10^6$  pictures of a 100 GeV/c Cerenkov-tagged enriched  $\bar{p}$  beam (30%  $\bar{p}$ /70%  $\pi^-$ ),  $0.4 \times 10^6$  pictures of a 100 GeV/c Cerenkov-tagged  $p/K^+/\pi^+$  (30%  $p$ /10%  $K^+$ /60%  $\pi^+$ ) beam, and 50,000 pictures of a 360 GeV/c  $\pi^-$  beam into the 30-inch hydrogen bubble chamber filled with hydrogen and containing thin metallic foils as heavy nuclear targets. An essential feature of this proposal is the planned use of both the Downstream Particle Identifier (DPI), in order to identify the antiprotons, protons, and charged kaons which emerge from the chamber, as well as a neutral calorimeter to identify forward antineutrons and photons. With such a system we expect to obtain a highly enriched sample of baryon annihilation events. Another extremely important use of the DPI is to identify a large fraction of the central region protons and kaons, produced in both annihilation and non-annihilation interactions. With this information, as well as with the neutral kaon and slow proton detection in the bubble chamber itself, one can study such topics as the  $\bar{p}p$  annihilation process, the quark structure of the incident hadrons, and central region physics such as  $p/\bar{p}$  production, the rapidity gap distribution for strangeness exchange, and two particle correlations between  $K^-\pi^-$ ,  $K^+\pi^+$  (and  $K\bar{K}$ ).

The data obtained in this experiment will be sufficient for the study of many topics other than those mentioned above. Many such topics are obvious. As has happened frequently in past bubble chamber experiments, other topics, as yet unconsidered, may ultimately be of greatest importance. The key factors for the physics of the experiment, in any case, are the combination of high statistics, improved secondary particle detection and identification,

and the capability of comparing strong interactions initiated by several different types of incident particles. In fact, an especially attractive feature of this proposal is the opportunity to study the interactions of a wide range of incident particles ( $\pi^+$ ,  $K^+$ ,  $p$ ,  $\pi^-$ ,  $\bar{p}$ ) and targets ( $p$ ,  $Mg$ ,  $Au$ ) in the same exposure. This provides for the most efficient use of the hybrid system, with full use being made of all the observed interactions, while also allowing for the intensive study of closely related interactions (e.g.  $\bar{p}p$  and  $pp$  or  $\pi^+p$  and  $\pi^-p$ ).

We wish to point out that one of the groups (Duke University) already has an approved experiment (#304) for studying high energy  $\pi^\pm$  interactions with heavy nuclei. We note that there are several advantages in considering #304 to be part of this proposal:

- (a) The nuclear interactions can be obtained at the same time as the hydrogen events with a corresponding saving of time and expense to Fermilab;
- (b) The present proposal includes the interactions with high  $Z$  of  $\bar{p}$ ,  $p$  and  $K^+$  in addition to the above mentioned  $\pi^\pm$ ;
- (c) The present proposal would consist of almost an order of magnitude more events than expected in #304; and
- (d) The present proposal would provide charged particle identification and neutral particle detection over much of the forward hemisphere.

### III. Beam and Bubble Chamber

The results of E-311 have shown that the enriched "halo"  $\bar{p}$  beam<sup>8</sup> at 100 GeV/c is appropriate for the current proposal. During that experiment a negative beam containing 20%  $\bar{p}$ 's at 100 GeV/c was obtained from the target "halo" produced by the decays of  $\bar{\Lambda}$ 's. Requiring there be 2 or more

$\bar{p}$ 's/pulse before taking a bubble chamber picture, we took 98,000 pictures containing 0.32  $\bar{p}$ 's/negative beam particle. With the collimators wide open, a flux of 30-40  $\bar{p}$ 's/ $10^{11}$  incident protons on target was obtained, which was more than adequate for the quadruple pulsing mode which was standard for the bubble chamber at that time.

The E-311 exposure was carried out with a 300 GeV incident proton beam. However, 400 GeV protons are now available on a regular basis. In fact, more recent  $\bar{p}p$  experiments utilizing the 30-inch bubble chamber (E-345, 100 GeV/c  $\bar{p}d$ ; and E-344, 50 GeV/c  $\bar{p}p$ ) and recent beam tests have shown that one can readily obtain a 100 GeV/c 30%  $\bar{p}$ /70%  $\pi^-$  beam at the 30-inch bubble chamber without triggering the bubble chamber flash, and with sufficient flux (i.e.  $\sim 6$  particles per picture) to octuple pulse the chamber with less than  $5 \times 10^{10}$  protons on target per accelerator cycle.

The currently existing beam line without any filtering is quite adequate for the 360 GeV/c  $\pi^-$  and proposed positive beams (30%  $p$ /10%  $K^+$ /60%  $\pi^+$ ), although a few shifts of beam time may be necessary to tune the beam for optimal  $K^+$  content. Again, octuple pulsing of the chamber is planned.

We plan to use the current upstream system of proportional wire chambers and beam Cerenkov counters in Enclosures 106 and 108 to tag each beam track entering the bubble chamber.

In summary, we will no longer need to trigger the bubble chamber flash. Hence the  $1.45 \times 10^6$  pictures could be taken in  $\sim 1.45 \times 10^6$  chamber expansions, or  $\sim 175$  K accelerator cycles, assuming 100% efficient octuple pulsing of the beam line and bubble chamber.

#### IV. Downstream Particle Identifier (ISIS and OSIRIS)

One of the primary goals of the proposed experiment is to identify as many of the produced charged particles as possible, i.e., one wants to

identify the leading particles (generally  $p$ ,  $\bar{p}$  or  $\pi^\pm$  with some  $K^\pm$ ) if they exist, as well as those particles produced in the central region (generally  $\pi^\pm$  or  $K^\pm$  with some  $p^\pm$ ).

The system we propose to use is the Downstream Particle Identifier (DPI) (see Fig. 1) which is currently under construction by the PHSC (ISIS) and the Michigan State University group (Cerenkov counter, named OSIRIS). At the current time, \$40,000 to start the project have already been allocated by Fermilab. It is expected the project will be concluded in FY78 at a total cost to Fermilab of ~\$200,000, with substantial additional support coming from the resources of the PHSC and MSU. Details of this system are described in the July 1976 issue of NALREP, which is included as Appendix B. Basically, the system consists of two elements behind the 30-inch bubble chamber: (a) an ISIS device<sup>9</sup> consisting of  $1 \times 1 \times 1 \text{ m}^3$  section followed by a  $1 \times 1 \times 2 \text{ m}^3$  section interspersed with drift chambers, and (b) a  $2 \times 2 \times 5 \text{ m}^3$  8-cell atmospheric pressure  $\text{N}_2$ -He Cerenkov detector, OSIRIS. In the ISIS device, ionization deposited in the detector is sampled by measuring the pulse height from each "cell" hit by a charged particle and, utilizing the relativistic rise effect, mass identification of particles traversing the device is possible. The circulating gas is a 80% Ar - 20%  $\text{CO}_2$  mixture, which gives a satisfactory relativistic rise. Monte Carlo calculations, substantiated by recent tests,<sup>10</sup> indicate that one can obtain ~7.8% FWHM ionization resolution on a track which passes through the entire device (3m.). With this resolution, it is anticipated useful particle separation can be achieved up to ~30-40 GeV/c.

To examine the acceptance of the ISIS detector for the proposed experiment, we have used ~4200 inelastic  $\bar{p}p$  events obtained from E-311, and ~4000 inelastic  $\pi^-p$  events from E-2B. To investigate the properties of the leading  $\bar{p}$  (or  $p$  in  $pp$  collisions), we have separated slow protons and  $\pi$ 's by ionization in the bubble chamber, transformed their laboratory 3-momenta

into the center-of-mass, reversed them, and then transformed them back into the laboratory system. For the  $\pi^-p$  study, all tracks not identified as protons have been assumed to be pions. Using these events, we find the following:

- (a) The acceptances as a function of the laboratory momentum of the produced pions are shown in Tables I and II. Typically  $\geq 85\%$  of the forward hemisphere pions from a given event make their way into ISIS (see Tables III and IV). Many slow (backward hemisphere) particles do not traverse the exit aperture of the bubble chamber magnet (see Table I and II) and thus could not be detected by any device outside the magnet. Typically  $\sim 50\%$  of the forward hemisphere particles traverse the entire ISIS device. The acceptances as a function of CM rapidity are shown in Figs. 2 and 3 for  $\pi^-p$  and  $\bar{p}p$  interactions, respectively.
- (b) For a sample of  $\bar{p}p$  events examined in detail (see Figs. 4 (a) to (c) for examples), we estimate that the average resulting resolution on ionization, after folding in the (negligible) probability of more than 1 track entering the same cell, for tracks that traverse the full 3 meters of ISIS is  $\sim 7.8\%$  FWHM. For tracks that do not traverse the full 3 meters, the average resolution is estimated to be  $\sim 11.7\%$  FWHM.

To effectively use the ionization information from ISIS requires that the momentum resolution be better than 10%. We note the proposed use of the drift chambers and the PWC's (see Fig. 1) will yield a momentum resolution of  $\Delta p/p = 0.06p\%/(GeV/c)$ . Thus the momentum uncertainty on a given particle will have little effect on the expected  $\sim 7.8\%$  ionization resolution from ISIS.

The second element of the DPI is the  $2 \times 2 \times 5m^3$  atmospheric pressure Cerenkov counter, OSIRIS. The thresholds and photoelectron response for

different He-N<sub>2</sub> mixtures ranging from 100% He to 100% N<sub>2</sub> are shown in Table V. It should be noted that because of the ability to vary the proton (kaon) threshold from 39 (21) to 116 (61) GeV/c, such a detector provides an extremely flexible system with which to identify the faster particles with momenta above the effective range of ISIS ( $\approx 30-40$  GeV/c) as well as the ability to identify some of the particles that are also identified by ISIS. Thus OSIRIS is complementary to the ISIS system and by using the information from both systems, the range of mass identification will be increased as will be the confidence one has of unique particle mass identification. In particular, for this proposal OSIRIS plays an essential role in identifying (in a passive veto mode) the fast  $\bar{p}$ 's with momenta typically above 50 GeV/c from the nonannihilation events (Fig. 5 shows the  $\bar{p}$  laboratory momentum spectrum deduced from slow protons).

It is intended that OSIRIS have 8 cells, consisting of 2 vertical sets, each of four mirrors of size 50, 20, 20 and 50 cm (high) x 70 cm (wide), respectively (see Fig. 6). Acceptance calculations, again using events from E-311, show that the overall acceptance for  $\bar{p}$ 's, is  $\approx 99\%$  based on the inversion (in the CM system) of protons with  $P_{lab} \leq 1.4$  GeV/c which are identified by ionization in the bubble chamber. Furthermore, 36% (46%) of the forward CM hemisphere  $\pi$ 's and K's from 100 GeV/c  $\bar{p}p$  ( $\pi^-p$ ) interactions will also hit the Cerenkov mirrors at 11 m. The acceptances as a function of the CM rapidity are also shown in Figs. 2 and 3. Again, this plot shows the complementarity of ISIS and OSIRIS.

We have also studied the likelihood of two or more particles striking the same mirror (overlap) and find for the  $\bar{p}p$  experiment the following: (a) only 3.6% of the  $\bar{p}$ 's have at least one other particle in the same mirror, and (b) only 12% of all  $\pi$ 's or K's have at least one other particle

striking the same mirror. For this calculation we have used the measured momentum of each pion and have assumed that (a) the proton threshold is set at 100 GeV/c (see Table V) and (b) the Cerenkov light is produced at the front of the counter (5m from the mirrors) thus yielding the maximum possible radius for the Cerenkov light cone. A  $\bar{p}$  is then considered to have no overlap (i.e. to be unique) if the Cerenkov light from that  $\bar{p}$  strikes a mirror which does not accept light from any other particle (i.e.  $\pi$  or K).

The ranges of particle separation are shown in Fig. 7(a) for the bubble chamber (ionization), ISIS and for two settings of OSIRIS ( $\check{C}_1$  has proton threshold at 70 GeV/c;  $\check{C}_2$  has proton threshold at 100 GeV/c). Fig. 7 (b) shows how particles from 100 GeV/c  $\bar{p}p$  interactions would be identified for each range of momentum. The dotted lines indicate no identification at all and the numbers indicate the percentage of each type of particle expected in a given momentum range. With such a system one should be able to identify almost all of the antiprotons in addition to  $\geq 70\%$  of the slow protons. Since many of the above 3.6%  $\bar{p}$ 's may be identified anyway (either by comparison with the expected pulse height for two particles with known momentum or from the expected momentum spectra of the produced  $\pi^-$ 's and  $\bar{p}$ 's - Fig. 7b shows that very few  $\pi^-$ 's have momentum above 70 GeV/c), we estimate that the overall detection efficiency for  $\bar{p}$ 's is  $\sim 97\%$ .

As another example of the complementarity of the OSIRIS and ISIS systems, let us consider central region particle identification with the two Cerenkov settings described above. With  $\check{C}_1$  ( $\check{C}_2$ ) as in Fig. 7, we can attain  $\pi/K$  separation from  $\sim 3$  to  $\sim 30$  GeV/c with ISIS and from  $\sim 10$  ( $\sim 15$ ) GeV/c to  $\sim 40$  ( $\sim 50$ ) GeV/c with OSIRIS;  $\pi/p$  separation from  $\sim 3$  to  $\sim 70$  GeV/c with ISIS and from  $\sim 10$  ( $\sim 15$ ) GeV/c to  $\sim 70$  ( $\sim 100$ ) GeV/c with OSIRIS; and K/p separation from  $\sim 5$  GeV/c to  $\sim 70$  GeV/c with ISIS and from  $\sim 40$  ( $\sim 50$ ) GeV/c to 70 (100) GeV/c

with OSIRIS. Thus we see that OSIRIS provides charged particle identification at the higher momenta as well as overlapping with ISIS in the momentum range ( $\sim 20$  to  $\sim 40$  GeV/c) where particle separation on the basis of ionization becomes more difficult.

The Michigan State group was granted \$5000 (by Fermilab in April 1977) for preliminary studies of the performance of OSIRIS. In December 1977, tests were made at SLAC with a prototype counter with 5m of helium and 1.4m of  $N_2$  with a single optical cell. The aim of these tests was to measure the "figure of merit" (denoted by A in Table V) which we estimated to be  $100 \text{ cm}^{-1}$ . A description of the results of these tests is included as Appendix C and indicates that this value of A has been attained.

#### V. Neutral Particle Calorimeter (Antineutron and Photon Detector)

One of the primary considerations of these high statistics exposures is to identify a "clean" sample of annihilation events. To do this, it is necessary to identify as many as possible of the events which have a leading baryon or antibaryon. The slow protons can be identified by ionization in the bubble chamber. The fast antiprotons, whose laboratory momentum spectra deduced from slow protons is shown in Fig. 5, must be identified by OSIRIS, since  $p/K/\pi$  separation in ISIS is only available for  $\lesssim 30-40$  GeV/c. Since slow neutrons are difficult to identify, to find all the annihilation final states ( $\bar{p}pX$ ,  $\bar{p}nX$ ,  $\bar{n}pX$  and  $\bar{n}nX$ ), a further necessary ingredient in rejecting nonannihilation events is the detection of forward  $\bar{n}$ 's. As will be discussed in detail in this section, a device of cross section 31" x 31" placed immediately behind OSIRIS at 11-12m (see Fig. 1) will view 40% of the  $\bar{n}$ 's produced at 100 GeV/c. The expected laboratory angular and momentum distributions of  $\bar{n}$ 's (total) and those viewed by the detector (shaded) are shown in Fig. 8.

(a)  $\bar{n}$  Detection

The DPI Workshop of May 7-8, 1976 recognized the possibility that other detectors, such as a neutral hadron calorimeter, might be considered for use behind OSIRIS (see MALREP, July, 1976, Appendix B). For this experiment, we plan to use a modified version of the  $\bar{n}$  calorimeter which we have already used in a 9 GeV/c  $\bar{p}p/pp$  experiment (BC-64) behind the 40-inch bubble chamber at SLAC. This device is shown in Fig. 9. In its modified configuration, there will be 2-4 radiation lengths of Pb followed by 3 planes of xy hodoscopes, each plane consisting of 15 2" x 30" scintillators. Two planes are oriented at an angle of 90° with respect to each other. The third plane is oriented at an angle of 45° with respect to the first two in order to resolve ambiguities due to multiple hits. Following the hodoscopes are 26 sections of steel-scintillator sandwich. Each of the first 11 sections contains 1" x 31" x 31" steel plates and 1/2" x 31" x 31" scintillator, and each of the last 15 sections contains 1 3/8" x 31" x 31" steel plates and 1/2" x 31" x 31" scintillator.

Since we intend to veto  $\bar{n}$  events, the  $\bar{n}$  detector must have high efficiency. Our results from the SLAC experiment show that the efficiency for detecting  $\bar{n}$ 's is given by<sup>11</sup>

$$\text{Eff.} \approx (0.95)(1 - e^{-x/6.4})(e^{-y/23}),$$

where x is the total length of steel (inches) and y is the amount of steel between any two scintillators (inches). The coefficient 0.95 reflects the probability that the antineutron interacted to produce only neutrals that were never detected. With x = 31.6" and y = 1.2", we find an efficiency of ≈90%.

The actual performance of this calorimeter has been well documented as the result of our experiment (BC-64) at SLAC. In Figs. 10 and 11 we show the mean ADC response per counter to the energy deposited by monoenergetic muon, hadron and electron beams (of various energies) versus the longitudinal position (counter number) in the calorimeter. The sum of the pulse heights from all of the 28 counters varies almost linearly with momentum over the tested range of 1.6 to 12 GeV/c. The energy resolution is measured to be  $150\%/\sqrt{E}$  (FWHM) for hadrons and  $63\%/\sqrt{E}$  for electrons.

Since  $\gamma$ -rays could possibly simulate antineutrons through electromagnetic showers in the detector, we have made estimates of the  $\gamma/\bar{n}$  ratio resulting from nonannihilation interactions in the bubble chamber. Using acceptance calculations based on the simultaneous production of a forward  $\bar{p}$  and  $\pi^\pm$  in E-311 events, we estimate that  $\pi^0/\bar{n}$  is  $\lesssim 7\%$  for  $\bar{n}$ 's and  $\pi^0$ 's ( $\rightarrow 2\gamma$ ) hitting the detector. We have not done a detailed calculation of the  $\pi^0$  decay; however, for the energies of the  $\pi^0$ 's produced with a  $\bar{p}$  or  $\bar{n}$  it is highly unlikely that both  $\gamma$ 's from  $\pi^0$  decay will enter the  $\bar{n}$  detector. Thus, our best estimate is that  $\sim 7\%$  of the  $\bar{n}$ 's in the detector will be accompanied by a single  $\gamma$ . For annihilations, we again estimate that  $\sim 7\%$  of the events will yield a  $\gamma$  in the  $\bar{n}$  detector. However, we anticipate that it will not be difficult to distinguish  $\gamma$ 's from  $\bar{n}$ 's on the basis of the distribution of energy deposited along the calorimeter. In fact our SLAC results show that electromagnetic and hadronic showers are readily distinguished (i.e. to better than 95%) on the basis of shower penetration alone (compare the data of Figs. 10 and 11).

In a manner similar to that for estimating the  $\pi^0/\bar{n}$  ratio, the ratio  $\pi^\pm/\bar{n}$  is estimated to be  $\sim 14\%$  for nonannihilation (this follows from  $\pi^0/\bar{n} \simeq 7\%$  and  $\pi^0 \simeq 1/2 \pi^\pm$ ). Hence, in about 14% of the cases an  $\bar{n}$  signal may be accompanied by a  $\pi^\pm$  interacting in the  $\bar{n}$  detector. Since we know the energy of any  $\pi^\pm$ 's that enter the calorimeter, the energy resolution should be good enough to discriminate between simultaneous  $\pi^\pm$  and  $\bar{n}$  interactions.

As we will see later, the importance of the  $\bar{n}$  detector in providing a "clean" sample of annihilation events is dependent upon the ratio of  $\bar{p}$ 's to  $\bar{n}$ 's produced in nonannihilation events. Hence, one consequence of such a detector will be a measurement of the ratio of inclusive  $p/n$  ( $\bar{p}/\bar{n}$ ) production in 100 GeV/c  $pp$  ( $\bar{p}\bar{p}$ ) interactions.

(b) Acceptances and Detection Efficiencies for  $\bar{n}$ 's

An acceptance calculation has been performed for  $\bar{n}$ 's. For this purpose, we assume a 31" x 31" detector placed immediately behind the Cerenkov counter. Since  $\bar{p}p \rightarrow \bar{n}$  data are not readily available, we have used neutron production data for  $pp \rightarrow n$  ( $0.2 < p_T < 0.8$  GeV/c)<sup>12</sup> at ISR energies (invariant cross sections  $E d^3_\sigma/d^3p$  have been assumed to scale to 100 GeV/c) as an approximation to the  $\bar{p}p \rightarrow \bar{n}$  distribution. Our calculations show that 90% of the  $\bar{n}$ 's will be "seen" by a 31" x 31"  $\bar{n}$  detector (see Fig. 8). When combined with the  $\sim 90\%$  detection efficiency of the calorimeter, we find an overall  $\bar{n}$  efficiency of 81%.

(c)  $\pi^0$  Detection

The 31.6" of steel and 4 radiation lengths of Pb in front correspond to a total of  $\sim 50 X_0$ . As mentioned above, the resolution of our calorimeter for electromagnetic showers has been measured to be  $\frac{\Delta E}{E}$  (FWHM) =  $\frac{63\%}{\sqrt{E}}$

for electrons from 1.6 to 7.2 GeV/c. While we do not anticipate attempting one constraint physics in this experiment, the above energy resolution should be more than adequate to do the  $\pi^0/\gamma$  physics that we will discuss below. Important types of physics we will want to do with photon detection will be (1) to count the number of  $\pi^0/\gamma$  produced in the forward region associated with diffractive events, and (2) to use the  $\gamma$  detection as a veto while studying exclusive four-constraint channels. With regard to the latter study, there is little doubt that our calorimeter will be adequate. With regard to the counting of forward gammas, we show in Fig. 12 the minimum opening angle and minimum separation distance at 12m of the 2  $\gamma$ 's from a single  $\pi^0$  decay as a function of the  $\pi^0$  laboratory momentum. The minimum separation of the 2  $\gamma$ 's at 12m is  $\geq 10$ cm. In addition, considerations of the lateral growth of the shower show<sup>13</sup> that after 2.5cm of lead, 99% of the shower lies inside a radial distance of 2.5cm. Given these numbers a 2" x 2" cell size should be quite adequate to measure the  $\gamma$  multiplicity striking the calorimeter. For this reason we have placed 3 scintillation hodoscopes (each with 15 elements, 2" wide) at a depth of 2-4 radiation lengths (0.1 - 0.2 interaction lengths) in order to discriminate between simultaneous  $\gamma$ 's from the same  $\pi^0$ .

We have investigated the geometrical acceptance of the calorimeter for  $\gamma$ 's by using 100 GeV/c  $\pi^-p$  events from E2B. From the inclusive sample we find that 26% of all  $\gamma$ 's produced (or 1.7  $\gamma$ 's/event) will strike the calorimeter.

## VI. Physics Justification

A large number of interesting features of strong interactions have been discovered in earlier experiments with the Fermilab 30-inch bubble chamber and hybrid systems. In many cases, such as studies of correlations among kinematic variables, the statistics available in the original experiments have been inadequate for detailed studies. Other phenomena of great interest, such as  $\bar{p}p$  annihilations, have been impossible to study because of the lack of secondary particle identification. Improved identification of charged secondaries, including  $K^\pm$  and  $p, \bar{p}$  at momenta too great to allow identification by bubble density in the 30-inch chamber, will also allow major advances in studies of multiparticle correlations and of central region particle production. Significant improvements in  $\pi^0$  detection are needed to test hypothesized similarities to charged particle production. Current questions about analogies between particle production in lepton-hadron interactions, electromagnetic interactions, and hadron-hadron interactions will benefit from the availability of high-statistics data on hadron-hadron interactions which can serve as a baseline for the lower-statistics studies of the other types of interactions.

In an experiment which will provide the fullest possible information about interactions of all charge multiplicities, it is difficult to predict exactly what topics will prove to be of greatest importance. In the following sections we enumerate several examples of why we believe this proposed research should be carried out but we wish to emphasize that these are just examples of the full range of physics possible in this experiment.

In Table VI we estimate the numbers of events that we expect in the requested  $1.45 \times 10^6$  pictures at 100 GeV/c with  $\sim 6$  particles/picture. In

addition to these events, we also expect an additional  $\sim 60K$  events off the metallic foils inserted in the front of the chamber.

(a)  $\bar{p}p$  Annihilation and its Relation to the Difference of  $\bar{p}p$  and  $pp$  Total Cross Sections

We are interested in carrying out a detailed study of the baryon annihilation component in  $\bar{p}p$  interactions at 100 GeV/c incident anti-proton momentum. One of the long-standing problems in  $\bar{p}p$  annihilation is the possible relationship of  $\sigma(\text{ann})$  to  $\Delta\sigma_T = \sigma_T(\bar{p}p) - \sigma_T(pp)$ . A summary of available data is shown in Fig. 13. Recently we have published<sup>3</sup> an analysis of the differences between  $\bar{p}p$  and  $pp$  topological cross sections, including 100 GeV/c data from our E-311  $\bar{p}p$  experiment. The analysis indicates that good fits may be obtained to the model of Eylon and Harari<sup>14</sup>, where the quantity

$$R_n = \frac{\sigma_n(\bar{p}p) - \sigma_n(pp)}{\sigma_n(pp)} \quad (1)$$

is predicted to be of the form

$$R_n = \beta^n s^{2\alpha_B - 2\alpha_M} - (1 - n_1)\gamma^n, \quad (2)$$

and  $s$  is the square of the  $\bar{p}p$  C.M. energy,  $n$  is the charge multiplicity,  $\alpha_M(\alpha_B)$  is the intercept of the leading exchanged meson (baryon) trajectory,  $n_1(\leq 1)$  is a constant, and  $\beta(>1)$  and  $\gamma(<1)$  are constants which, in a simple form of the model, are  $3/2$  and  $1/2$ , respectively. Our fits shown in Figures 1 and 2 of our paper<sup>3</sup> with the further definition  $\alpha = 2\alpha_M - 2\alpha_B$  are consistent with a contribution from the first term of Eq. (2) only (implying  $n_1 \simeq 1$  or  $\gamma \simeq 0$ ). In the Eylon-Harari model the first term of Eq. (2) represents annihilations due to the Pomeron exchange term in the total cross section, whereas the second term represents

nonannihilations due to Pomeron and meson exchange terms. Thus, the data support the conjecture that the annihilation component in  $\bar{p}p$  interactions is due to the Pomeron and not meson exchange contributions to the total cross section.

The Eylon-Harari model is very much in contradiction with the "classical" approach to the difference in the total cross sections. That is, in Regge terminology one usually writes

$$\sigma_T(\bar{p}p) = \text{Im}(P + \rho + \omega + f + A_2)_{t=0} \quad (3)$$

$$\sigma_T(pp) = \text{Im}(P - \rho - \omega + f + A_2)_{t=0} \quad (4)$$

and hence,

$$\Delta\sigma_T = 2\text{Im}(\rho + \omega)_{t=0}, \quad (5)$$

indicating the difference is due to the vector meson exchange part of the total cross section. In fact, the energy dependence of  $\Delta\sigma_T$  from Eq. (5) is  $s^{\alpha_V(0)-1} \sim s^{-0.5}$ , which is a good representation of the data (see Fig. 13). In both the "classical" and Eylon-Harari models as well as related phenomenologies<sup>15</sup> it is argued that  $\sigma(\text{ann})$  may equal  $\Delta\sigma_T$ . To a certain extent this is obviously false, since (1) the  $\bar{p}p$  system is an equal mixture of isospin one and zero states, whereas  $pp$  is pure isospin one and (2) there are nonannihilation states ( $\Lambda^0\bar{\Lambda}^0$  for example) which are available to  $\bar{p}p$  but which are not open to  $pp$ . Obviously, if the various models discussed above which claim to address the question of annihilations via  $\Delta\sigma_T$  are to be proven valid, the experimental relationship of  $\Delta\sigma_T$  to  $\sigma(\text{ann})$  must be established. We propose to do this with a high statistics sample (~10 K events) of "clean" annihilations.

Somewhat surprisingly, no clean event-by-event identification of annihilation events has been made above ~2 GeV/c incident antiproton

momentum. This is the result of several factors: (1) the high multiplicity final states in both annihilation and nonannihilation interactions belong to the domain of the bubble chamber technique with its well known high multi-track efficiency; (2) annihilation cross sections are relatively large ( $\sim 3.5$  mb at 100 GeV/c, see Fig. 13), further lending their study to bubble chambers; (3) ambiguities among  $\bar{p}$  and  $\pi^-$  ( $K^-$ ) tracks cannot be resolved in the bubble chamber above  $\sim 1.5$  GeV/c and (4) neutrons and antineutrons cannot be identified in the bubble chamber. Attempts have been made up to 12 GeV/c to statistically separate the annihilation component.<sup>15-16</sup> These are interesting first steps in isolating annihilations and have been extremely illuminating in their own right. However, they require assumptions which might bias the final result. Clearly better measurements free of possible systematic errors are required.

As mentioned earlier, the Cambridge-MSU collaboration has been approved for a similar  $\bar{p}p$  and  $pp$  experiment (BC-64) at 9 GeV/c at the SLAC 40-inch hybrid bubble chamber facility. Because of the similarities between these two experiments, we expect to be able to study the energy dependence of many of the annihilation properties by comparing our 9 GeV/c data with the results we would obtain at 100 GeV/c from this proposed experiment.

(b) Baryon Annihilations and Comparison with  $e^+e^- \rightarrow$  hadrons

(i) Charged Particle Multiplicities

The  $\bar{p}p$  topological cross sections at 100 GeV/c from E-311 show interesting differences when compared to  $pp$  results at 100 GeV/c. The trend seems to be for the low multiplicity  $\bar{p}p$  cross sections to be

smaller than the pp ones, while the higher charged multiplicity (i.e.,  $\geq 14$  prongs) cross sections are significantly larger than the corresponding pp values. This suggests that annihilations occur mainly in the high multiplicity events. (If this is true, it will be difficult to study these events in anything but a bubble chamber.) With an increase in statistics by a factor of 10 for both  $\bar{p}p$  and pp, we will be able to study this difference in much greater detail.

The possibility that hadron interactions are reducible in some sense to interactions of constituent quarks is of fundamental importance to hadron physics. Arising from such a possibility are relationships between  $\bar{p}p$  annihilations and  $e^+e^- \rightarrow$  hadrons, such as

$$\bar{n}_{\bar{p}p\text{ann}}(\sqrt{s}) = 3 \bar{n}_{ee}(\sqrt{s}/3), \quad (6)$$

which follow naturally from a scheme visualizing particle production via jets associated with interactions of individual quarks (see Fig. 14). More recently, Rossi and Veneziano<sup>17</sup> have used the topological expansion approach to place these ideas on a more sound theoretical framework, and have also suggested more detailed tests of the jet structure of hadronic final states; we shall return to these below. Meanwhile we note that Eq. (6) is not very successful, because it fails to take into account fluctuations in the partition of energy between the jets. On trying to do so, one finds<sup>18</sup> that one should replace  $\sqrt{s}/3$  by  $\sqrt{s}/\eta$ , with  $\eta \approx 4.5$ . The current experimental situation then appears as in Fig. 15, a plot of  $\langle n \rangle$  versus  $s$ . There is a 100 GeV/c estimate for  $(\bar{p}p - pp)$  obtained in our exploratory Fermilab experiment (E-311) but it is clearly of great interest to obtain as reliable and precise a measurement from identified annihilations at as high an energy as possible to see whether

$\bar{p}p$  and  $\bar{e}e$  are becoming equal asymptotically. Note that the energy of this proposal ( $s = 189 \text{ GeV}^2$ ) is equivalent (for  $n^2 \approx 20$ ) to  $e^+e^-$  annihilations at  $\sqrt{s} = 3.1 \text{ GeV}$ , within the SPEAR, DORIS energy range. The statistics available in this proposal will yield a value of  $\langle n_- \rangle$  to  $\sim 1-2\%$ .

Muirhead<sup>19</sup> has pointed out a number of intriguing similarities between the annihilation processes

$$e^+e^- \rightarrow \text{hadrons} \quad (7)$$

and

$$\bar{p}p \rightarrow \text{hadrons} \quad (8)$$

where for these purposes "hadrons" is limited to pions or kaons. For example, Figures 16-18 directly compare the  $f_2^{--}$ ,  $\langle E_{\text{neutral}} \rangle / \langle E_{\text{negative}} \rangle$  and inclusive cross sections for the two processes. In some cases off-shell (below threshold) low mass  $\bar{p}p$  data are obtained by examining virtual  $\bar{p}p$  interactions in the u-channel for the reaction  $K^-p \rightarrow \Lambda^0 + \text{pions}$ . The similarities in the data are indeed remarkable. With the exception of the lowest energies the  $\bar{p}p$  points must be viewed as only approximate since "clean" samples of annihilation events have not been identified in the "bare" bubble chamber experiments. For example, taken at face value the  $\bar{p}p$  data of Fig. 17 do not exhibit the "energy crisis" observed in  $e^+e^-$  data. On the other hand, a measurement of  $\langle E_{\text{neutral}} \rangle / \langle E_{\text{negative}} \rangle$  at  $100 \text{ GeV}/c$  ( $s = 189 \text{ GeV}^2$ ) with "clean" events free of nonannihilation contamination and comparisons with new data from high energy  $e^+e^-$  experiments could be most revealing.

As a result of these comparisons, the potential of a high statistics, "clean" comparison of  $\bar{p}p$  and  $e^+e^-$  annihilations seems intriguing to us

and could be extended to the details of topological features, specific exclusive channels, resonance production, etc., with the added feature of kaon identification as will be discussed later. It appears to us that the  $\sim 10,000$  annihilation events (based on  $\sigma_{\text{ann}} \sim 3.5$  mb, see Fig. 13) should be adequate for a preliminary  $e^+e^-$ ,  $\bar{p}p$  annihilation comparison. It should be pointed out that the comparisons of  $\bar{p}p$  and  $e^+e^-$  annihilations at the same  $\sqrt{s}$  will also be of interest. This  $\sqrt{s}$  value will correspond to the CESR energy range (and possibly the low energy range of PEP and PETRA). We note that recent dual quark model calculations of Webber<sup>20</sup> indicate that  $f_2^- \rightarrow 1.39$  for  $\bar{p}p$  annihilations at high energy and we should obtain a 100 GeV/c estimate to  $\pm 0.2$  to test this asymptotic prediction.

(ii) Single Particle Inclusive Distributions

Data<sup>6</sup> on inclusive  $\pi^\pm$  production at 100 GeV/c based on  $\sim 12,000$   $\bar{p}p$  events has suggested, for example, that the rapidity spectrum is broader in  $\bar{p}p$  annihilations than in non-annihilations. The dual quark model<sup>20</sup> envisages  $\bar{p}p$  annihilations in terms of the emission of meson clusters in three strongly-ordered sequences associated with each individual quark annihilation, and makes detailed predictions about the distributions of produced particles (including  $K^\pm$ ,  $K^0$ ) e.g. rapidity structure, leading particle effects, etc. With 10,000 events we should be able to investigate such features and test the underlying quark dynamics.

(iii) Two-particle Correlations of Produced Particles in High Energy Annihilations

Although certain correlation parameters have been mentioned above, we single out for emphasis a detailed study of correlations, particularly among hadrons produced in the central region. Such a study will make possible entirely new tests of fundamental aspects of hadronic processes

in a previously unexplored area, e.g. of correlations involving strange particles.

The measurement of the correlation function

$$R(y_1, y_2) = \sigma_{\text{inel}} \frac{d^2\sigma}{dy_1 dy_2} / \frac{d\sigma}{dy_1} \frac{d\sigma}{dy_2} - 1 \quad (9)$$

for the production of two  $\pi^-$ 's will permit a test of the recent prediction by Giovannini and Veneziano<sup>21</sup>, that for  $y_1^* \approx y_2^* \approx 0$ ,

$$(R^{--}-1)_{\bar{e}e} : (R^{--}-1)_{pp} : (R^{--}-1)_{\bar{p}p_{\text{ann}}} = 3 : 1.5 : 1 \quad (10)$$

which amounts to a sensitive test of the  $\bar{q}q$  jet structure of lepton - and hadron - induced processes via Bose-Einstein (BE) effects. Existing data suggest  $R_{pp}^{--} \approx 0.5$ , so we have the clear prediction

$$R_{\bar{e}e}^{--} = 0 \quad (11)$$

$$R_{\bar{p}p_{\text{ann}}}^{--} = 0.67. \quad (12)$$

We believe we can measure  $R_{\bar{p}p_{\text{ann}}}^{--}$  to perhaps  $\pm 15\%$ , for comparison with a future PEP, CESR or PETRA value from  $e^+e^-$ . We note that the BE effect is predicted to be small in  $\bar{e}e$  and largest in  $\bar{p}p$  annihilations. This comes from the fact that two  $\pi^-$ 's in the same jet (as with  $\bar{e}e$ ) cannot be neighbors and tend to have different momenta, whereas two  $\pi^-$ 's in different jets (3 jets in  $\bar{p}p$ ) can be essentially dynamically uncorrelated and allow the BE effect to become strong. We note also that the predictions (11) and (12) are in striking disagreement with those of "universal emission" models, e.g. of Ref. (22), which imply a universal value for  $R^{--}$ . In a recent report, G. Goldhaber has shown<sup>23</sup> that SPEAR data from 3 to 7.4 GeV cm energy exhibit a striking phenomenon: the GGLP (Bose-Einstein) effect, clearly present below  $\sim 4.5$  GeV, disappears

suddenly and is not seen at 6.2, 7.4 GeV, in the region where jet structures become clear.

An equivalent prediction for  $\pi^+\pi^-$  correlations exists, namely

$$R_{e^+e^-}^{+-} : R_{pp}^{+-} : R_{pp_{ann}}^{+-} = 3 : 1.5 : 1 \quad (13)$$

which should hold at all  $(y_+^*, y_-^*)$  in the central region. It should be possible to test this result in the central region.

(c) Study of ( $\bar{p}p - pp$ ) Differences

Apart from their possible connection with  $\bar{p}p$  annihilations, ( $\bar{p}p - pp$ ) differences are of intrinsic physics interest in their own right because they permit detailed tests of the Mueller-Regge formalism free from the complications of the pomeron. Clearly most of the inclusive and correlation data discussed above can be interpreted in this light, the unifying concept being that ( $\bar{p}p - pp$ ) is dominantly a result of  $\rho$  and  $\omega$  exchanges.

Data have already appeared from E-311 relating to single and double pion production in  $\bar{p}p$  at 100 GeV/c. Among the phenomena investigated have been

- (1) Scaling of  $(\bar{p}p - pp) \rightarrow \pi^-$  in the target fragmentation region, which shows that data at 12 and 100 GeV/c scale according to the difference in the  $\bar{p}p$  and  $pp$  total cross sections.<sup>6</sup>
- (2) Comparison of  $\pi^\pm$  production in the target fragmentation region from  $(\bar{p}p - pp)$ ,  $(\pi^-p - \pi^+p)$  and  $(K^-p - K^+p)$  differences as a function of  $s$ , leading to estimates<sup>24</sup> of the appropriate reggeon particle vertices; the  $\pi^-$  production data are shown in Fig. 19.
- (3) Central region production of charged pions in  $(\bar{p}p - pp)$ , which is shown to have the required  $s$ -dependence (Fig. 20), and leads to

estimates<sup>24</sup> of the appropriate reggeon - particle couplings (of relevance to dual theories) when compared with  $(\pi^-p-\pi^+p)$  data.

- (4) An understanding of double fragmentation in terms of a product of single fragmentation distributions; factorization is shown<sup>7</sup> to hold in pomeron and reggeon exchange independently.

These can be thought of as preliminary results from an exploratory experiment since the present proposal will have ten times the statistics for pion production.

(d)  $\pi\pi$  (and  $K\pi$ ) Interactions

It will be possible to study  $\pi\pi$  interactions over a range of  $\pi\pi$  masses up to perhaps 4-5 GeV. Among the important topics to be studied are:

1.  $\pi\pi$  total and elastic cross sections as a function of  $\pi\pi$  mass;
2. multiplicity of charged secondaries as a function of  $\pi\pi$  mass;
3. neutral pion multiplicity as a function of  $\pi\pi$  mass;
4. comparison of  $I = 2$  and  $I = 0, 1$   $\pi\pi$  cross sections;
5. diffractive dissociation of pions by pions.

We will study  $\pi\pi$  interactions by isolating primary interactions of the type

$$\pi^\pm p \rightarrow \Delta^{++} + X.$$

Our previous studies of  $\Delta^{++}$  production in 100, 200 and 360 GeV/c  $\pi^-p$  interactions yield an inclusive  $\Delta^{++}$  cross section of about 1.2 mb for  $t_{p\Delta} < 1 \text{ GeV}^2$  with relatively small backgrounds under the  $\Delta^{++}$ . The inclusive  $\Delta^{++}$  cross section is relatively independent of incident pion momentum. Significant  $\Delta^{++}$  production can be found for charge multiplicities at least up to  $n_c=12$ . The  $\Delta^{++}$  density matrix elements are compatible with  $\Delta^{++}$  production via one-pion exchange with absorption. Other data suggest

comparable  $\Delta^{++}$  production cross sections for 100 GeV/c interactions of all types. Thus we might expect 2,000-8,000  $\Delta^{++}$  events in the  $\pi^+p$  and  $\pi^-p$  samples and up to 400  $\Delta^{++}$  events in the  $K^+p$  data. This should be sufficient for studies of the topics mentioned above.

The comparison of multiplicities in  $\pi\pi(K\pi)$  interactions with those in  $pp$  and  $\bar{p}p$  will be of special interest in terms of quark models. Qualitatively, each meson quark is expected to carry, on the average, half the energy of the meson while each nucleon quark should carry one third of the nucleon energy. Thus the average available energy and the average secondary particle multiplicity should be greater in meson-meson interactions than in meson-nucleon and nucleon-nucleon interactions at the same total energy.

In addition to providing information on neutral pion multiplicities in  $\pi\pi$  interactions, the photon detector will be especially useful in obtaining pure samples of 4-prong 4C events for measuring  $\pi\pi$  elastic scattering in the reactions  $\pi^-p \rightarrow \pi^-\pi^-\Delta^{++}$  and  $\pi^+p \rightarrow \pi^+\pi^-\Delta^{++}$ . It can be used to veto events where a photon is detected even if an acceptable 4C kinematic fit is obtained. Similarly it can improve the purity of 6 prong 4C samples which can be used to search for specific channels of pion diffractive dissociation such as  $\pi^+p \rightarrow (A^\pm\pi^\mp)\Delta^{++}$ .

(e) Tests of the Quark-Parton Model in Low  $P_T$  Hadronic Collisions

The quark-parton hypothesis has been used successfully to describe hard processes such as the production of high-mass meson and lepton pairs (Drell-Yan) and of hadrons at large transverse momentum. These processes involve the hard scattering<sup>1</sup> of two elementary constituents (partons): one from the projectile and one from the target. These two partons undergo an elastic collision followed by quark fragmentation or decay into the observed hadrons.

More recently it has been shown<sup>26-27</sup> that quark-parton effects may also appear in "soft" (low  $P_T$ ) processes. In the simple  $q\bar{q}$  recombination model a fast valence quark from the projectile combines with an antiquark from the sea to form the hadronic fragment. Additional evidence in favor of this model has come from considerations<sup>27</sup> of the inclusive two-particle processes in the proton fragmentation region: i.e. "trigger" on a fast hadron at Feynman  $x_a$  and study the cross section - or ratios of the cross sections - for other hadrons at  $x_b$ .

In particular, let the trigger particle be a  $K^0$  ( $= d\bar{s}$ ) or  $\pi^-$  ( $= d\bar{u}$ ) and let the second particle be either a  $\pi^+$  or  $\pi^-$ . It has been shown<sup>27</sup> that the  $\pi^+/\pi^-$  ratio is expected to be the same for either the  $K^0$  or  $\pi^-$  trigger data, despite the different charges of the two trigger mesons. While the data suggest this equality, further data of greater statistical accuracy would be welcome. In addition there are many other processes e.g. triggering on a  $K^+$  ( $= u\bar{s}$ ) and  $\pi^+$  ( $= u\bar{d}$ ) which will provide interesting tests of the recombination or quark fusion model. The 30-inch chamber and DPI with the charged particle identification in the forward hemisphere is an obvious set-up for obtaining "triggered" data with a minimum of bias as well as the ability to study what occurs in the rest of the collision. It will also be of great value to have data with different projectiles ( $\bar{p}$ ,  $p$ ,  $\pi^\pm$ ,  $K^\pm$ ) in order to provide extensive tests of this model.

(f) Central Region Physics

(i) Two-Particle Correlations and Resonance Production

Current studies of two particle correlations have revealed a number of interesting effects. For example, the two-particle correlation

functions for  $\pi^+ \pi^-$  pairs and for  $\pi^+ \pi^+$ ,  $\pi^- \pi^-$  pairs are found to differ significantly.<sup>28</sup> The correlation between like pions is greatly enhanced when the two pions are required to have momenta similar in both magnitude and direction and appears to be consistent with what is expected from Bose-Einstein statistics.<sup>29</sup> Among the areas in which advances could be expected from this experiment in the study of two-particle correlations are:

- (1) Improved studies of semi-inclusive correlations;
- (2) Improved charged-particle identification will allow comparisons of  $K^\pm \pi^\pm$  correlations with  $\pi^\pm \pi^\pm$  correlations;
- (3) Current studies of meson production in interactions over a range of energies have suggested the importance and possible dominance of meson production via the decay of intermediate states which may possibly be identified with known meson and baryon resonances. If such decays are the major source of final state pions it should be possible to determine the effects for the observed multi-particle correlation functions when better statistics are available. The explanation of observed correlations as primarily due to decays of known meson resonances would be of interest. The demonstration that observed correlations cannot be understood solely in terms of such decays would be even more exciting.
- (4) Studies of second-order interference effects, analogous to the Hanbury Brown-Twiss effect in optics have recently been presented. Interpretation of the observations has been severely hampered by limited statistics. Improved statistics may lead to a possible better understanding of the space and time evolution of particle production.

(ii) Local Conservation of Quantum Numbers

Current studies of charge exchange along the rapidity axis in high-energy interactions provide evidence for local conservation of charge.<sup>30</sup> This observation has led to considerable speculation about local conservation of other quantum numbers such as strangeness and of variables such as transverse momentum. With the identification of  $K_S^0$ ,  $K^\pm$ ,  $\Lambda$  and  $\bar{\Lambda}$  in a large number of events (see summary in Table VI) one might expect to study the processes of strangeness exchange in hadronic interactions. For example, what is the rapidity gap distribution between the two strange particles? How locally is strangeness conserved? The answers to these questions (along with the analogous questions relating to charge exchange) could be most revealing.

(g) Exclusive Channels

Figure 21 shows a summary of the 4 and 6 body final states in  $\bar{p}p$  interactions. By extrapolation to 100 GeV/c, one can estimate the numbers of events expected for various annihilation and nonannihilation final states. These are given in Table VI along with the analogous values for  $pp$ ,  $\pi^\pm p$  and  $K^\pm p$  interactions. At 100 GeV/c the momentum resolution of the downstream hybrid system will be sufficient to provide reliable kinematic fitting. Contamination of 4C event samples with events involving neutral secondaries can be further reduced with information from the neutral calorimeter since these data can be used to veto events with associated photons.

With the expected numbers of  $\bar{p}p\pi^+\pi^-$ ,  $pp\pi^+\pi^-$ , and  $\pi^\pm p\pi^+\pi^-$  events one will be able to make interesting comparisons at 100 GeV/c. The number of annihilation events expected in the low ( $\leq 6$ ) multiplicities

will be too small to permit much analysis, but it could be that the cross sections for annihilations to  $8\pi$  and up will be large enough to permit some interesting studies.

(h) Studies of the Events in Mg and Au Interactions

Much of the physics we intend to study in these events is described in Fermilab proposal #304 which has already been approved for 200K pictures of 300 GeV/c  $\pi^-$  with high Z nuclei (a revised version of the proposal is included as Appendix D). In this section we summarize the major topics to be studied.

(i) Incoherent  $\pi$ -A Collisions

By using both  $\pi^+$  and  $\pi^-$  incident beams it will be possible to make a detailed study of both  $\pi$ -Mg and  $\pi$ -Au collisions. This means that we can measure the multiplicities and rapidity distributions for  $\pi^\pm$ ,  $K^\pm$ ,  $\pi^0$  and  $K^0$  as well as the distributions for the knocked-on protons and neutrons. The determination of the number of knocked-on protons makes it possible to perform a detailed check of KNO scaling for magnesium and gold as compared to  $\pi p$  collisions.

(ii) Diffraction and Coulomb Studies

We should be able to measure inclusively the coherent events for Mg and Au. We expect of the order of 10% of all events to be coherent (these are the 3,5 and 7 prong events). Of these coherent events about one third of the events in gold should be Coulomb induced.

(iii)  $\alpha$ -Centauri Events

We propose to look for this process in which large charged multiplicities are encountered with very few  $\pi^0$ 's produced. We intend to study the high multiplicity events in detail. With the sample size

available ( $\sim 60,000$  high A events) we can look at the high charged multiplicity events to see if there are any indications of basically new phenomena such as events with few  $\pi^0$ 's.

(iv) A Study of Direct Pair Production in Condensed Matter

(v) A Study of High  $P_T$  Phenomena in Heavy Nuclei

This will be a by-product of our comprehensive studies of interactions in a heavy nucleus.

(vi) 360 GeV/c  $\pi^-$ -Nucleus Interactions

We propose a 50K picture exposure of the 30" hydrogen bubble chamber with Mg and Au thin foil targets to a 360 GeV/c  $\pi^-$  beam in order to make an exploratory study of the multiplicities produced by the highest possible energy  $\pi^-$  interactions with heavy nuclei to look for possible new physics.

VII. Efficiency for Separating Annihilation from Nonannihilation Events

The efficiencies determined in previous sections are summarized in Table VII. In Table VIII we show the separate efficiencies for detecting the four nonannihilation final states: (1)  $\bar{p}pX$ ; (2)  $\bar{p}nX$  and (3)  $\bar{n}pX$  and (4)  $\bar{n}nX$ . An important input into these considerations is the anticipated relative abundance of these four states. Assuming  $pp$  and  $\bar{p}p$  (nonannihilation) reactions are factorizable, the results<sup>31</sup> of Bøggild et al. for  $pp$  at 19 GeV/c suggest the above reactions should scale in accordance with the ratio  $p:n = 0.7 : 0.3$ . We conclude that 97% of the nonannihilations will be identified.

The resultant purity of the annihilation sample is now easily calculated. With  $\sigma_T = 42$  mb,  $\sigma(\text{ann}) \sim 3.5$  mb,  $\sigma_{e1} = 7.4$  mb, we calculate

$$\text{Purity} = 1 - \frac{(42-3.5-7.4) \times 0.03}{3.5} = 73\% \quad (14)$$

where we assume elastic events can be readily removed using kinematics. Furthermore, any impurity will probably manifest itself as departures from C-invariance in  $\pi^\pm$ ,  $K^\pm$  distributions.

In addition to the use of symmetry arguments, we would also expect to make detailed corrections for the inefficiencies in the detection system by using pp data run under identical conditions. By using those pp events in which we do not identify any baryon (since every pp event must produce two baryons, such events result from inefficiencies in the system), we will obtain distributions (e.g.,  $y^*$ ,  $x$ ,  $p_T$ ,  $\langle n_C \rangle$ , etc.) which may then be used to obtain corrected annihilation samples. From Table VI and our estimated efficiencies, we calculate that by using  $\sim 300,000$  pp pictures (with the  $0.3p/0.1K^+/0.6\pi^+$  ratios) as a calibration run, the errors resulting from these corrections should be comparable to or smaller than the statistical errors in individual bins in a typical differential distribution. Thus, in addition to the informative physics studies to be done in the pp experiment, an extremely important aspect of the pp exposure is as a calibration run for the  $\bar{p}p$  annihilation physics.

### VIII. Analysis of Experimental Data

Physicists at all six institutions on this proposal have had extensive past experience with measurements and analysis in experiments involving the Fermilab 30-inch bubble chamber. Appendix A lists the publications from these groups for the following experiments:

- #2B (Notre Dame, Duke, Fermilab, Michigan State): 100 GeV/c  $\pi^-p$ ,  
200 GeV/c  $\pi^-p$ , 200 GeV/c pp and 300 GeV/c pp.
- #163A (Duke): 200 GeV/c  $\pi^-Ne$

#281 (Notre Dame, Michigan State): 360 GeV/c  $\pi^-p$

#311 (Cambridge, Fermilab, Michigan State): 100 GeV/c  $\bar{p}p$

#345 (Stockholm): 100 GeV/c  $\bar{p}d$ .

Thus we have demonstrated our capability for measuring and analyzing significant numbers of events of all multiplicities in the 30-inch bubble chamber.

The six institutions have measuring systems ranging from semi-automatic machines (Spiral Reader, Sweepnik, SAMM, RIPPLE) to conventional film-plane and image-plane devices of high precision with experienced operators and on-line computer sequencing and checking. We estimate that the combined measuring power of the collaborating institutions amounts to about 170K events per year. This should insure that all of the events in the  $1.45 \times 10^6$  pictures are measured in  $\sim 2$  years. We anticipate, however, that many physics results will be obtained prior to completion of measurements on the entire film obtained in this experiment.

REFERENCES

1. R. D. Field and R. P. Feynman, Phys. Rev. D15, 2590 (1977).
2. R. E. Ansorge et al., Physics Letters 59B, 299 (1975).
3. J. G. Rushbrooke et al., Physics Letters 59B, 303 (1975).
4. D. R. Ward et al., Physics Letters 62B, 237 (1976).
5. R. Raja et al., Phys. Rev. D15, 627 (1977).
6. J. Whitmore et al., Phys. Rev. Letters 38, 996 (1977).
7. J. G. Rushbrooke et al., Phys. Rev. Letters 39, 117 (1977).
8. W. W. Neale, Fermilab Report FN-259, June, 1974; see also Refs. 2-7.
9. W. W. M. Allison et al., Nucl. Instr. Methods 119, 499 (1974).
10. Private Communication, V. Kistiakowsky (12/23/77).
11. M. L. Marshak and P. Schmuser, Nucl. Instr. & Methods 88, 77 (1970).
12. J. Engler et al., Nucl. Phys. B84, 70 (1975).
13. Yu. B. Bushnin et al., Nucl. Instr. Methods 106, 493 (1973).
14. Y. Eylon and H. Harari, Nucl. Physics B80, 349 (1974).
15. H. Muirhead, Proceedings of the Symposium on  $\bar{N}N$  Interactions, Liblice-Prague, CERN 74-18 (1974), p. 488. P. S. Gregory, Proceedings of the Inter. Symposium on  $\bar{p}p$  Interactions, Loma-Koli, U. of Helsinki Report No. 103 (1975), p. 256.
16. C. Walck, ibid, p. 65.
17. G. C. Rossi and G. Veneziano, Nucl. Phys. B123, 507 (1977).
18. B. R. Webber, Private Communication.
19. H. Muirhead, Ref. 15, p. 300.
20. B. R. Webber, Nucl. Phys. B117, 445 (1976).
21. A. Giovannini and G. Veneziano, TH-2347-CERN (1977).
22. J. D. Bjorken and J. Kogut, Phys. Rev. D8, 1341 (1973); S. J. Brodsky and J. F. Gunion, Phys. Rev. Letters 37, 402 (1976).

23. G. Goldhaber, LBL Note, TG-287 (1977).
24. J. G. Rushbrooke and B. R. Webber, Phys. Reports C, to be published (1978).
25. J. W. Chapman et al., Phys. Letters 47B, 465 (1973); M. Alston-Garnjost et al., Phys. Rev. Letters 35, 142 (1975); J. Erwin et al., Phys. Rev. Letters 32, 254 (1974); C. Bromberg et al., Phys. Rev. Letters 31, 1563 (1973).
26. W. Ochs, Nucl. Phys. B118, 397 (1977); K. P. Das and R. Hwa, Phys. Letters 68B (1977); T. A. DeGrand and H. I. Miettinen, SLAC Preprint (1977); D. W. Duke and F. E. Taylor, Fermilab-Pub 77/95-THY (1977).
27. E. Lehman, M. Pratap, J. Pumplin, J. Whitmore et al., MSU Preprint (1978).
28. B. Y. Oh et al., Phys. Letters 56B, 400 (1975); N. N. Biswas et al., Phys. Rev. Letters 35, 1059 (1975).
29. N. N. Biswas et al., Phys. Rev. Letters 37, 175 (1976).
30. J. W. Lamsa et al., Phys. Rev. Letters 37, 73 (1976); V. A. Sreedhar et al., Phys. Rev. D14, 2894 (1976).
31. H. Bøggild et al., Nucl. Phys. B27, 285 (1971).

Table I

Pion Acceptance of ISIS as a Function of Laboratory  
Momentum for 100 GeV/c  $\bar{p}p$  Interactions

<u>Momentum (GeV/c)</u>	<u>No. of Pions Produced</u>	<u><math>\pi</math>'s Escaping Magnet</u>		<u><math>\pi</math>'s Escaping Magnet and Thru <math>1 \times 1 \times 3 \text{m}^3</math> ISIS</u>	
		<u>No.</u>	<u>% of <math>\pi</math>'s Produced</u>	<u>No.</u>	<u>% of <math>\pi</math>'s Produced</u>
0-5	16135	8389	52.0	691	4.3
5-10	3752	3734	99.5	2034	54.2
10-15	1692	1678	99.2	1522	90.0
15-20	916	910	99.3	887	96.8
20-30	919	913	99.3	910	99.0
30-40	393	390	99.2	389	98.9
40-50	164	159	97.0	159	97.0
50-60	63	61	96.8	61	96.8
60-70	33	30	90.9	30	90.9
70-100	12	10	83.3	10	83.3
Totals	24079	16274	67.6	6693	27.8

Table II

Pion Acceptance of ISIS as a Function of Laboratory Momentum for 100 GeV/c  $\pi^- p$  Interactions

Laboratory Momentum (GeV/c)	No. of Pions Produced		$\pi^-$ 's Escaping Magnet			$\pi^-$ 's Escaping Magnet and Thru $1 \times 1 \times 3m^3$ ISIS				
	$\pi^-$	$\pi^+$	No. $\pi^-$	% of $\pi^-$ Produced	No. $\pi^+$	% of $\pi^+$ Produced	No. $\pi^-$	% of $\pi^-$ Produced	No. $\pi^+$	% of $\pi^+$ Produced
0 - 5	6352	7227	3529	55.6	3818	52.8	352	5.5	245	3.4
5 - 10	2029	1696	2027	99.9	1689	95.6	1297	63.9	731	43.1
10 - 15	1139	848	1139	100.0	847	99.9	1093	96.0	727	85.7
15 - 20	633	483	633	100.0	483	100.0	632	99.8	466	96.5
20 - 30	791	448	791	100.0	448	100.0	789	99.7	446	99.6
30 - 40	427	176	427	100.0	176	100.0	427	100.0	175	99.4
40 - 50	278	85	278	100.0	85	100.0	278	100.0	85	100.0
50 - 60	183	43	183	100.0	43	100.0	182	99.5	43	100.0
60 - 70	169	25	169	100.0	25	100.0	169	100.0	25	100.0
70 - 100	812	60	812	100.0	60	100.0	812	100.0	60	100.0
Total	12813	11091	9988	78.0	7674	69.2	6031	47.1	3003	27.1

Table III

Hemispheric Pion Acceptance of ISIS for 100 GeV/c  $\bar{p}p$  Interactions

	No. of Pions Produced	% of Pions Produced	C.M. Hemisphere			
			Backward		Forward	
			No.	%	No.	%
Total produced	24079	100.0	12043	100	12036	100
Leave magnet	16274	67.6	4310	35.8	11964	99.4
Enter 1mx1m ISIS at 2.1m	12664	52.6	1987	16.5	10677	88.7
Exit 1mx1m ISIS at 5.3m	6693	27.8	375	3.1	6318	52.5

Table IV

Hemispheric Pion Acceptance of ISIS for 100 GeV/c  $\pi^-$  p Interactions

	C.M. Hemisphere															
						Backward					Forward					
	No. $\pi^-$	% $\pi^-$	No. $\pi^+$	% $\pi^+$	No. $\pi^-$	% $\pi^-$	No. $\pi^+$	% $\pi^+$	No. $\pi^-$	% $\pi^-$	No. $\pi^+$	% $\pi^+$	No. $\pi^-$	% $\pi^-$	No. $\pi^+$	% $\pi^+$
Total Produced	12813	100.0	11091	100.0	4267	100.0	5376	100.0	8546	100.0	5715	100.0	8546	100.0	5715	100.0
Leave Magnet	9988	78.0	7674	69.2	1454	34.1	1960	36.5	8531	99.8	5715	99.8	8531	99.8	5715	100.0
Enter 1 m x 1 m ISIS at 2.1 m	8851	69.1	5638	50.8	782	18.3	733	13.6	8069	94.4	4905	85.8	8069	94.4	4905	85.8
Exit 1 m x 1 m ISIS at 5.3 m	6031	47.1	3003	27.1	139	3.3	154	2.9	5892	68.9	2849	49.9	5892	68.9	2849	49.9

Table V

Thresholds and Photoelectron Response (OSIRIS)

Assuming: 1 atmosphere, L = 5m length, and  $N(P) = 2A (n-1)[1-(P_T/P)^2]L$ , with  
 $A = 100 \text{ cm}^{-1}$  (Figure of Merit)  $n = \text{index of refraction}$  and  
 $P_T = \text{threshold momentum}$

Threshold, $P_T$ (GeV/c)			Gas Mix	Index	Momentum	# Photoelectrons (N)			Maximum Light Cone Radius
$p$	K	$\pi$	%He-%N <sub>2</sub>	$(n-1) \times 10^6$	P(GeV/c)	$N^\pi$	$N^K$	$N^p$	$R^\pi_{\text{max}}(\text{cm})$
116	61.0	17.3	100 - 0	32.7	100	3.2	2.1	0	4.0
					50	2.9			
					20	0.8			
100	52.6	14.9	95.5-4.5	44.02	100	4.4	3.2	0	4.7
					50	4.0			
					25	2.8			
					20	2.0			
					15	1.5			
70	36.8	10.4	77.5-22.5	89.83	100	8.9	7.8	4.6	6.7
					50	8.6	4.1		
					25	7.4			
					15	4.7			
					10	3.0			
55	29.0	8.3	55.3-44.7	145.5	100	14.5	13.4	10.2	8.5
					50	14.2	9.7		
					35	13.8	4.6		
					20	12.1			
					10	4.5			
39.3	20.7	5.9	0 - 100	285	100	28.4	27.3	24.1	11.9
					50	28.1	23.6	10.9	
					25	27.0	9.0		
					15	24.2			
					10	18.8			
					7	8.6			

Table VI

Estimates of Number of Events to be Obtained  
(With 6 Particles/Picture)

Pictures Beam	<u>Negative Beam</u>		<u>Positive Beam</u>		
	1,000,000		400,000		
	$\bar{p}p$ (a)	$\pi^-p$ (b)	$pp$ (c)	$\pi^+p$ (c)	$K^+p$ (c)
Events/ $\mu$ b	2.70	6.30	1.08	2.16	0.36
Total Events	113,510	151,830	41,500	50,400	6790
Total Inelastic	93,420	131,990	33,910	43,200	5840
Elastic	20,010	19,850	7,560	7,190	950
Inelastic 2 prong	9,720	12,290	5,300	5,140	840
Inelastic 4 prong	21,740	30,180	7,890	10,050	1260
Inelastic 6 prong	22,280	32,570	7,570	10,410	1120
Inelastic 8 prong	18,710	27,090	6,050	7,840	1360
Inelastic 10 prong	11,100	15,750	4,030	5,700	660
Inelastic 12 prong	5,910	8,880	1,830	2,700	360
Inelastic 14 prong	2,430	3,780	870	1,060	170
Inelastic 16 prong	970	840	230	280	--
Inelastic 18 prong	320	280	76	86	65
Inelastic 20 prong	110	90	11	43	--
Inelastic 22 prong	24	50	--	--	--
$K_S^0$	2,300	1,710	535	1,013	260
$\Lambda/\bar{\Lambda}$	1,570	1,080	350	325	43
$\gamma$	6,280	3,750	1,200	1,870	243
$\bar{p}p\pi^+\pi^-/pp\pi^+\pi^-/\pi^\pm p\pi^+\pi^-$	2,700	3,600	990	1,200	150
$4\pi/6\pi/8\pi$	<2/5/13	--	--	--	--
Total Annihilation	9,450	--	--	--	--

(a) Based on Ref. 2

(b) Based on E. L. Berger et al., Nucl. Phys. B77, 365 (1974)

(c) Based on Ref. 25 and W. M. Morse et al., Phys. Rev. D15, 66 (1977)

Table VII

Detection Efficiencies for Individual Particles in  $\bar{p}p$  Interactions

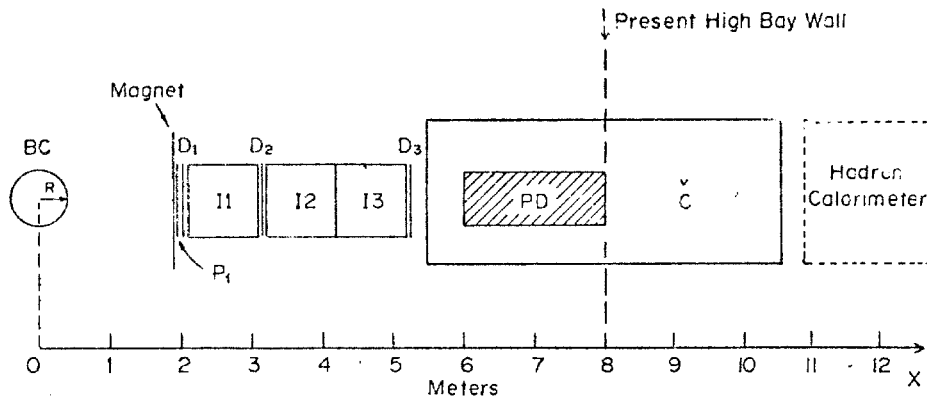
<u>Particle</u>	<u>Efficiency</u>	<u>Detector</u>	<u>Value</u>
$\bar{p}$	$\epsilon(\bar{p})$	OSIRIS	$\sim 97\%$
$\bar{n}$	$\epsilon(\bar{n})$	$\bar{n}$ Detector	$\sim 90\% \times 90\% = \sim 81\%$
$\pi^\pm$	$\epsilon(\pi)$	ISIS and OSIRIS	$\sim 36\%$ (of forward hemisphere)
		ISIS	$\sim 53\%$ (of forward hemisphere)
p	$\epsilon(p)$	30-inch B.C.	$\sim 70\%$

Table VIII

Overall Efficiency for Tagging Nonannihilation Events

<u>Reaction</u>	<u>Relative Abundance*</u>	<u>Efficiency X Rel. Abundance</u>
$\bar{p}pX$	0.49	$(1-0.03 \times 0.30)0.49 = 0.49$
$\bar{p}nX$	0.21	$0.97 \times 0.21 = 0.21$
$\bar{n}pX$	0.21	$(1-0.30 \times 0.19)0.21 = 0.20$
$\bar{n}nX$	0.09	$0.81 \times 0.09 = 0.07$
TOTAL	1.00	0.97

\*Assuming  $\bar{p}:\bar{n} = 0.7:0.3$ .



The particle identification system proposed in the recommendations of the workshop for the Fermilab 30 inch bubble chamber hybrid system. I1, I2, and I3 are 1m x 1m x 1m ISIS-type modules. (Since the time of the workshop it has been decided to combine I2 and I3 into a single 1m x 1m x 2m module I2'.) C is a 2m x 2m x 5m 8-cell Cerenkov detector; P1 is a proportional wire counter; and D1, D2, and D3 are drift chambers. The locations of the photon detector (PD) and the neutral particle calorimeter for  $\bar{n}$  and photon detection are also shown.

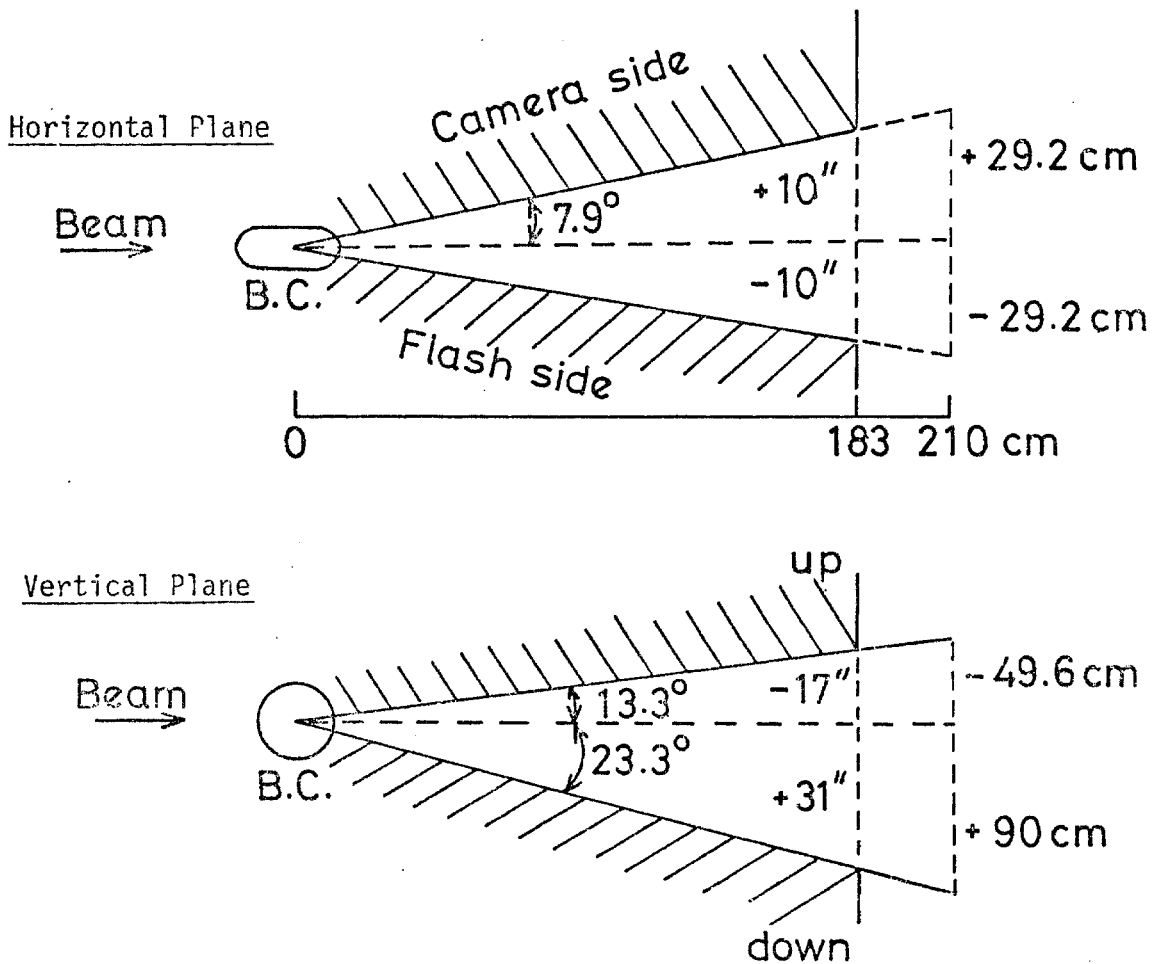


Fig. 1

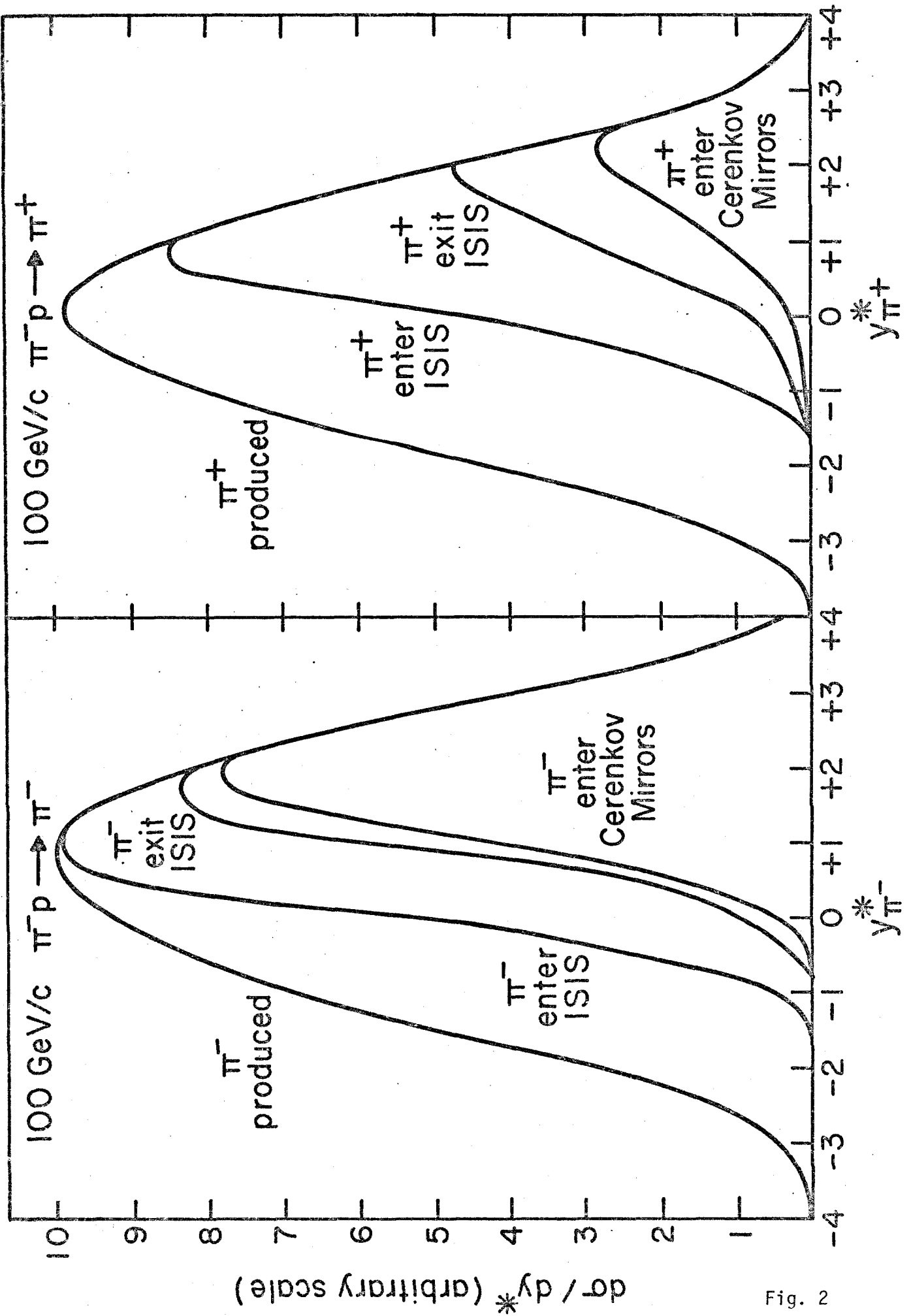


Fig. 2

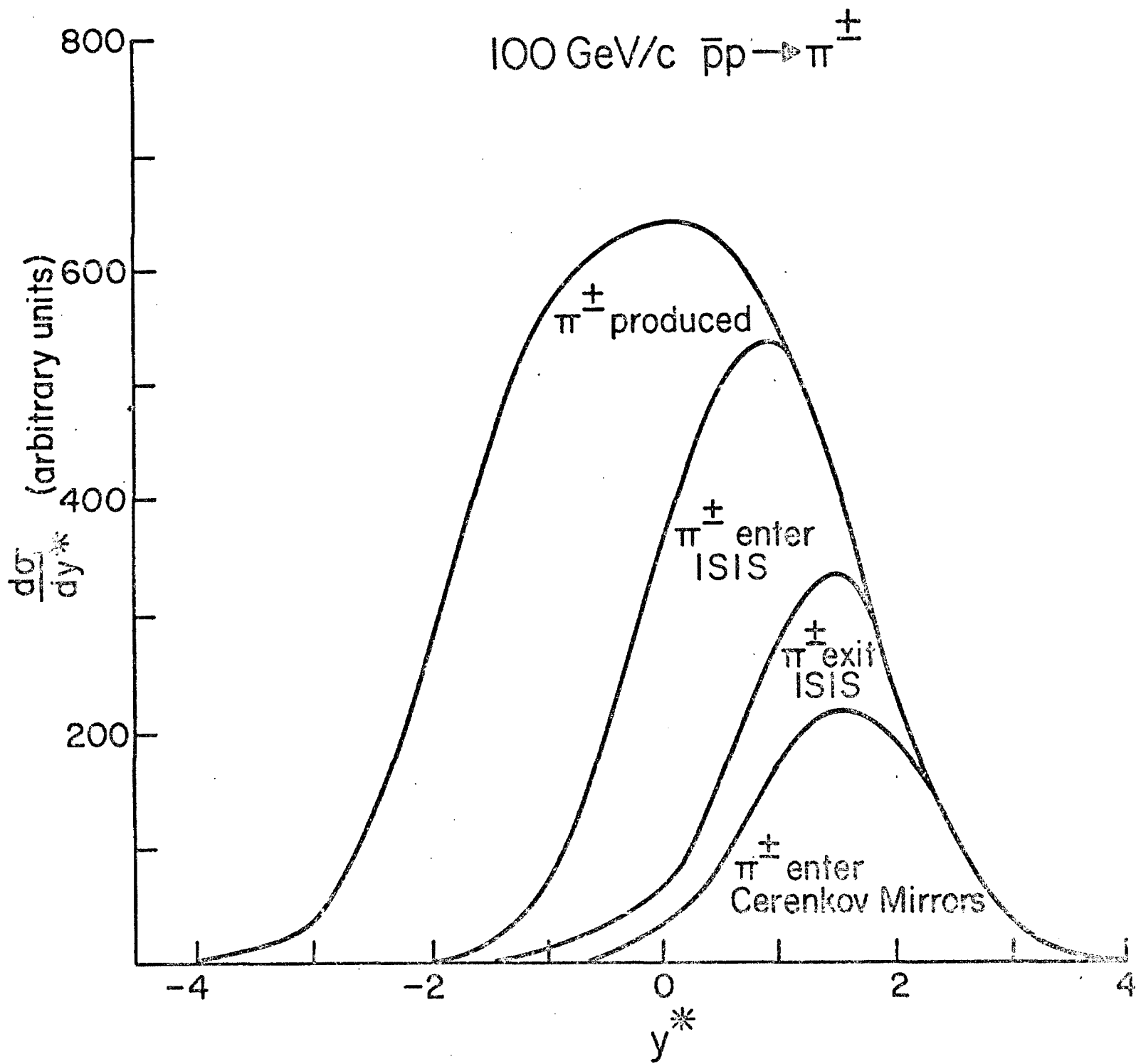


Fig. 3

### 4 prong event

A typical four-prong event as "seen" by the DPI after the tracks have been swum through the fringe field.

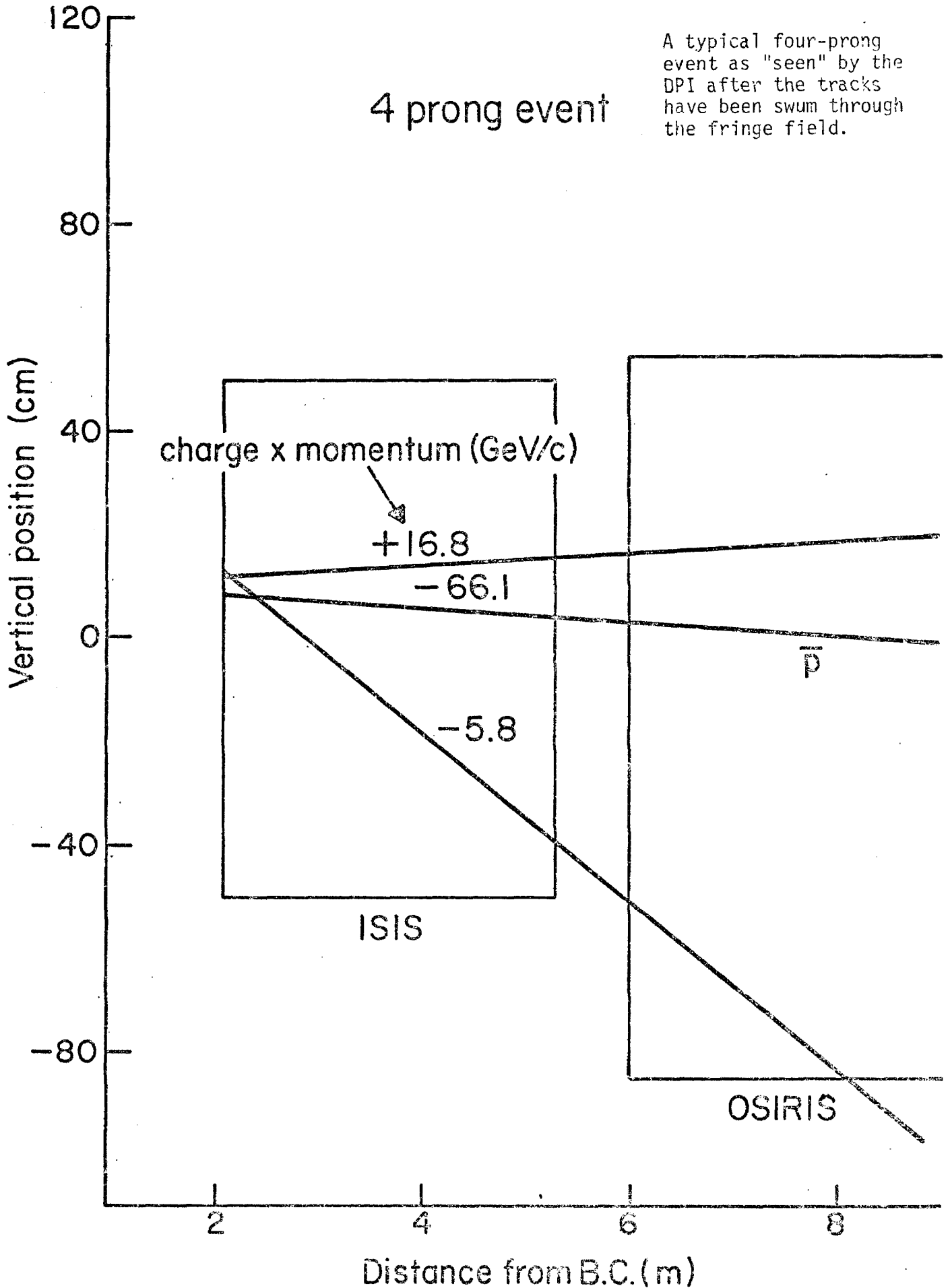


Fig. 4a

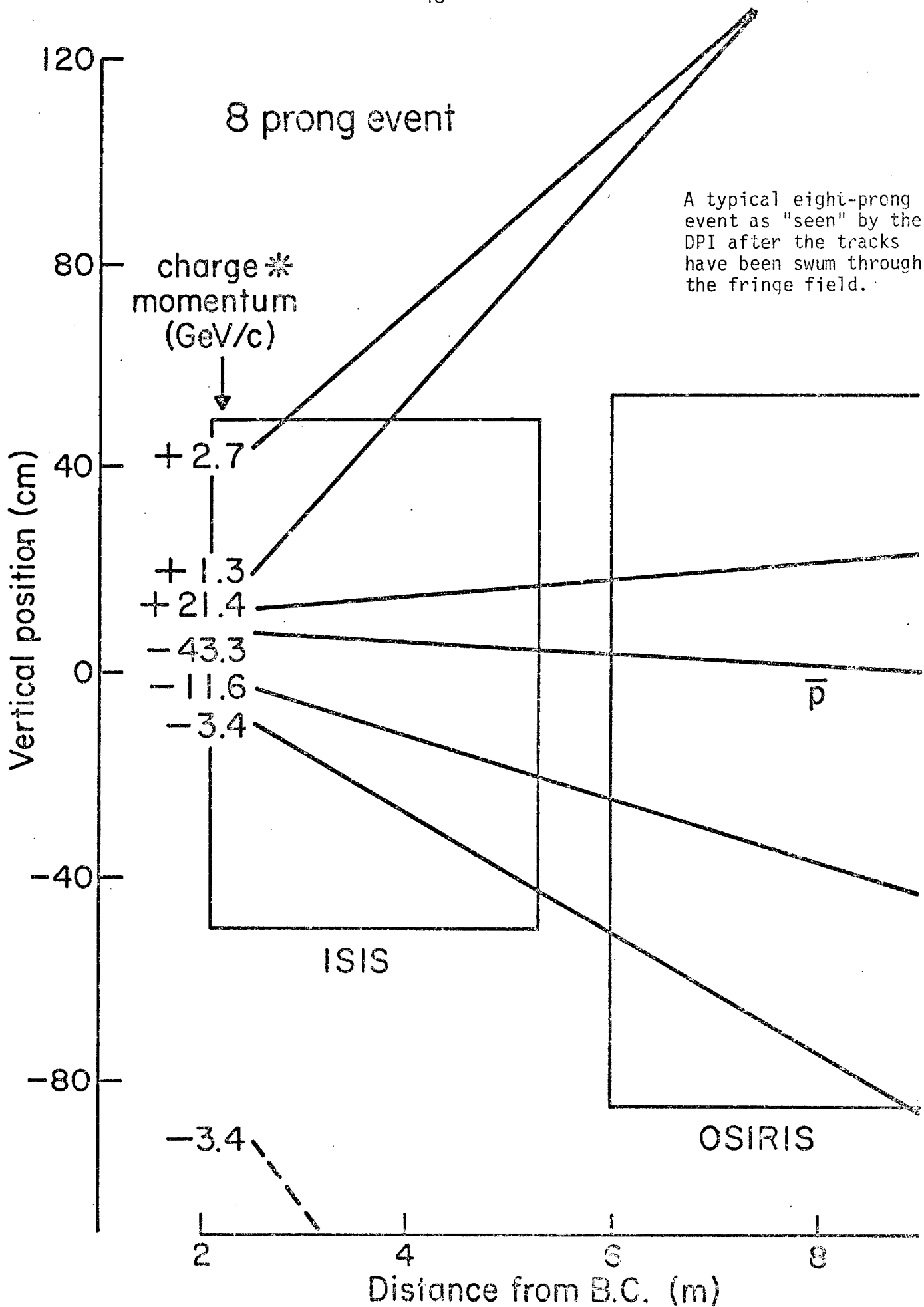


Fig. 4b

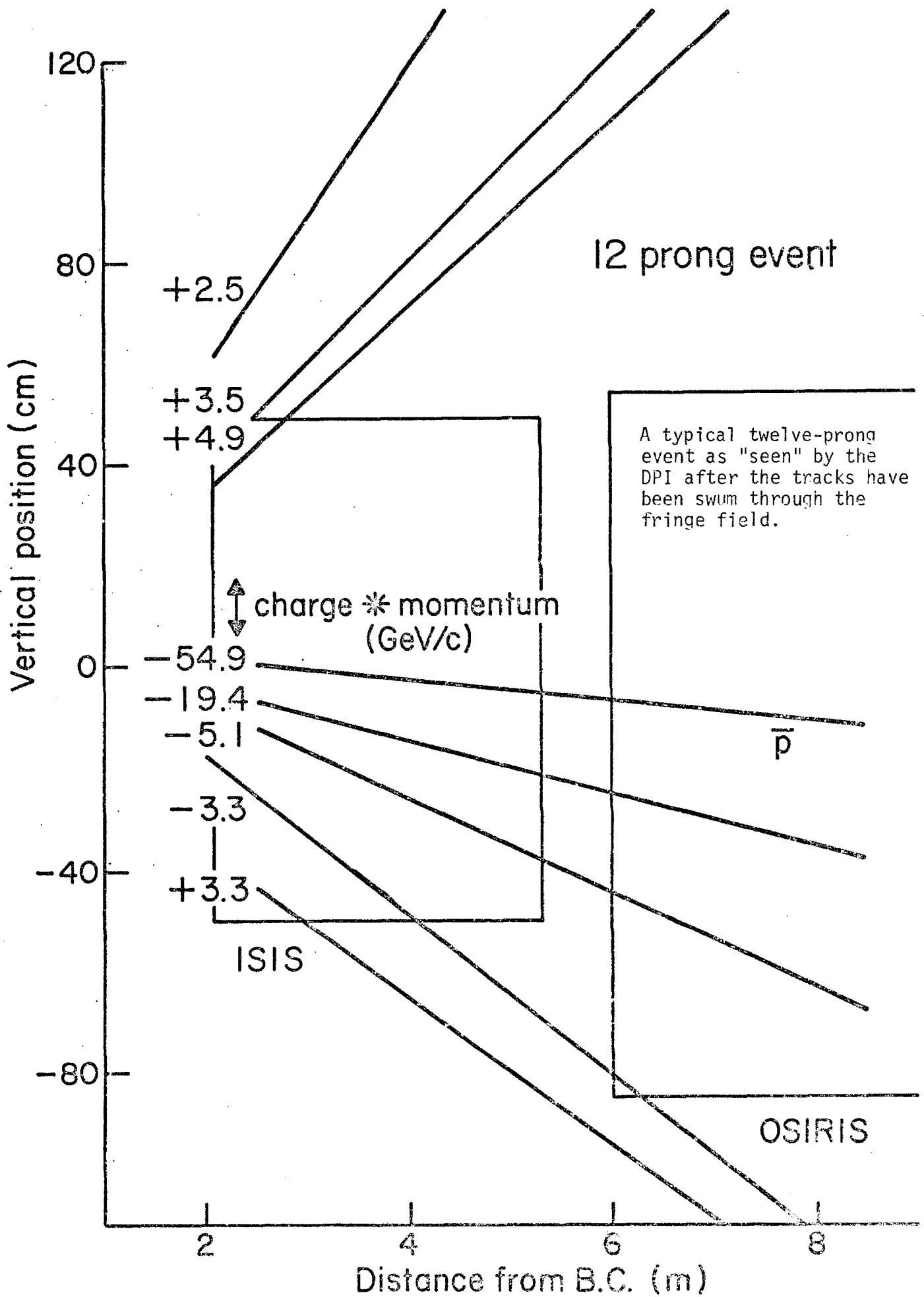


Fig. 4c

100 GeV/c  $\bar{p}p \rightarrow \bar{p} + X$

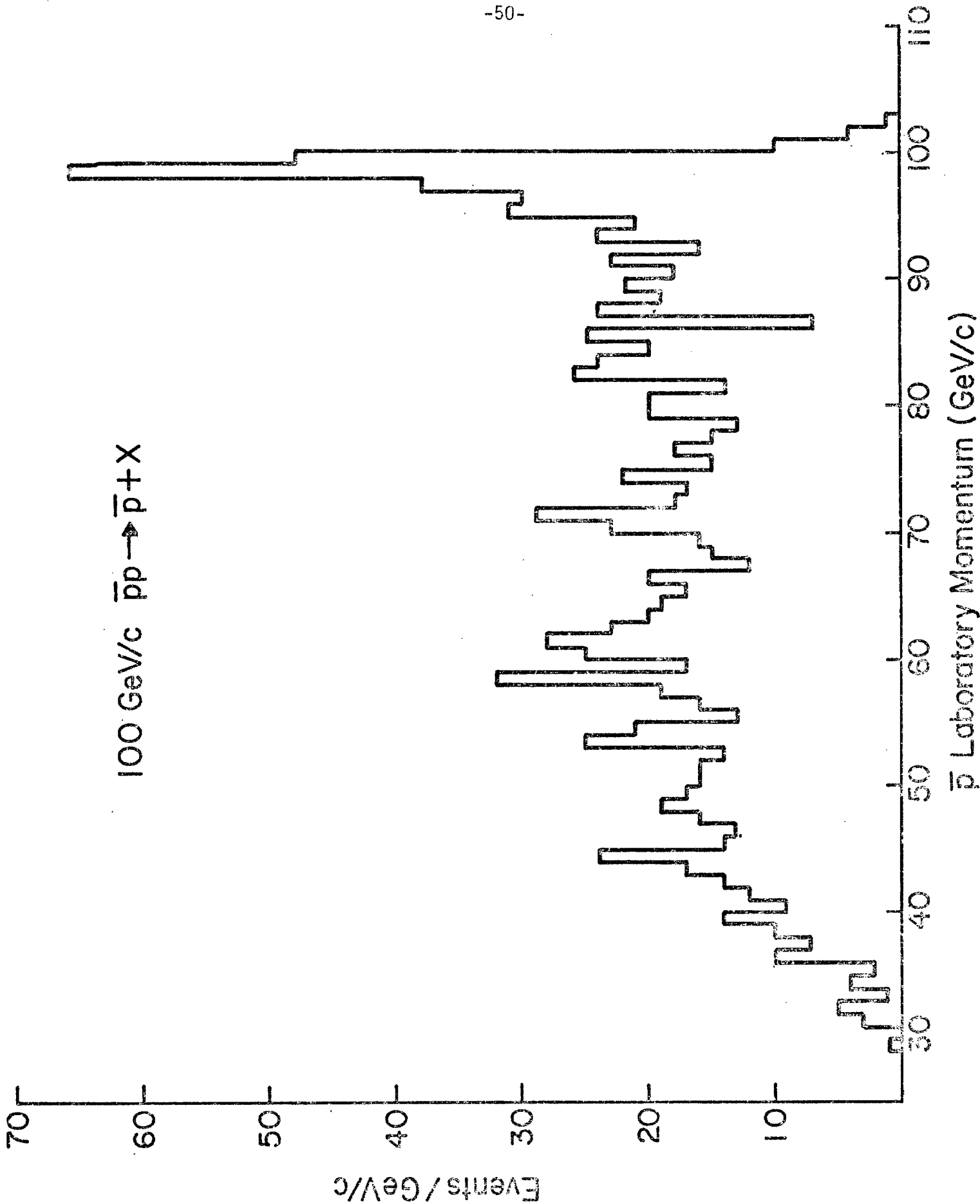
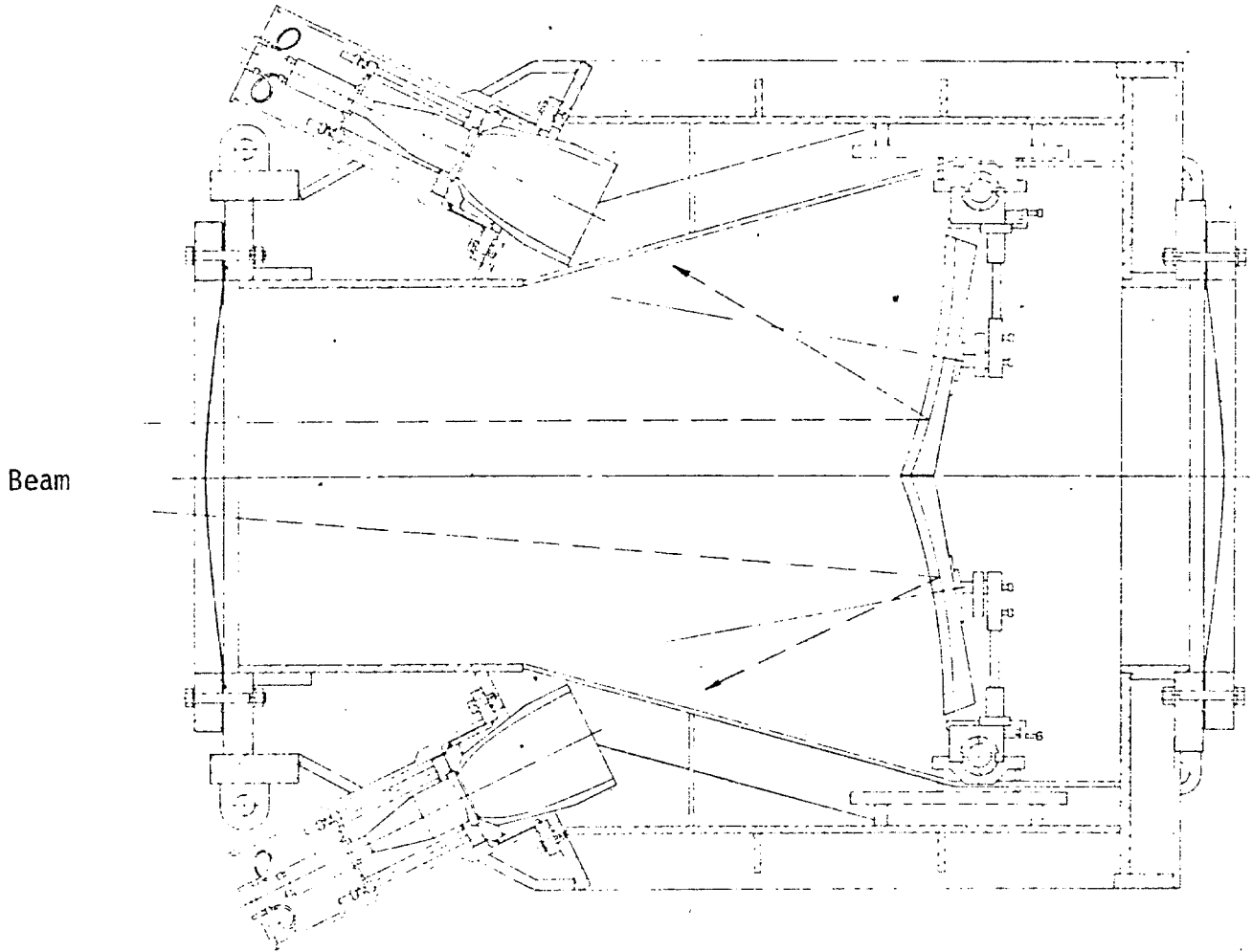


Fig. 5

Horizontal Plane



70 cm

70 cm

Schematic Beam  
View of Mirrors

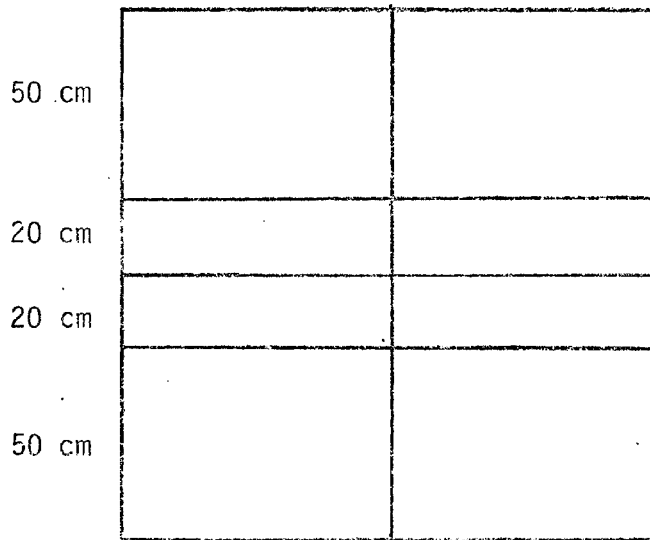
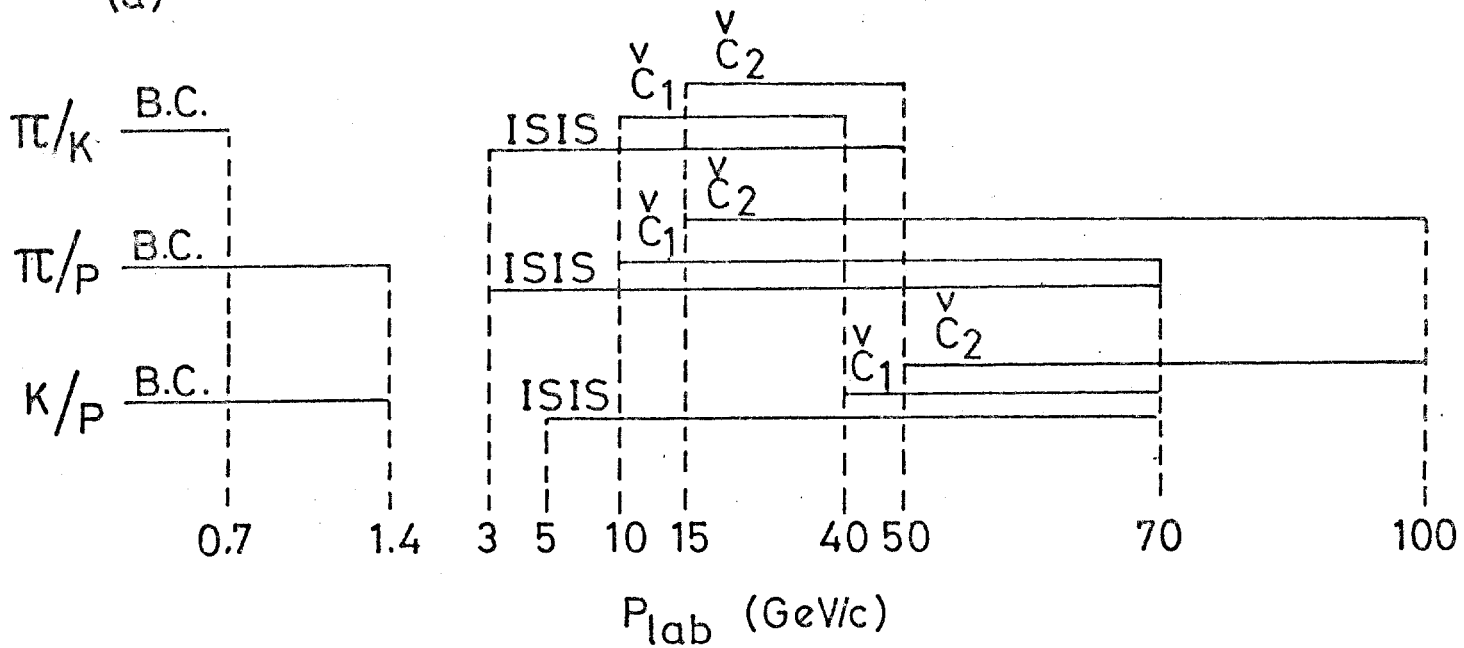


Fig. 6

(a)



(b)

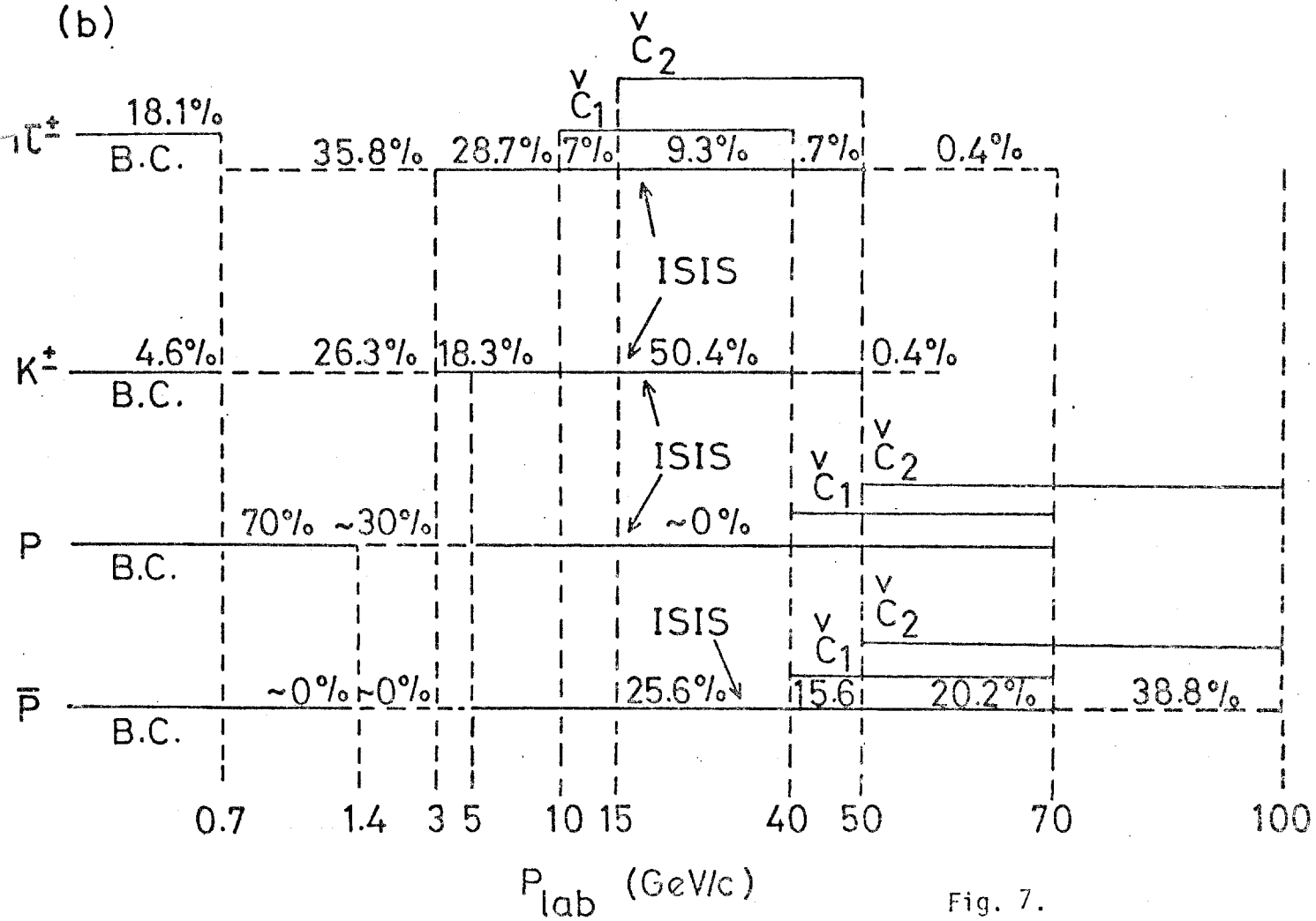


Fig. 7.

### Estimated Laboratory Distributions for $\bar{p}p \rightarrow \bar{n} X$ at 100 GeV/c

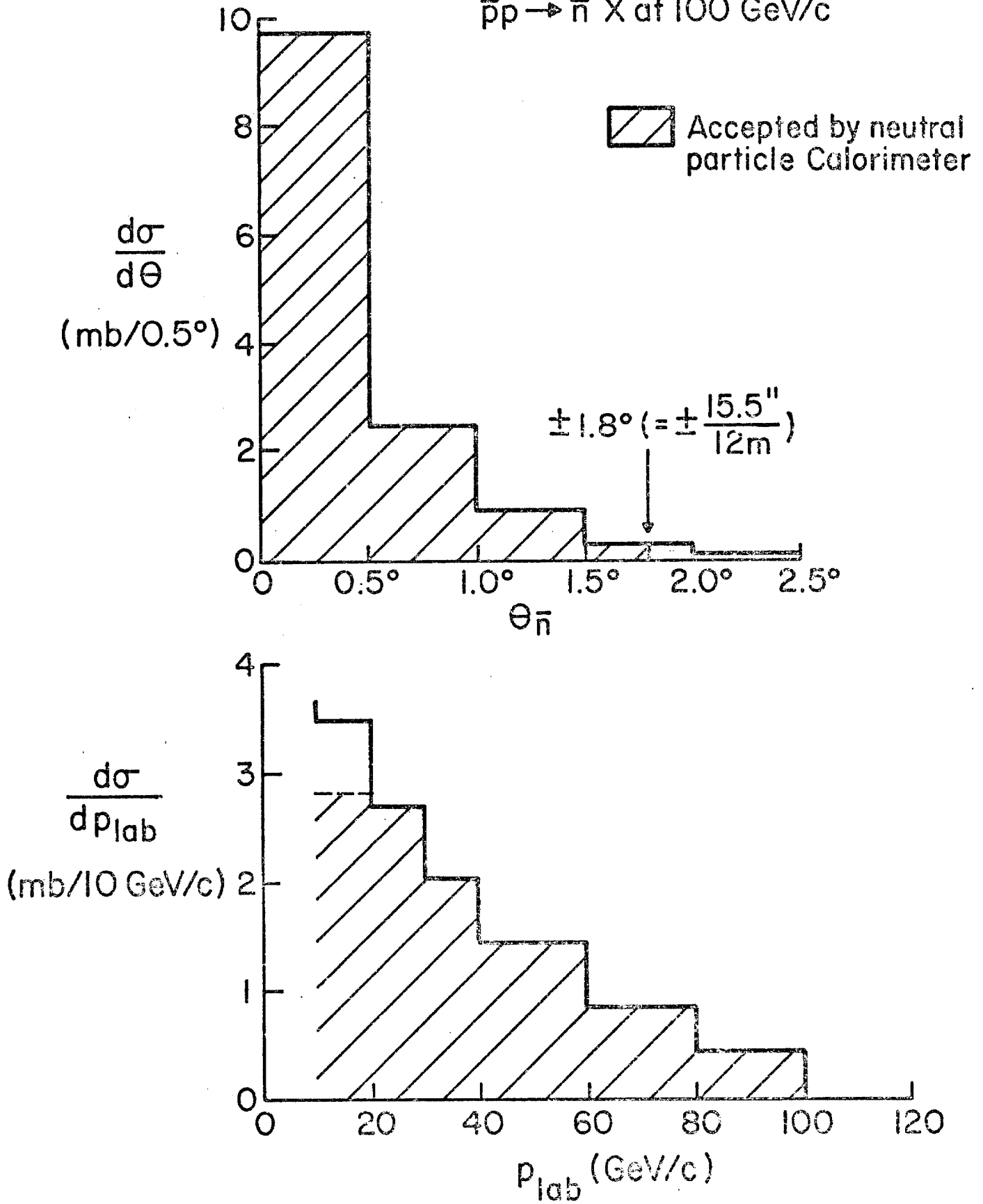
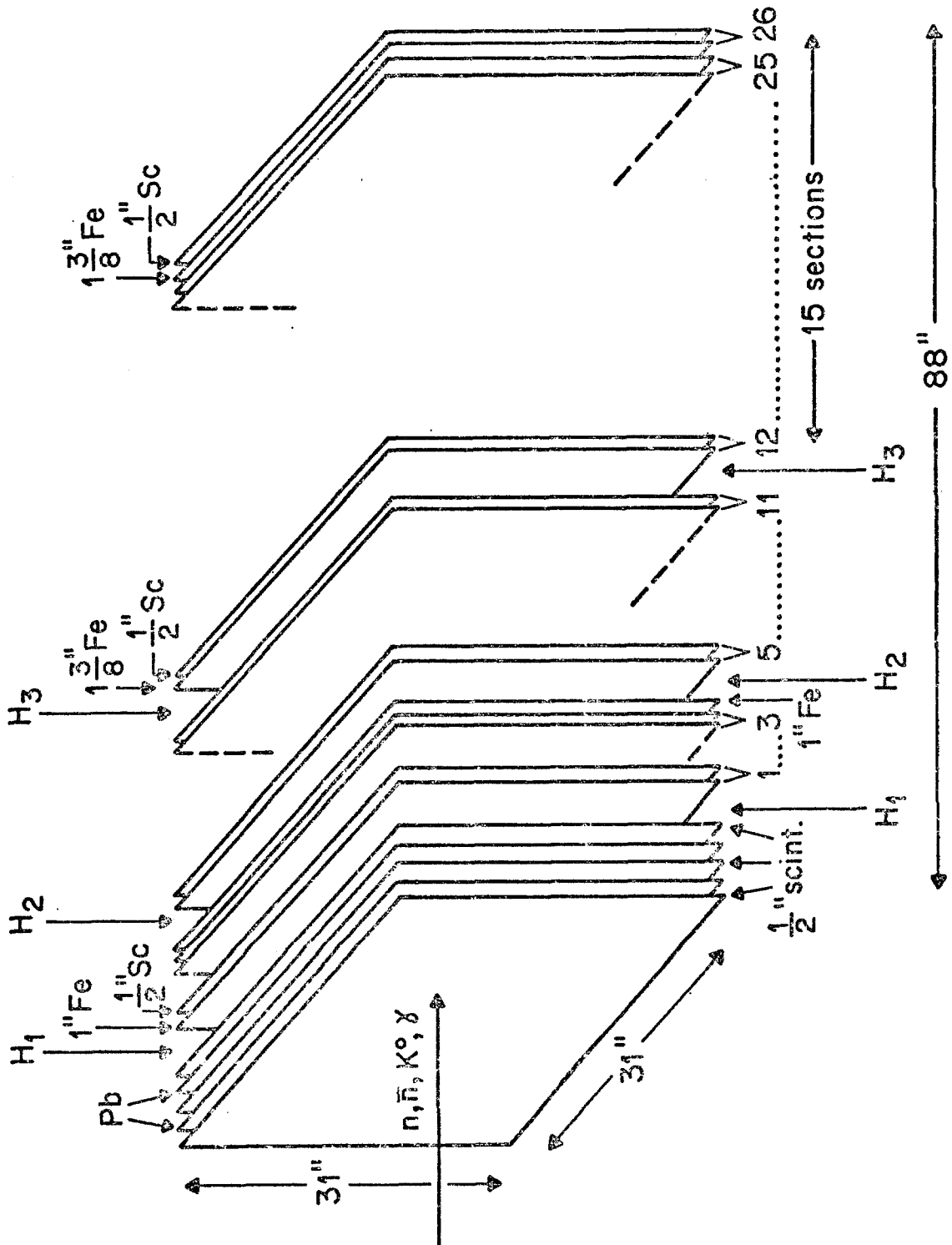


Fig. 8



Schematic view of neutral hadron calorimeter for SLAC BC-64. For P-394 H<sub>1</sub>, H<sub>2</sub>, H<sub>3</sub> will be expanded to a 15 x 15 matrix and placed consecutively behind the Pb in a X-U-V pattern.

Fig. 9

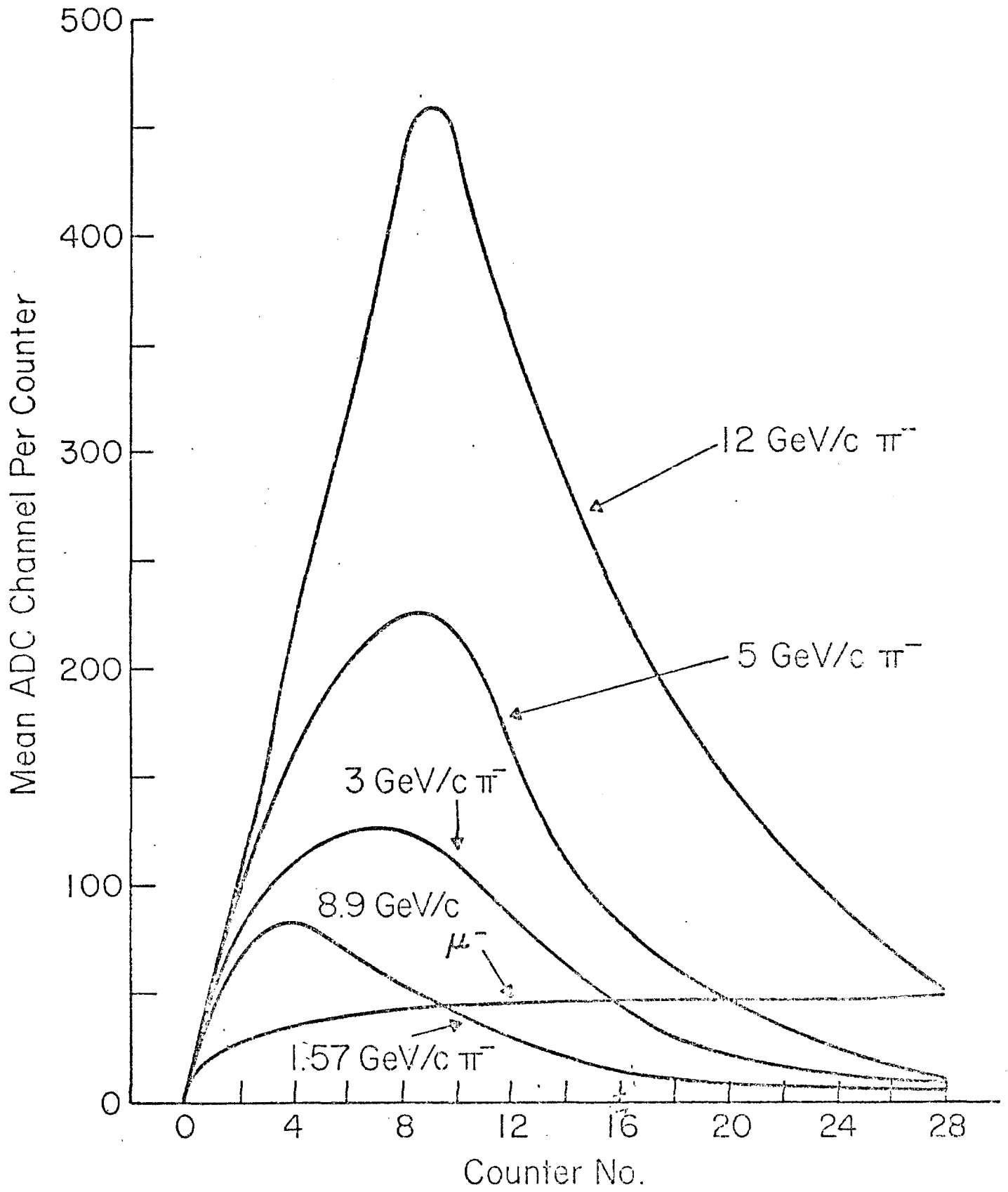


Fig. 10

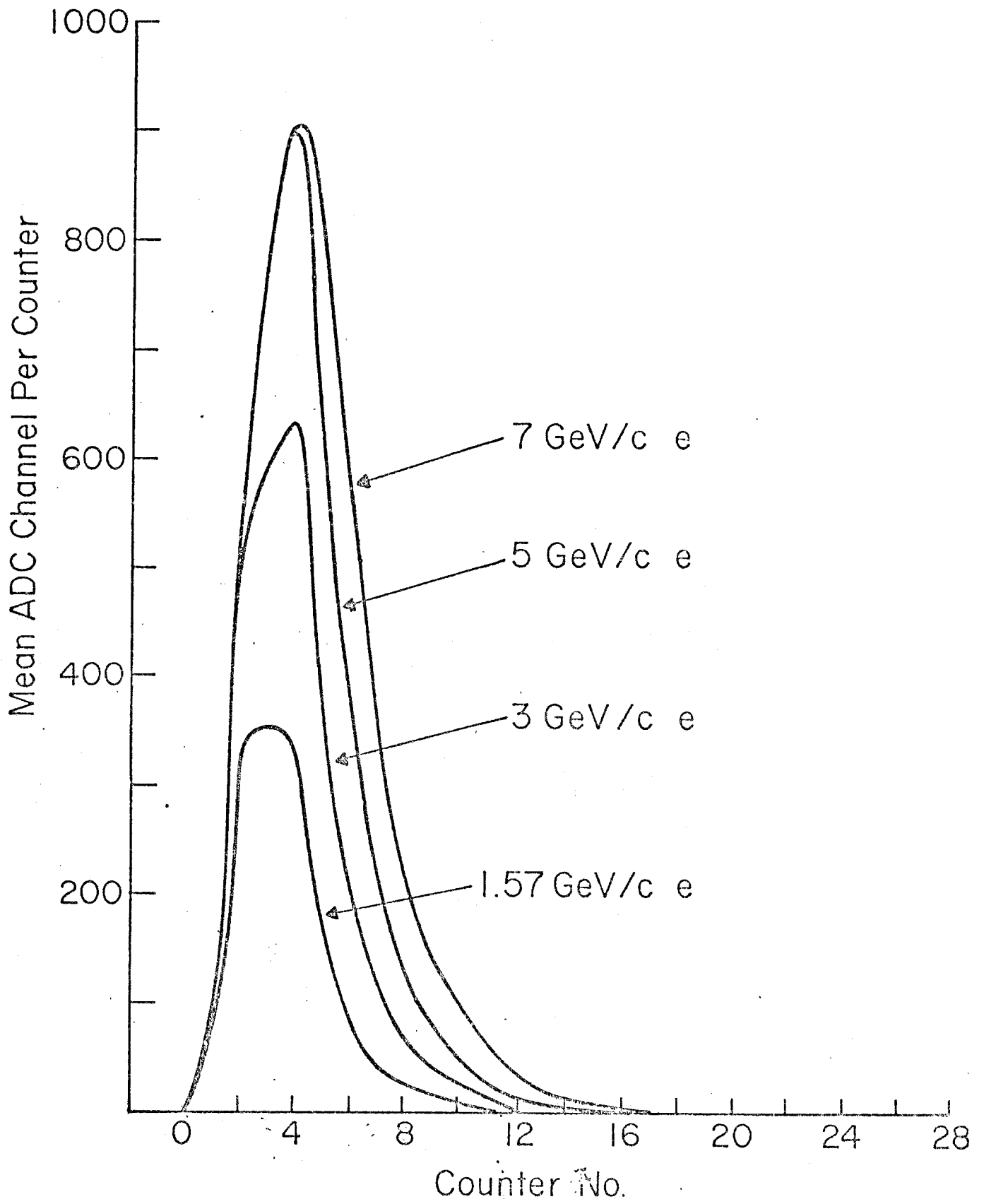


Fig. 11

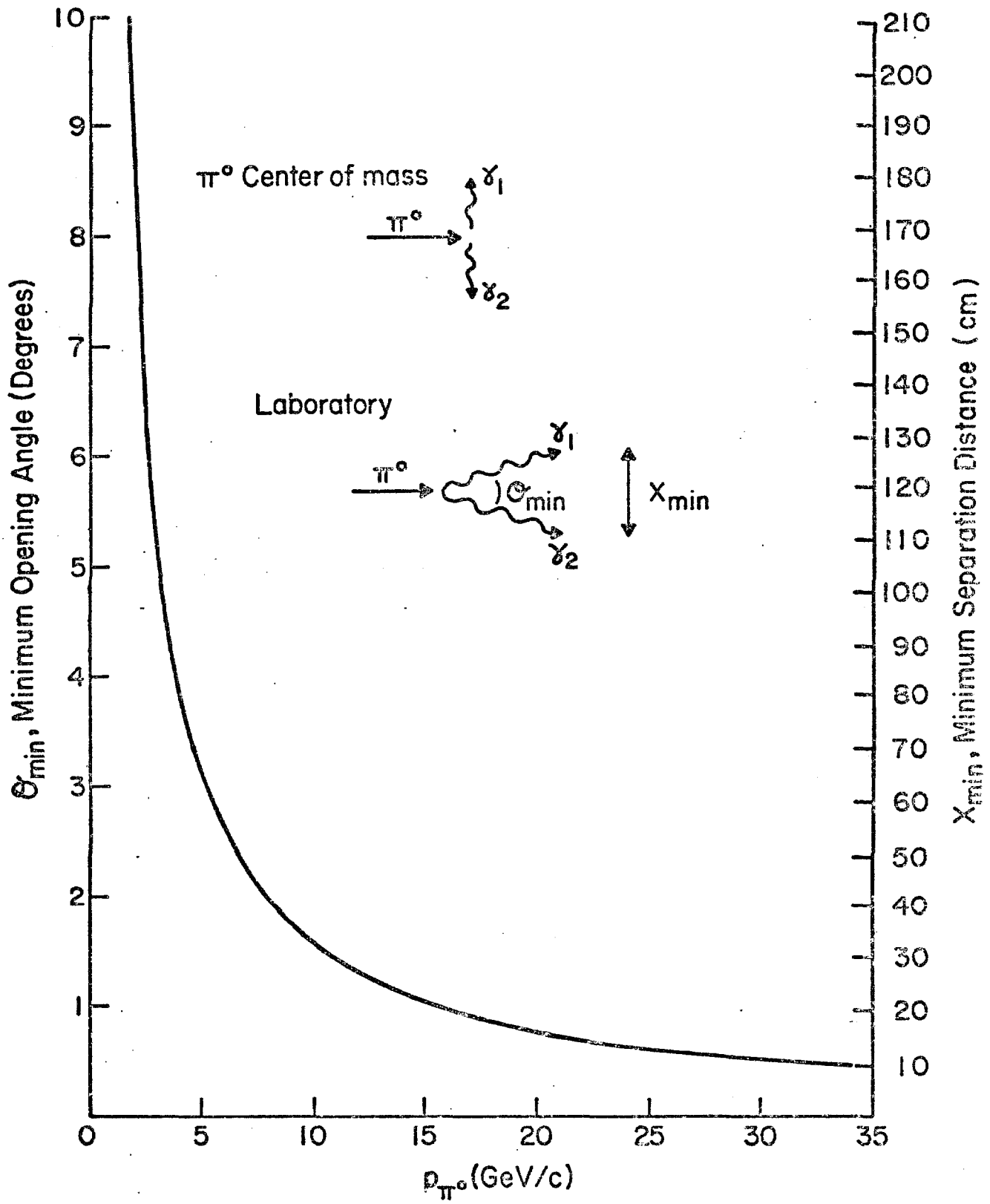


Fig. 12

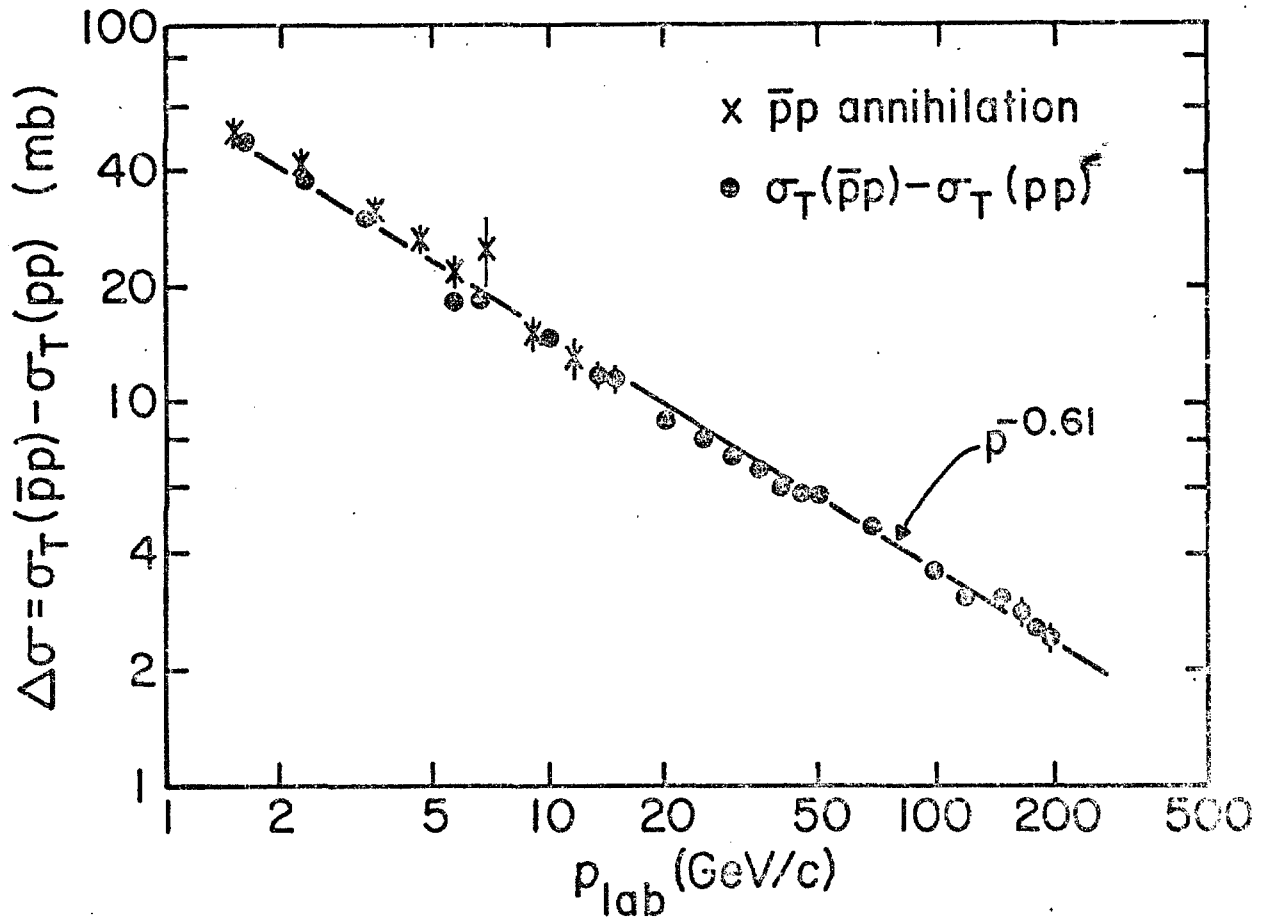


Fig. 13. Difference in total cross section for  $\bar{p}p$  and  $pp$  interactions as a function of the incident beam momentum. Also shown is the measured annihilation cross section at low energies (see J. Whitmore, proceedings of the APS/DPF Meeting, Seattle, 1975).

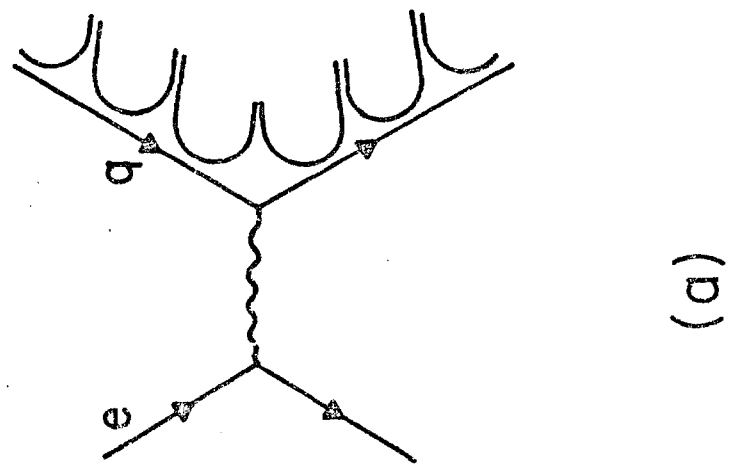
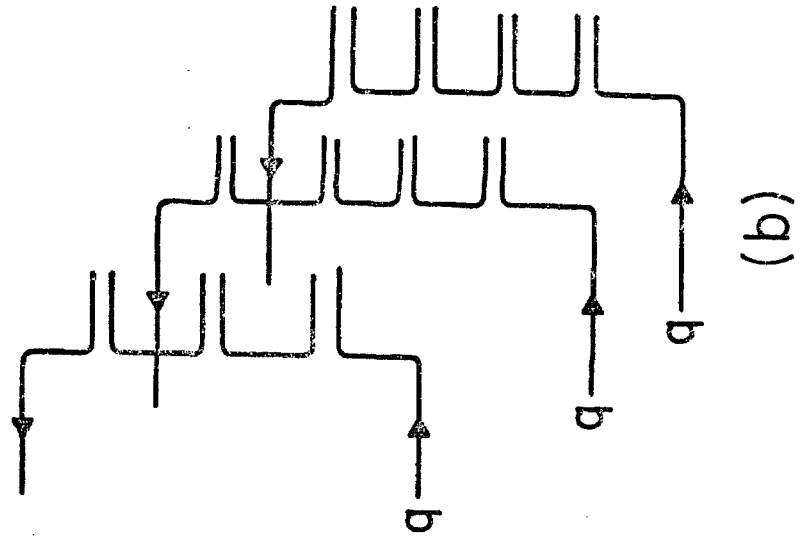


Fig. 14

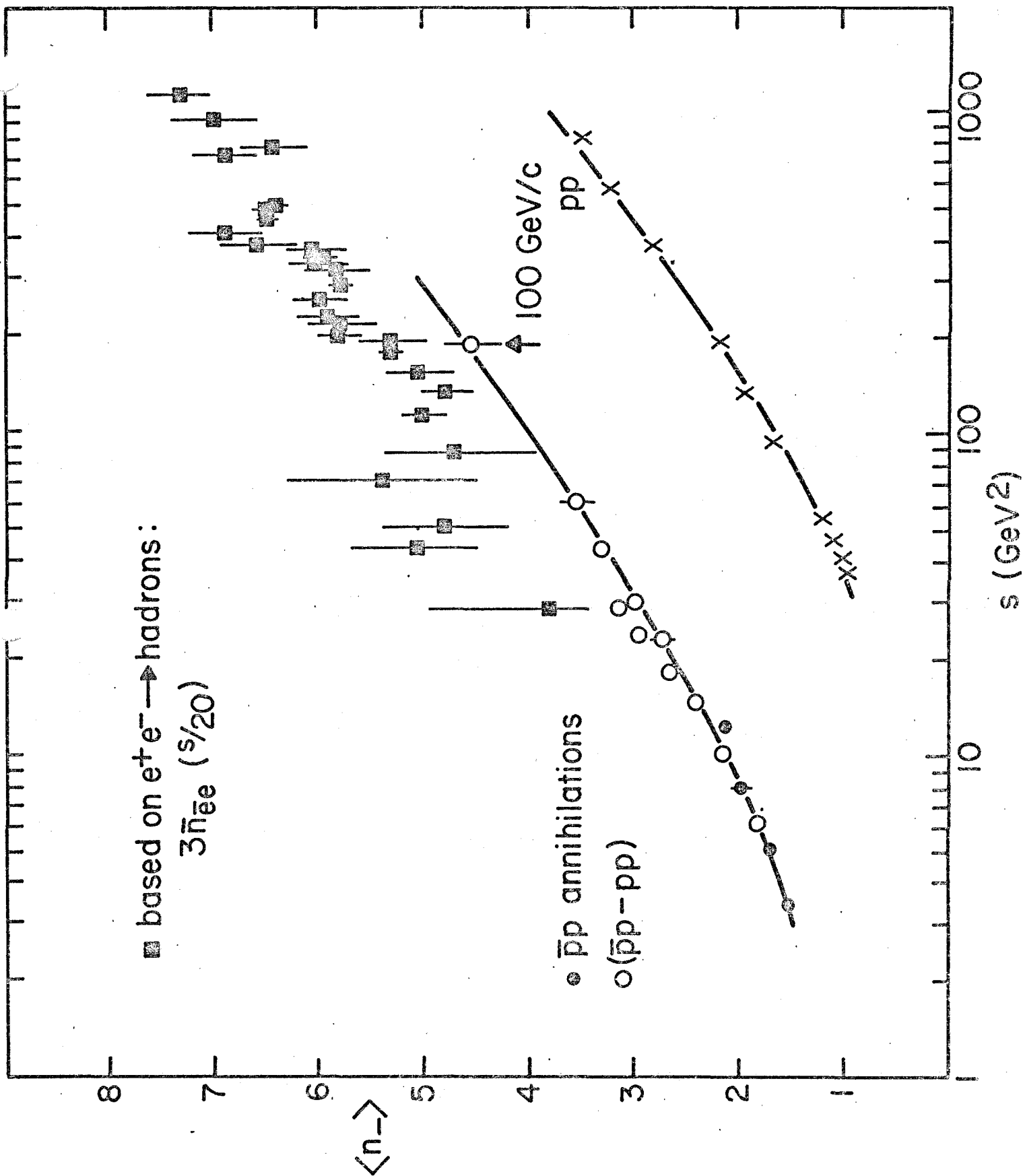


Fig. 15

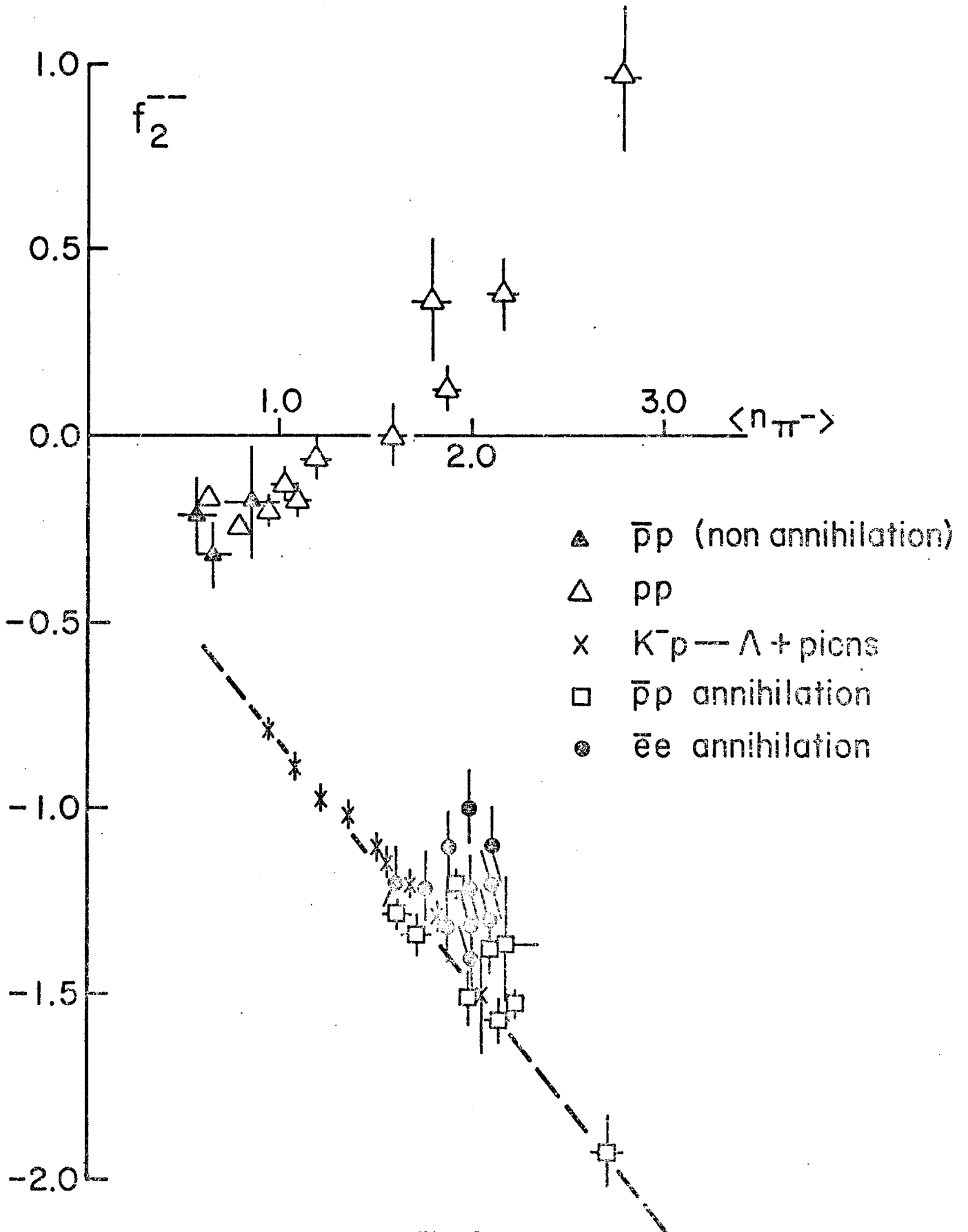


Fig. 16

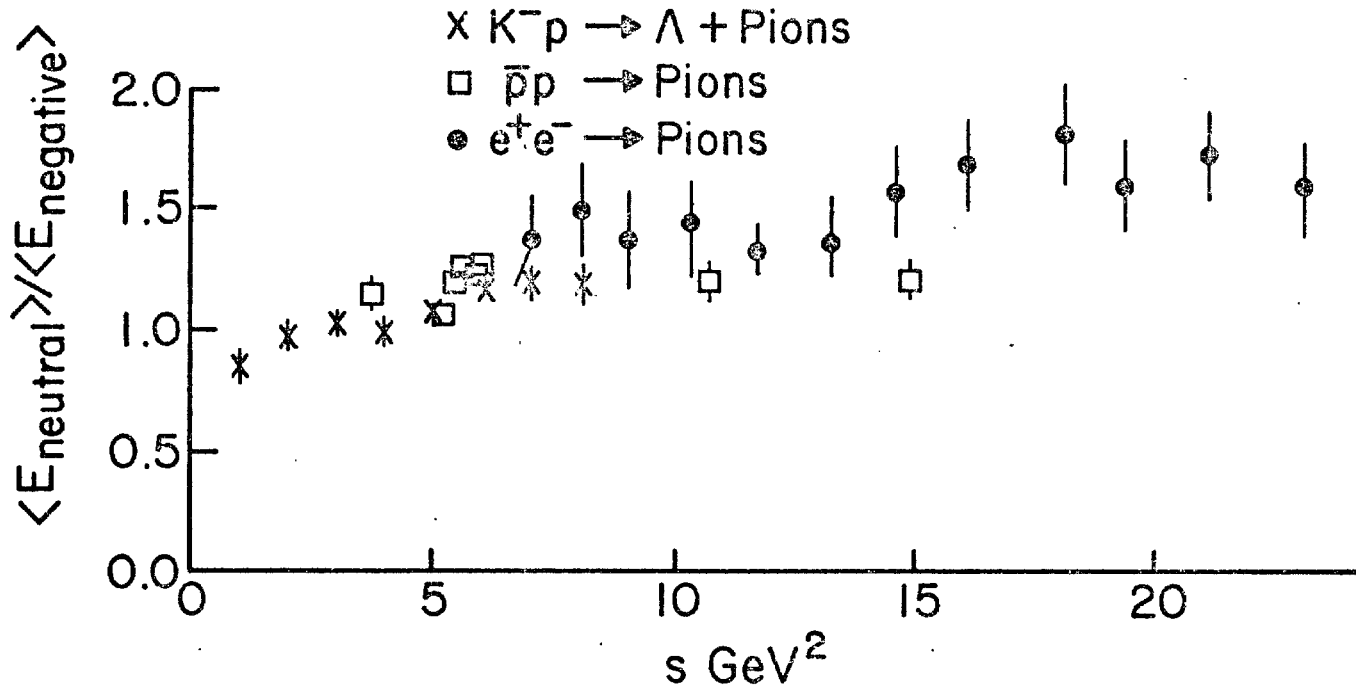


Fig. 17

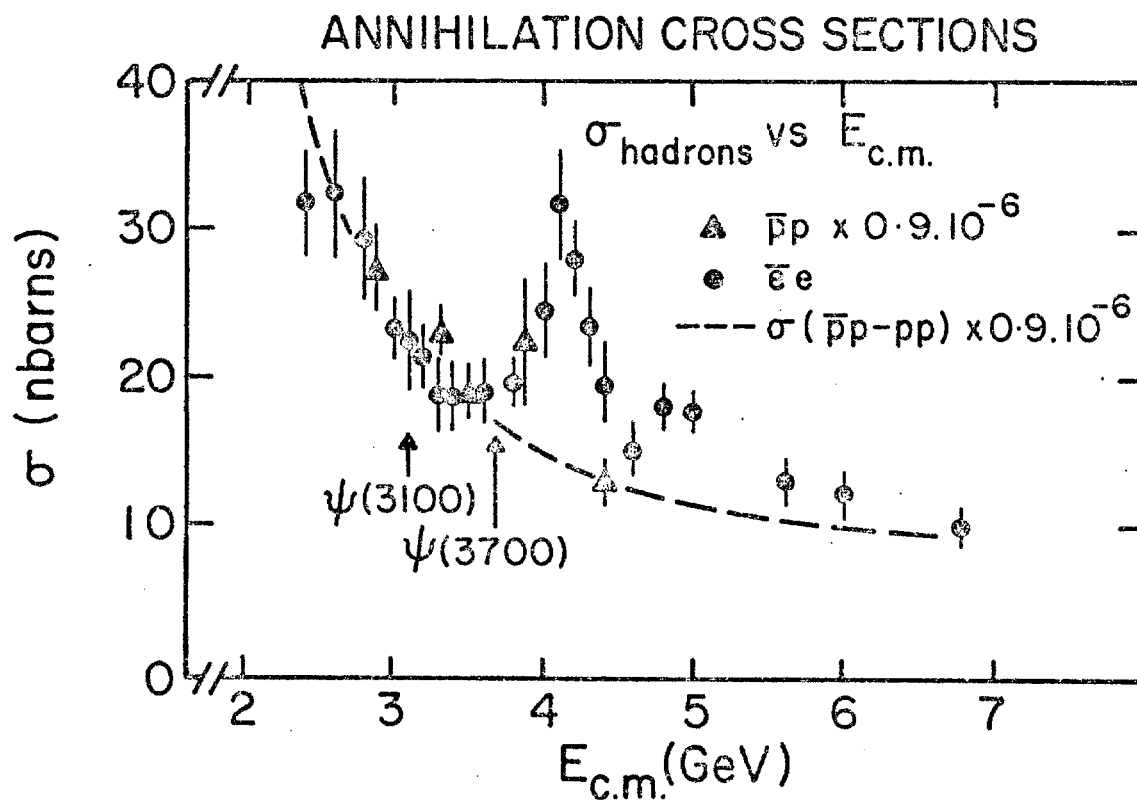


Fig. 18

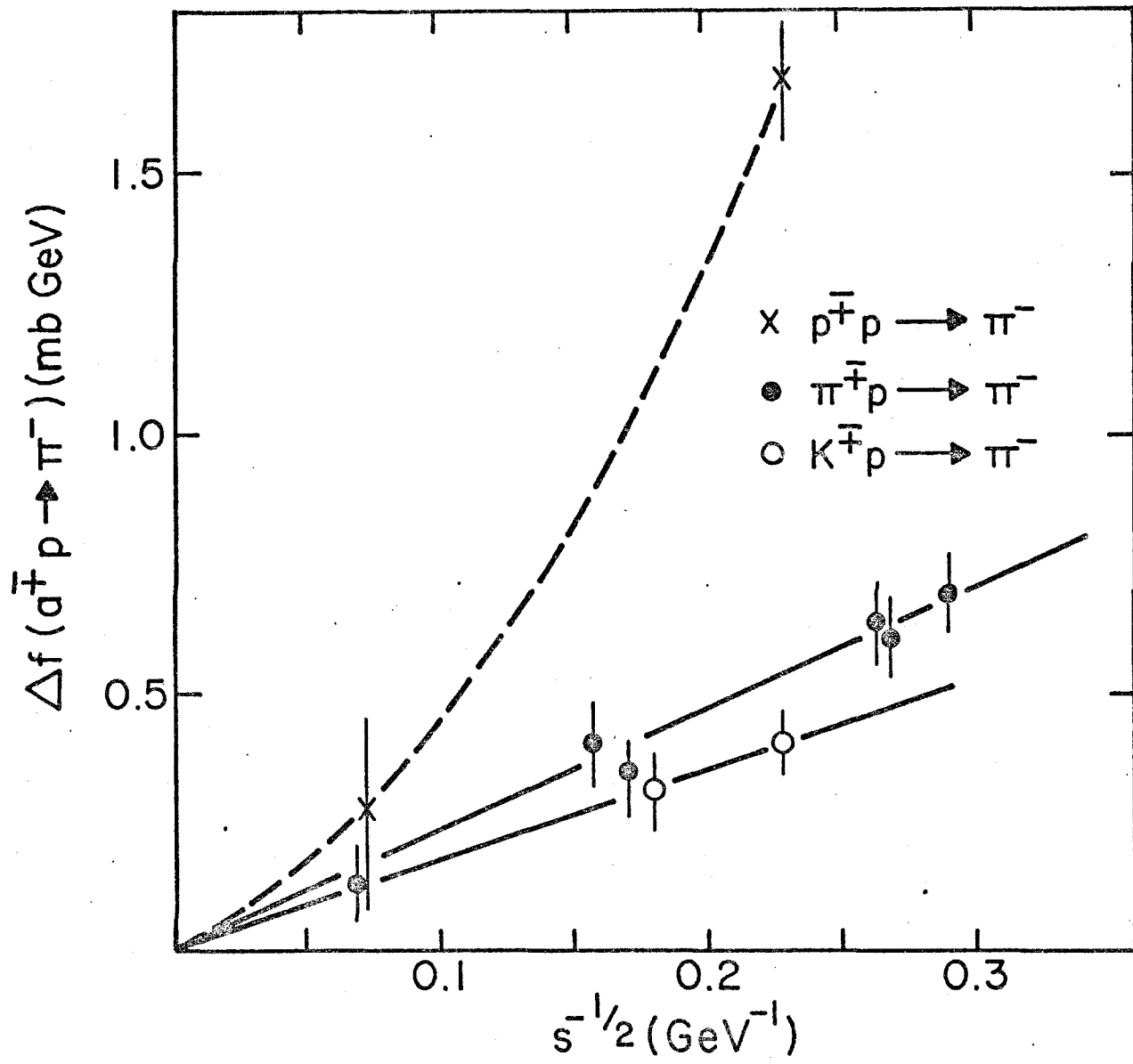


Fig. 19

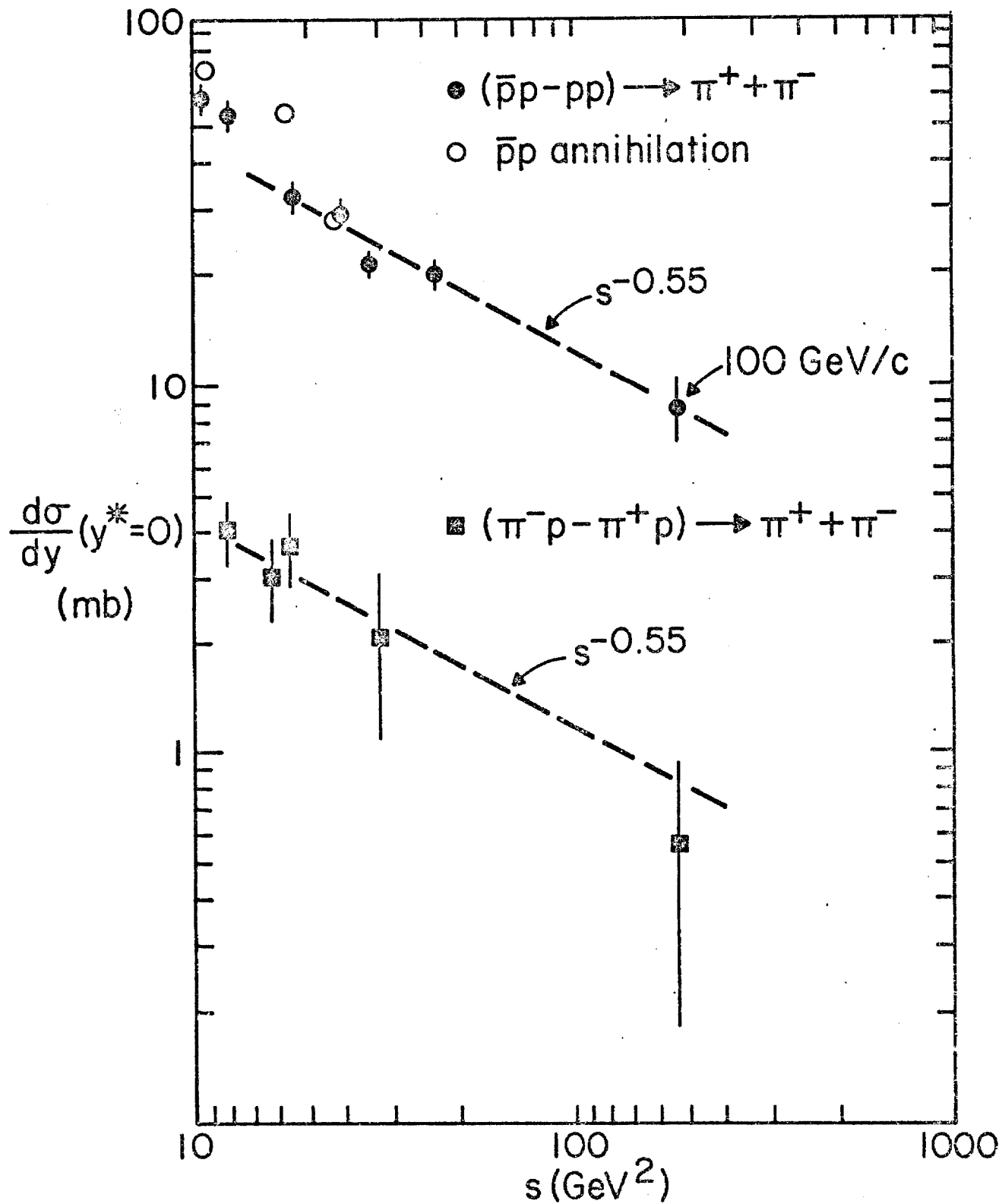


Fig. 20

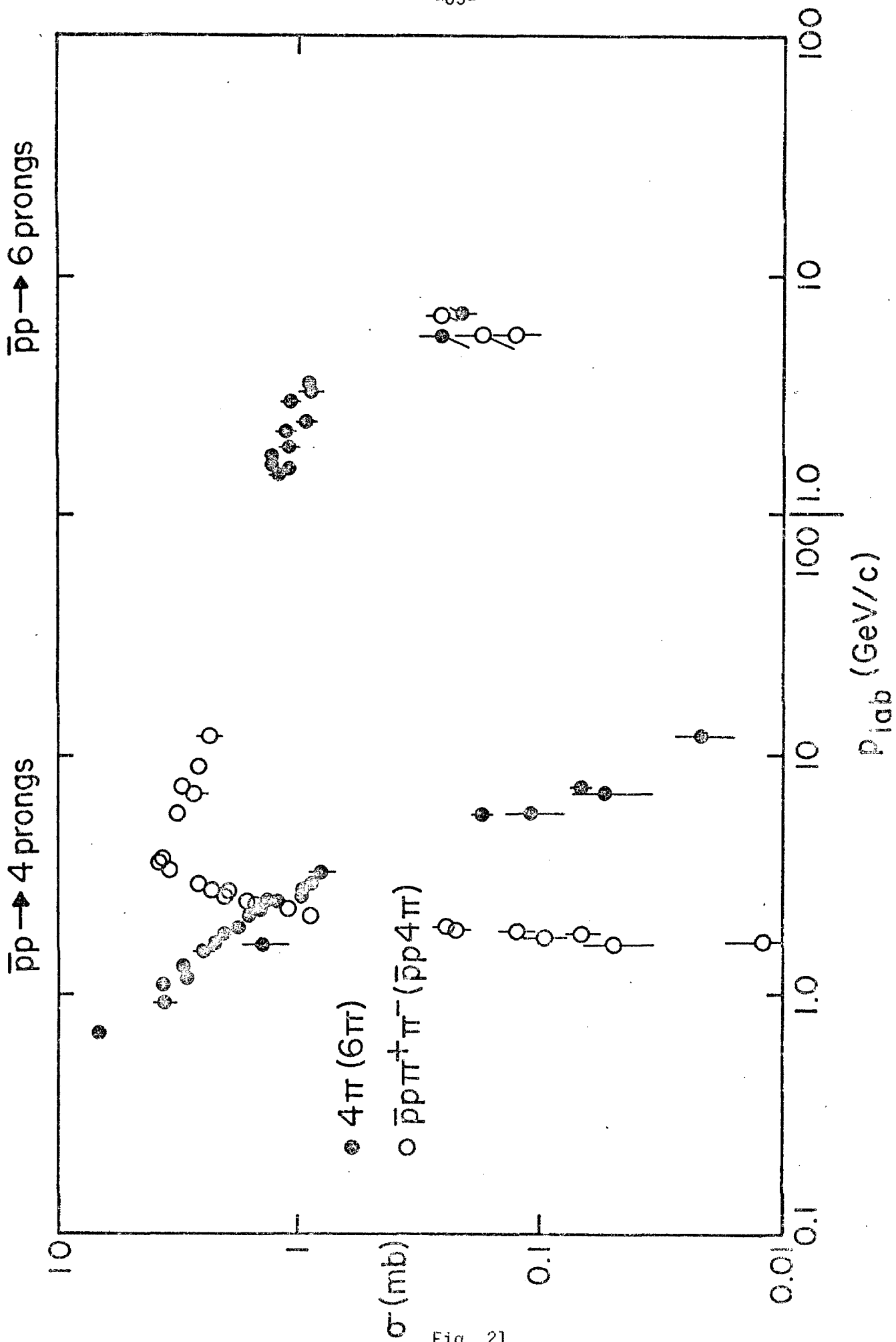


Fig. 21

Compilation of Refereed Journal Publications  
from  
Experiments 2B and 281  
(Spokesman: G. Smith)

Experiment 2B

1. "Study of the Energy and Charged Multiplicity Dependence of Inclusive  $\pi^-$  Production in  $\pi^-p$  Interactions up to Fermilab Energies", W. Morris et al., Phys. Letters 56B, 395 (1975).
2. "Two Particle Correlations in the Central Region of pp and  $\pi^-p$  Interactions at 100-300 GeV/c", B. Y. Oh et al., Phys. Letters 56B, 400 (1975).
3. "Two-Particle Correlations in Inclusive and Semi-Inclusive  $\pi^-p$  Reactions at 200 GeV/c", N. N. Biswas et al., Phys. Rev. Letters 35, 1059 (1975).
4. "Study of the Approach to Scaling and Factorization in Proton Fragmentation into  $\pi^+$ ", J. Whitmore et al., Phys. Letters 60B, 211 (1976).
5. "Three and Higher Order Rapidity Distributions in pp Collisions at 200 GeV/c", M. Pratap, et al., Nucl. Phys. B116, 1 (1976).
6. "Semi-Inclusive  $\pi^-$  Cross Sections in pp Interactions up to 300 GeV/c", B. Y. Oh et al., Nucl. Phys. B116, 13 (1976).
7. " $\pi^-p$  Charge-Transfer Cross Sections at 205 GeV/c, and an Apparent Universality of the Charge-Transfer Spectrum", G. Levman et al., Phys. Rev. D14, 711 (1976).
8. "Study of the Charge Structure of Events Produced in 200 GeV/c  $\pi^-p$  Collisions", V. A. Sreedhar et al., Phys. Rev. D14, 2894 (1976).
9. "Observation of a Universal Charge Exchange Dependence Across Rapidity Gaps in 200 GeV/c  $\pi^-p$  Interactions", J. W. Lamsa et al., Phys. Rev. Letters 37, 73 (1976).
10. "Direct Evidence for the Bose-Einstein Effect in Inclusive Two-Particle Reaction Correlations", N. N. Biswas et al., Phys. Rev. Letters 37, 175 (1976).
11. "Evidence for Local Compensation of Transverse Momentum in pp Collisions at 200 and 300 GeV/c", D. Weingarten et al., Phys. Rev. Letters 37, 1717 (1976).
12. "Inclusive  $\Delta^{++}$  (1236) Production in the 200 GeV/c  $\pi^-p$  Reaction", N. N. Biswas et al., Phys. Rev. D15, 2090 (1977).
13. Comparison of Inclusive Charged-Pion Production in  $\pi^\pm p$  Interactions at 100 GeV/c", J. Whitmore et al., Phys. Rev. D, (to be published) (1977).

Experiment 281

1. " $\pi^-p$  Interactions at 360 GeV/c: Measurement of the Total and Elastic Cross Sections and the Charged-Particle Multiplicity Distribution", A. Firestone et al., Phys. Rev. D14, 2902 (1976).
2. "Direct  $e^+e^-$  Pair Production by 360 GeV/c  $\pi^-$  in Hydrogen", E. W. Anderson et al., Phys. Rev. Letters 37, 1593 (1976).

Published Conference Proceedings from  
Experiments 2B, 281

1. "The NAL 30-inch Bubble Chamber-Wide Gap Spark Chamber Hybrid System", G. A. Smith, Proceedings of the Berkeley Meeting of APS/DPF, Berkley (1973), p. 500.
2. "Leading Clusters in 200 GeV/c  $\pi^-p$  Interactions", V. P. Kenney, Proceedings of the EPS International Conference, Palermo (1975), p. 815.
3. "Two Particle Correlations in the Central Region of pp Interactions at 200 GeV/c", G. A. Smith, Proceedings of the IIIrd International Meeting on Fundamental Physics, Sierra Nevada, Spain (1975), p. 97.
4. "Study of the Energy Dependence of Diffractive Excitation in  $\pi^-p$  Interactions up to Fermilab Energies", G. A. Smith, Proceedings of the IIIrd International Meeting on Fundamental Physics, Sierra Nevada, Spain (1975), p. 141.
5. "Inclusive Study of Beam Dissociation into 'Leading Clusters' at FNAL Energies", V. P. Kenney, Proceedings of the Seattle Meeting of APS/DPF, Seattle (1975), p. 192.
6. "Multiplicities and Inclusive and Exclusive Reactions at Fermilab Energies", J. Whitmore, Proceedings of the Seattle Meeting of APS/DPF, Seattle (1975), p. 234.
7. "Multiparticle Correlations", V. P. Kenney, Proceedings of the Seattle Meeting of APS/DPF, Seattle (1975), p. 254.
8. "Multiparticle Processes at Fermilab Energies", J. Whitmore, Proceedings of the BNL Meeting of APS/DPF, Brookhaven (1976), p. F37.
9. "Track Chamber Experiments at Fermilab Energies: Recent Developments in Strong Interactions", W. D. Shephard, Proceedings of the VII International Colloquium on Multiparticle Dynamics, Tutzing, Germany (1977), p. 41.

Compilation of Refereed Journal Publications  
from Experiment 311 (Spokesman: W. W. Neale)

1. "Charged Particle Multiplicities in 100 GeV/c  $\bar{p}p$  Interactions", R. E. Anson et al., Phys. Letters 59B, 299 (1975).
2. "On the Difference Between  $\bar{p}p$  and  $pp$  Topological Cross Sections up to 100 GeV/c", J. G. Rushbrooke et al., Phys. Letters 59B, 303 (1975).
3. "Comparison of Neutral Particle Production in 100 GeV/c  $\bar{p}p$  and  $pp$  Interactions", D. R. Ward et al., Phys. Letters 62B, 237 (1976).
4. "Neutral Particle Production in 100 GeV/c  $\bar{p}p$  Interactions", R. Raja et al., Phys. Rev. D15, 627 (1977).
5. "Properties of Inclusive  $\pi^\pm$  Production in 100 GeV/c Antiproton - Proton Interactions", J. Whitmore et al., Phys. Rev. Letters 38, 996 (1977).
6. "Tests of Factorization from Single- and Double-Pion Production in 100 GeV/c  $\bar{p}p$  and  $pp$  Collisions", J. G. Rushbrooke et al., Phys. Rev. Letters 39, 117 (1977).
7. "Inclusive  $\rho^0$  and  $f^0$  Production in 100 GeV/c  $\bar{p}p$  Interactions", R. Raja et al., Phys. Rev. D (to be published) (1977).

Published Conference Proceedings from Experiment 311

1. "Analysis of Antiproton Reactions at 100 GeV/c", W. W. Neale, Proceedings of the International Conference on High Energy Physics, Palermo, Italy (1975).
2. "Charged-Particle Multiplicities in 100 GeV/c  $\bar{p}p$  Interactions", J. Whitmore, Proceedings of the IV International Symposium on Nucleon-Antinucleon Interactions, Syracuse (1975), p. III-115.
3. "High Energy Antinucleon-Nucleon Annihilation Interactions", J. G. Rushbrooke, Proceedings of the Third European Symposium on Antinucleon-Nucleon Interactions, Stockholm (1976), p. 277.
4. "Two-Particle Correlations in 100 GeV/c  $\bar{p}p$  Interactions", M. Pratap, et al., Proceedings of the Third European Symposium on Antinucleon-Nucleon Interactions, Stockholm (1976), p. 485.

Compilation of Refereed Journal Publications  
from Experiment 163A (Spokesman: W. D. Walker)

1. "Multiple Pion Production in  $\pi$ -Ne Collisions at 10.5 and 200 GeV", J. R. Elliott et al., Phys. Rev. Letters 34, 607 (1975).
2. "Direct Electron-Positron Pair Production by 200-GeV Negative Pions", L. R. Fortney et al., Phys. Rev. Letters 24, 907 (1976).

APPENDIX B (Copied from July 1976 Issue of NALREP)

PARTICLE IDENTIFIERS FOR HADRON PHYSICS

Vera Kistiakowsky, Massachusetts Institute of Technology

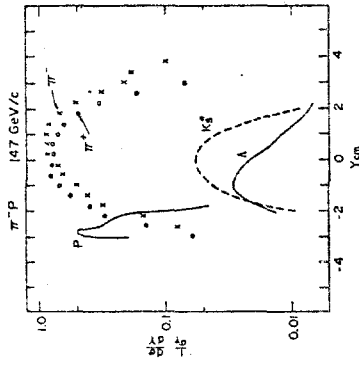
A workshop was held at Fermilab on May 7-8, 1976, to discuss what system of particle identifiers would be optimum for further studies of hadron collisions with the Fermilab hybrid bubble chamber proportional wire chamber system. The meeting was attended by about 40 physicists from various institutions.

What Can Be Learned?

The bare bubble-chamber experiments and the experiments with the two hybrid systems have already yielded many interesting results concerning hadron physics at Fermilab energies. For example, leading-particle studies have demonstrated the factorization of the Pomeron. Inclusive  $\pi^{\pm}p$  studies have shown that the leading particles and clusters retain the charge of the given incoming particle to low Feynman  $x$  and studies of the distribution of charge as a function of rapidity have indicated the absence of a central neutral plateau. Studies of two-particle correlations have shown a strong dependence of this correlation on the respective charges and on the azimuthal and rapidity separations of the two particles. The new results on  $\bar{p}p$  charged multiplicities and a comparison with  $pp$  data have yielded hints of some of the interesting properties of high energy  $\bar{p}p$  annihilations.

T. Ludlam (Yale) discussed some of the physics questions pertaining to particles produced in the central region of rapidity. The graph on the next page gives the differential cross sections for various particles from  $\pi^{-}p$  interactions at 147 GeV/c and it can be seen that, except for elastic scattering and beam and

target fragmentation, most of the particle production is between  $y = -2$  and  $y = +2$ . Investigations already being carried out on the charge structure of the particles in the central region of rapidity indicate the presence of short-range correlations and of local conservation of charge and raise the question of whether neutral clusters exist. An obvious extension of charge-transfer studies lies in similar investigations of strangeness. With charged-particle identification it should be possible to study strangeness transfer and it would be very interesting to determine whether the Quigg prediction of local strangeness conservation is verified. Turning to two-body resonances, charged-particle identification would permit investigation of  $K^*$ ,  $\phi$ , and  $Y^*$  production and, together with previous results on  $\rho^0$  and  $\Delta^{++}$  production, this would again permit an enlightening comparison between charge- and strangeness-dependent effects. Since a photon detector will shortly be part of the hybrid system, this will permit  $\pi^0$  identification and thus studies of  $\rho^\pm$  and  $\omega$  production. Finally, the recent observation at the ISR that in pp interactions there is apparently a sizable cross section ( $\sim 1$  mb) for events where both protons come almost to rest in the center-of-mass system raises the question whether the pions associated with such events are produced in jets or distributed isotropically. In conclusion, a rich source of information would be



The fractional differential cross section as a function of c. m. rapidity for p,  $\pi^+$ , n, and  $K^0$  produced in 14.7 GeV/c  $\pi^+p$  interactions.

opened up if clean  $\pi/K/p$  separation were possible over most of the central region and if programmatic studies with several incident beams and reasonably good statistics were carried out.

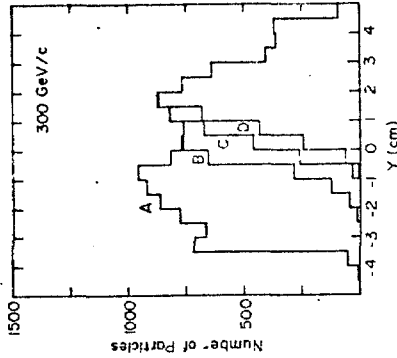
J. Whitmore (Michigan State) emphasized the physics question which could be studied in  $\bar{p}p$  and  $pp$  interactions, but also mentioned the interest in the central-region physics from the  $\pi^\pm$  interactions which could be obtained in the same exposures. One topic of considerable interest is a measurement of the relative contributions of annihilation and nonannihilation final states in  $\bar{p}p$  interactions and the study of baryon annihilations at high energy. The study of the annihilation channels is of particular importance since this process has not been studied at all above approximately 12 GeV/c and has not been studied in any detail above approximately 7 GeV/c. It is estimated that for  $\bar{p}p$  at 100 GeV/c (P-394) about 97% of the nonannihilation events could be identified by a suitable combination of particle identifiers, and the consequent identification of annihilation events would permit a comparison of the annihilation cross section with the difference between the  $\bar{p}p$  and  $pp$  total cross sections, as well as a study of the annihilation multiplicity distributions and related topics.  $\pi\pi$  correlations and single particle inclusive studies would also be possible and would contribute to a much better understanding of the annihilation channels at high energies. With respect to the central-region physics, in addition to the topics already mentioned, it would be interesting to determine the cross sections for production of  $K\bar{K}$  and  $NN$  pairs in  $\bar{p}p$ ,  $pp$ , and  $np$  interactions and to determine the properties of such events. Studies of this variety would require  $\pi/K/p$  separation both for leading particles and in the central region, a neutral-hadron detector, and high-statistics experiments.

W. Walker (Duke) reviewed the results of hadron-nucleus interaction studies, which have shown that the multiplicity, momentum and rapidity distributions are very similar to those for hadron-nucleon collisions. The differences, which are relatively small, indicate that the characteristic time for particle production is considerably longer than the collision time for hadron-nucleus collisions. It is necessary to measure the production spectra for K's, pi's and nucleons separately to further illuminate this result.

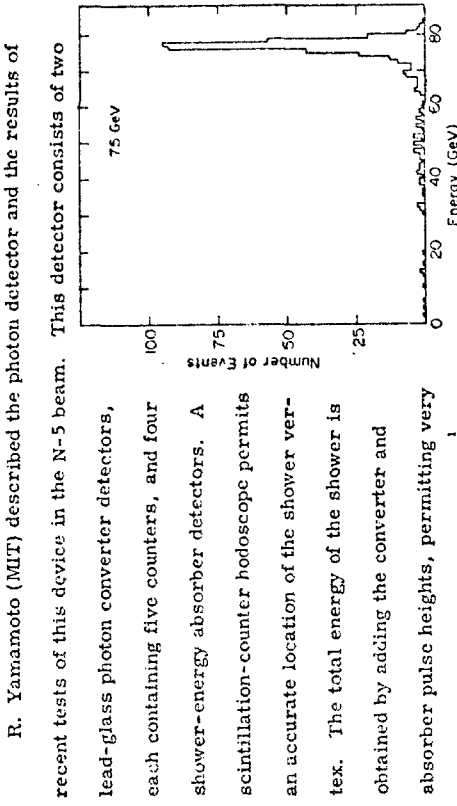
Fermilab Hybrid System

R. Plano (Rutgers) presented some possible configurations of the Fermilab hybrid system with downstream particle identifiers and described acceptance studies for these systems. The next phase of the hybrid system will include drift chambers and a photon detector, as well as proportional wire chambers. A downstream charged-particle identifier would be the next addition desired, and two possibilities have been considered by the

Proportional Hybrid System Consortium (PHSC). The first consists of three 4 m x 4 m x 4 m sections of a relativistic rise detector (ISIS) and the second of a 2 m diam x 3 m tall Cerenkov detector (CANUTE). Both detectors can only separate pi/K/p above 5 GeV/c and this corresponds kinematically to a limitation on the region of rapidity for which particle identification is possible. This limitation is less severe at higher incident-particle momenta and thus acceptance studies have been carried out at 300 GeV/c as well as 150 GeV/c, both based on data from the 147-GeV/c pi p (E-154) exposure. The graph at the top of the next page shows the 300 GeV/c distribution of particles with p > 5 GeV/c as a function of rapidity which traverse a 3 m ISIS located 2.25 m from the bubble chamber center.



The number of particles from simulated 300 GeV/c pi p interactions as a function of rapidity: A) all particles, B) particles which leave bubble chamber magnet, C) particles with p > 5 GeV/c which leave bubble chamber magnet and D) which pass through ISIS.



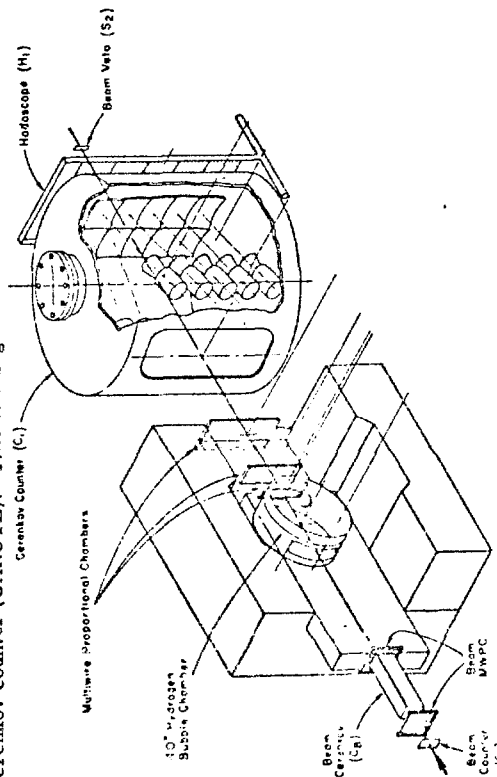
The number of events in the photon detector as a function of energy with 75-GeV electrons incident on the detector.

R. Yamamoto (MIT) described the photon detector and the results of recent tests of this device in the N-5 beam. This detector consists of two lead-glass photon converter detectors, each containing five counters, and four shower-energy absorber detectors. A scintillation-counter hodoscope permits an accurate location of the shower vertex. The total energy of the shower is obtained by adding the converter and absorber pulse heights, permitting very good energy resolution ( $\Delta E \approx 0.15E^{1/2}$ , where E is in GeV). Tests with electrons of various energies have verified

this prediction. The figure at the bottom of page 17 shows the pulse-height distributions of showers generated by 75-GeV/c particles tagged as electrons by a Cerenkov counter. The events observed at low energies are probably from pions which produce knock on electrons in the Cerenkov counter. This detector is currently being installed and will be used in Experiment 299 as soon as the schedule permits.

Charged-Particle Identifiers

R. Lewis (SLAC) described the Cerenkov counter operating in the SLAC hybrid facility and showed some experimental results on  $K/\pi$  separation obtained in a  $\pi^+ p \rightarrow K^+ Y^*$  experiment at about 12 GeV/c. The figure below shows the experimental layout and the 3 m diameter by 3 m high cylindrical Cerenkov counter (CANUTE). This is a segmented device with two rows of

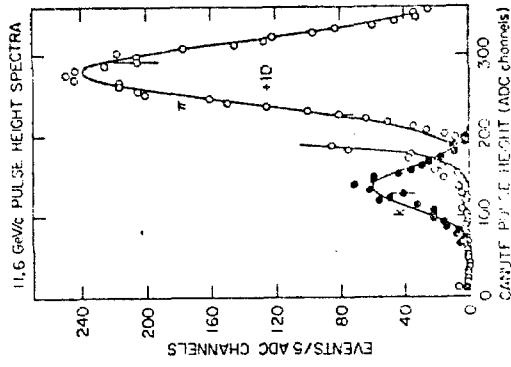


The layout of the SLAC 40-in. bubble chamber hybrid system including the Cerenkov detector (CANUTE).

five 75 cm wide by 50 cm high black lucite mirrors focusing the light on phototubes on either side of the beam line. CANUTE has been designed both mechanically and optically to operate with freon at pressures from slightly above atmospheric up to 4 atmospheres. With a filling of 45 psia of freon 100 photoelectrons are produced by particles with B of order 1 and thus  $K/\pi$  separation by pulse-height analysis is possible. It can be seen from the figure at the right that a good separation of  $K^+$  from  $\pi^+$  is achieved at 11.6 GeV/c.

G. Smith (Michigan State) discussed the particle-identification considerations necessary to a 9 GeV/c  $\bar{p}p$  experiment to be carried out at the SLAC 40-in. hybrid facility by a Cambridge-Michigan State collaboration (BC-64) and considered the same questions for the 100 GeV/c  $\bar{p}p$  experiment proposed for the Fermilab hybrid spectrometer (P-394). The two essential components of the SLAC experiment are CANUTE and the UCLA neutron detector, suitably modified, used for antineutrons.

This device will contain 26 layers of iron alternated with scintillator and three hodoscopes for accurate location of the  $\bar{n}$  interaction. This device will have an efficiency of approximately 88% for  $\bar{n}$ . A possible particle-identification scheme for the Fermilab 100 GeV/c  $\bar{p}p$  experiment would involve a CANUTE-type Cerenkov counter to separate  $\pi/K/p$  for central-region

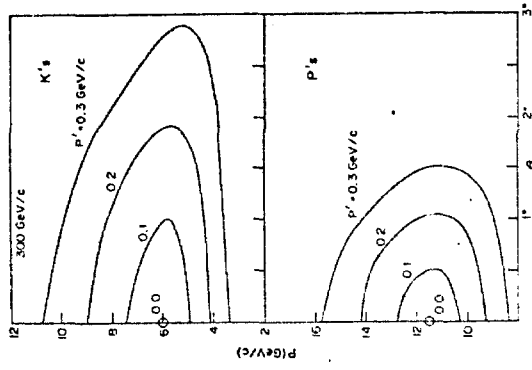


The number of events as a function of pulse height for 11.6 GeV/c  $\pi$  mesons and K mesons in CANUTE.

physics followed by a multi-cell  $2\text{ m} \times 2\text{ m} \times 5\text{ m}$  atmospheric pressure Cerenkov counter ( $C_2$ ) similar to that constructed at Michigan State for E-366, which when filled with approximately 95% helium and 5% nitrogen would permit a  $\pi/K/\bar{p}$  separation between 53 GeV/c (K threshold) and 100 GeV/c (p threshold). Acceptance calculations yield a 97% overall detection efficiency for  $\bar{p}$  by  $C_2$ . An antineutron detector similar to that planned for SLAC would follow the Cerenkov counters and would have about 90% acceptance. This, together with the conversion efficiency, would yield an overall detection efficiency of about 80% for antineutrons. These estimates, together with cross-section information, yield a 73% estimated purity of the annihilation sample. The cost for building  $C_1$  would be approximately \$410,000 (based on the construction cost of CANUTE) and for  $C_2$  approximately \$30,000 (based on the Michigan State E-366 Cerenkov cost).

V. Kistiakowsky (MIT) discussed the problems associated with using Cerenkov detectors for central-region physics and presented some estimates of the separation expected from a CANUTE-type detector at 150 GeV/c and 300 GeV/c. The graph on the following page gives the laboratory momentum  $p$  as a function of laboratory angle  $\theta$  for K-mesons and protons produced with very low c.m. momenta  $p'$  by 300 GeV/c interactions. It is seen that the region where particle separation would be desired stretches from  $p$  approximately 3 to 16 GeV/c. For lower incident momenta, these curves are shifted downward in laboratory momentum. Currently attainable K thresholds are  $\geq 5.3\text{ GeV/c}$  (4 atmospheres freeon) due to safety considerations. Using the experimental results for the number of photoelectrons in CANUTE,

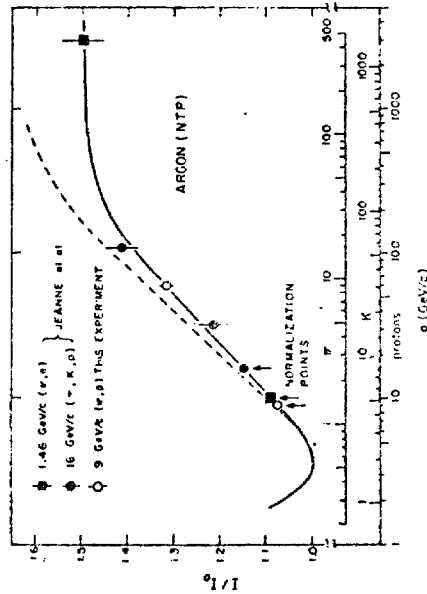
the efficiency for distinguishing  $\pi/K/p$  has been estimated. From about 5.5 GeV/c to 11 GeV/c K's can be identified by pulse-height analysis, but there is an overlap between the pulse-height distributions for  $\pi$ , K and p which results in the misidentification of up to 30% of the K-mesons. Another problem which seriously affects the detection efficiency of such a detector is the overlap of Cerenkov light spots from different particles. This cannot be improved by



decreasing the CANUTE mirror size, since at 4 atmospheres of freeon the size of the spots is comparable to that of the mirrors. At 300 GeV/c, the acceptance of a CANUTE-type detector located 6 m from the bubble chamber would be 46% for particles with momenta  $5.5 < p < 11\text{ GeV/c}$ . However, only 43% of the particles accepted would have sufficient separation to permit identification. The advantages of such a device are that it is guaranteed to work and that engineering costs could be minimized by copying CANUTE (estimated cost about \$110,000). The disadvantages are the limited region of  $\pi/K/p$  separation, the limited particle spatial resolution, and the incompatibility of such a device and the photon detector.

J. Whitmore (Michigan State) described the CERN External Particle Identifier (EPI) and discussed the pros and cons of constructing such a device

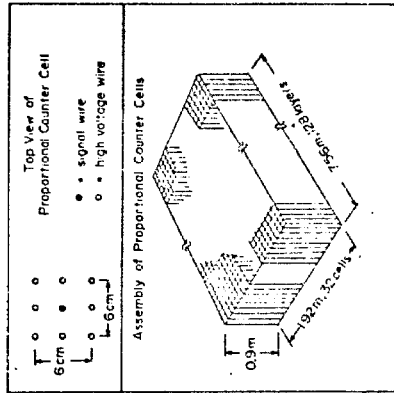
for the Fermilab hybrid system. This device is being built (75% completed) for use at BEBC and extensive tests which have been made with prototypes are very promising. This device measures the ionization of the particles in the region (3 to 100 GeV/c) where  $dE/dx$  for  $\pi$ , K, and p is different due to the rise at relativistic velocities (see figure below). Since an individual



The relative ionization as a function of momentum for  $\pi$  mesons, K mesons, and protons. The dashed line is that calculated by Sternheimer, the solid line is hand drawn through the points which are the results of experiments carried out by the group developing the BEBC EPI.

ionization measurement can yield a wide range of values for  $dE/dx$  with a probability given by the Landau distribution, the ionization of a given particle must be sampled a large number of times and an average of these measurements (or an equivalent quantity) used to typify the particle. With a large enough number of samples, good resolution can be achieved for the distribution of the average values for a given particle type at a given momentum. The CERN EPI will consist of 128 layers of 32 individual proportional

counters, each of which is 6 cm x 6 cm x 90 cm (see figure below). The active volume of each proportional counter is defined by eight high-voltage

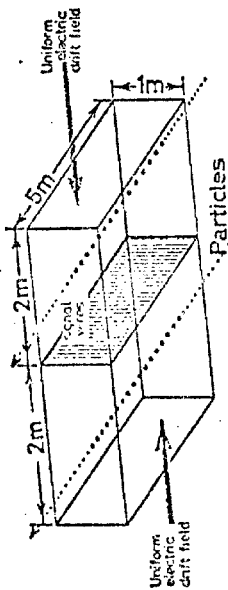


wires and the device is filled with 95% A-5% CH<sub>4</sub>. Based on experimental studies, 5.5% FWHM resolution is anticipated for 128 6 cm ionization samples suitably analyzed. The acceptance of an EPI located 2.5 m from the bubble chamber center has been estimated using data from a 100 GeV/c  $\bar{p}p$  experiment (E-314), and 59.1% of all particles and 97.3% of

all forward-hemisphere particles would enter the device. A consideration of the track-overlap problem indicates that in 4-prong events, typically, the information from approximately 34% of the cells must be discarded because of particles passing through the same cell, with a corresponding reduction in resolution to 6.6% FWHM (for 128 layers). In 12-prong events, the loss is approximately 4% with essentially no decrease in resolution. A recent estimate made at CERN for the cost of a 64-layer EPI was \$188,000 plus salaries.

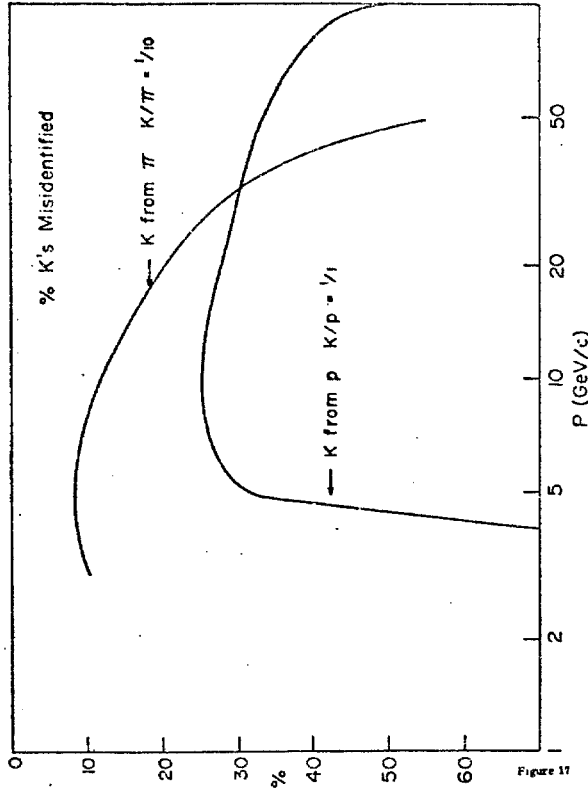
W. Dugg (Tennessee) described another relativistic-rise detector and presented some estimates of its anticipated performance with the Fermilab hybrid system. This device is a smaller version of ISIS, the device being developed at Oxford for use with the CERN rapid-cycling bubble-chamber hybrid system. ISIS consists of a 1 m x 4 m x 5 m drift chamber which

contains 330 signal wires with a 1.5 cm spacing (see the illustration below).



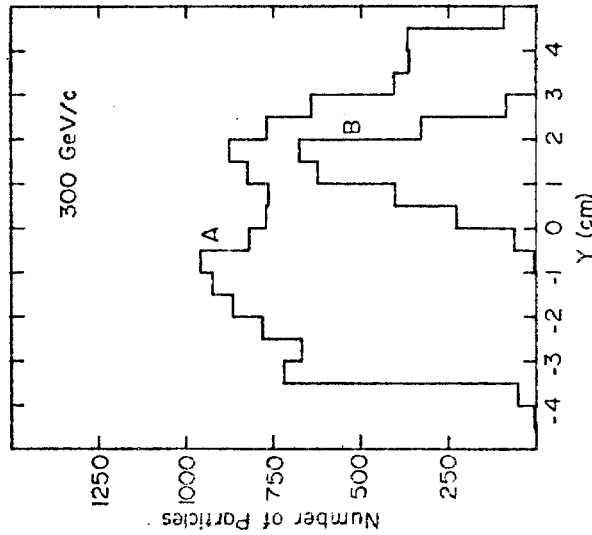
Schematic representation of the Oxford ISIS.

The pulse-height resolution predicted for the mean of the 330 1.5 cm samples is 6.2% FWHM. The time resolution of the signal collection is 250 nsec and thus, with a 2 cm/μsec drift velocity, measurements on tracks within roughly 1 cm of each other cannot be used. A full-scale ISIS has not yet been tested, but extensive studies of both its drift chamber and relativistic-rise aspects have been carried out. There are some stringent constraints on gas purity and field uniformity for operation with a full 2 m drift space, but these disappear if the drift-space dimension is decreased to 50 cm. Such a device could be operated with commercial bottled gas (purity 2 ppm) and an off-the-shelf power supply. Thus it is proposed that three sections of a 1 m x 1 m x 1 m ISIS-type device be constructed, each containing 66 wires at a 1.5 cm spacing, permitting a total of 198 1.5 cm samples of the ionization and a corresponding 7.3% FWHM resolution. The figure at the top of the next page gives the percentage of misidentified K-mesons as a function of particle momentum corresponding to this resolution and this device is seen to give better than 70% K identification from 5 to 30 GeV/c. The figure at the top of page 26 gives the rapidity distribution both for all particles and for those



The percentage of K mesons which are misidentified in a relativistic rise detector with 8% FWHM resolution at a function of momentum for  $\pi/K/p = 10/1/1$ .

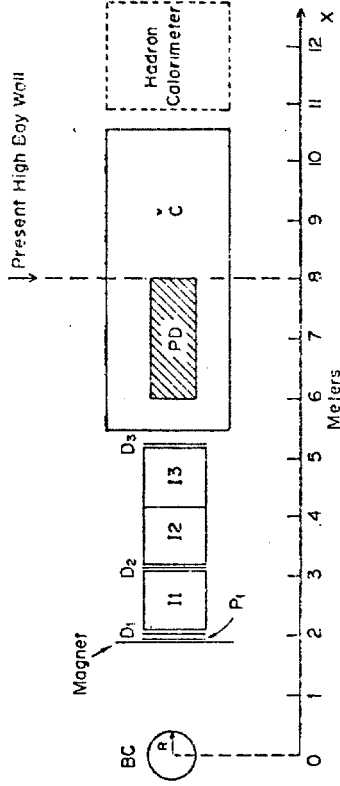
which both pass through ISIS and have momentum,  $5 < p < 40$  GeV/c. At 300 GeV/c, 48% of all particles and 30% of those escaping the magnet satisfy these criteria. One topic of importance to all varieties of particle identifiers is the question of charged-particle background, since a background particle passing through the same cell as a particle from the event renders the information from that cell not useable. A background study has been carried out using the proportional wire counter data for several hundred events chosen at random from E-154 ( $\pi^+p$  at 147 GeV/c) and E-299 ( $\pi^+p$  at 150 GeV/c). The percentage of cells which must be discarded is estimated to be 25% for



The number of particles as a function of rapidity from simulated 300 GeV/c p-p interactions: A) all particles, B) those particles with  $5 < p < 40$  GeV/c which pass through 43 in the figure on page 27.

an ISIS (1 cm cells) and 54% for an EPI (6 cm cells), both located 2 meters from the bubble chamber center, with the current-bubble chamber configuration. Improvements in the background could be made by reductions in the amount of matter downstream of the bubble chamber. The cost estimated by the Oxford group for a 4 m x 1 m x 1 m ISIS module is \$47,200; thus, including provision for contingencies, a conservative estimate would be \$30,000 per module. The first module could be constructed in 6-9 months and the remaining modules could be completed within a year at a total cost of \$100,000 plus salaries.

I. Pless (MIT) presented a proposal agreed upon by the workshop for a system which would permit both "central-region" physics (5-50 GeV/c) and "leading-particle" physics (50-100 GeV/c). This system is shown in the figure below and would consist of three elements: an ISIS consisting of three 1 m x 1 m x 1 m sections interspersed with drift chambers (5-50 GeV/c), a 2 m x 2 m x 5 m multi-cell atmospheric pressure N<sub>2</sub>-He Cerenkov detector (50-100 GeV/c), and the photon detector. The photon and Cerenkov detectors



The particle identification system proposed in the recommendations of the workshop for the Fermilab 30-in. bubble chamber hybrid system. 11, 12, and 13 are 1 m x 1 m x 1 m ISIS-type modules; C is a 2 m x 2 m x 5 m multi-cell Cerenkov detector; P1 is a proportional wire counter; and D1, D2, D3 are drift chambers. The location of the photon detector (PD) and possible location of a future hadron calorimeter are also shown.

could not be used simultaneously and would be mounted on rails for easy interchange. This arrangement would necessitate an addition to the present high-bay area which would accommodate either the Cerenkov or the photon detector when not in use. At a future date, this could be expanded to include a neutral-hadron calorimeter for n/π detection. The workshop had been asked to consider 12 aspects of particle identifier systems (NALREP, p. 19,

March, 1976). The proposed system has (1) operating parameters of  $\pi/K/p$  separation from 5-100 GeV/c and (2) an acceptance that is reasonably well matched to the geometric profile of the particles leaving the bubble chamber. (3) The background sensitivity is acceptable and (4) the problems of gas handling and purity are minimized since commercially available bottled gas (2 ppm impurity) is satisfactory. (5) The readout electronics can use elements already available and this problem and (6) that of off-line computing are already solved in principle. (7) The system is compatible with photon detection and high-resolution momentum measurements and (8) requires no drift chambers or proportional wire counters other than those already in existence or under construction for the hybrid system. (9) A modest extension of the building will be necessary, but not a crane. (10) The maintenance requirements will be about the same as those of the present system, and (11) the system poses no safety problems. (12) The construction and testing of ISIS would be carried out by the PHSC and that of the Cerenkov detector, by Michigan State University. Conservative estimates of the costs are respectively \$100,000 and \$30,000. The construction, initial test and installation schedule would involve 6 to 9 months for construction, 1 to 2 months for testing and 3 months for installation, for a total of 12 to 15 months. The PHSC would assume overall responsibility for the integration of these detectors with the proportional hybrid system.

J. Whitmore  
High Energy Physics  
Michigan State University  
January 1978

Preliminary Results of Tests on Components  
of the Proposed Multicelled Cerenkov  
Counter for the Fermilab DPI

In December, 1977, various tests were performed in Test Beam 6 at SLAC on a prototype for the 8 cell  $2 \times 2 \times 5\text{m}^3$  Cerenkov Counter (OSIRIS) to be used in the Downstream Particle Identifier (DPI) System behind the Fermilab 30-inch bubble chamber. These tests were made in an 8 GeV/c electron/pion beam tagged with a beam Cerenkov Counter. The beam was run at  $\sim 1$  particle/burst at 10pps and  $\sim 30\%$  of the beam was tagged as electrons.

The prototype, shown schematically in Fig. 1(a), consisted of a single optical cell with three window-phototube configurations and two gases being tested. The three configurations were:

- (i) Quartz window with a bare phototube;
- (ii) Quartz window with pTp waveshifter on the phototube; and
- (iii) pTp on a pyrex window with a bare phototube.

The phototubes were two RCA 8854 quantacon (tubes A and B) and one Amperex XP 2041 (tube C) 5" phototubes. The Cerenkov media used were 5m of helium and 1.4m of nitrogen.

The Cerenkov light was reflected to the phototube by a plane mirror of black lucite surfaced with aluminum and  $\text{MgF}_2$  vacuum deposited. The advantage of these optics is that the light probes the full surface of the photocathode. Light from different beam particle trajectories illuminates different regions of the photocathode, resulting in a superposition of pulse height spectra from strong and weak areas of the photocathode.

The technique used for calibrating the pulse height spectra is illustrated in Fig. 1(b). Calibrations were made in conjunction with each run, using an LED mounted inside the Cerenkov tank. The calibration spectra of Fig. 1(b) are simulated by a Monte Carlo program which generates a Poisson distribution statistically broadened according to a function compatible with the shape of the measured single photoelectron peak. A cross check is provided by comparing the expected inefficiency with the number of events corresponding to zero pulse height; the agreement is excellent.

The results of the following four tests are shown in Figs. 2(a) - 2(d):

	<u>Phototube</u>	<u>pTp on tube?</u>	<u>Cerenkov Medium</u>	<u>Window Configuration</u>	<u><math>\bar{n}</math> (p.e.)</u>	<u>A (cm<sup>-1</sup>)</u>
(a)	B	Yes	5m H <sub>e</sub>	quartz (ii)	3.0	86 ± 8
(b)	B	Yes	1.4 N <sub>2</sub>	quartz (ii)	6.5	77 ± 8
(c)	A	No	1.4 N <sub>2</sub>	quartz (i)	8.7	104 ± 10
(d)	A	No	1.4 N <sub>2</sub>	pTp on Pyrex (iii)	11.5	137 ± 13

The results tabulated above represent mean pulse heights, converted to a number of photoelectrons using the calibration data. Hence they correspond to a performance averaged over the photocathode. The figure of merit is defined as the value of the coefficient A in the relation  $\bar{n} = AL\theta^2$ , where  $\bar{n}$  is the average number of photoelectrons, L is the radiator length (cm) and  $\theta$  is the Cerenkov angle. The curves in Fig. 2(a) - 2(d) are simple Poisson distributions whose mean values correspond to those tabulated above and are reasonable representations of the data.

We note that configurations (a) and (b) indicate a figure of merit of  $A \approx 80 \text{ cm}^{-1}$ , while (c) and (d) show that we have attained a value of A greater than  $100 \text{ cm}^{-1}$ . The difference between these two results is consistent with

being due to the fact that phototube A has a manufacturer's rating for the cathode sensitivity which is a factor of 1.4 higher than that for tube B. This sensitivity is undoubtedly more important than any other variables tested. The results for tube C, an Amperex XP 2041, were generally a factor of two worse than the RCA tubes.

We conclude that a figure of merit of  $A \geq 100 \text{ cm}^{-1}$  has been achieved, consistent with our earlier expectation ( $A = 100 \text{ cm}^{-1}$ ) stated in Fermilab proposal #394.

### Prototype Cerenkov Cell

(a)

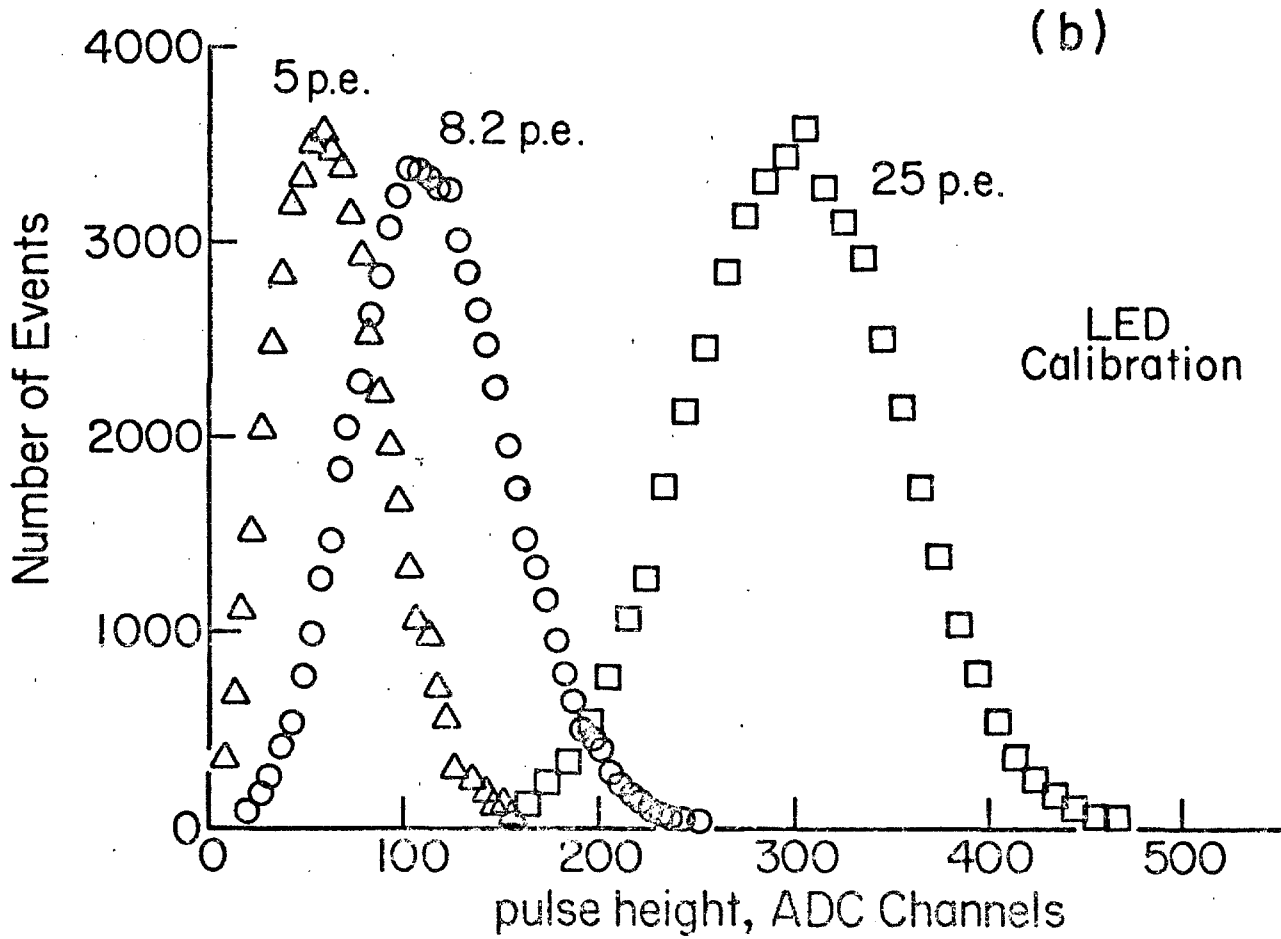
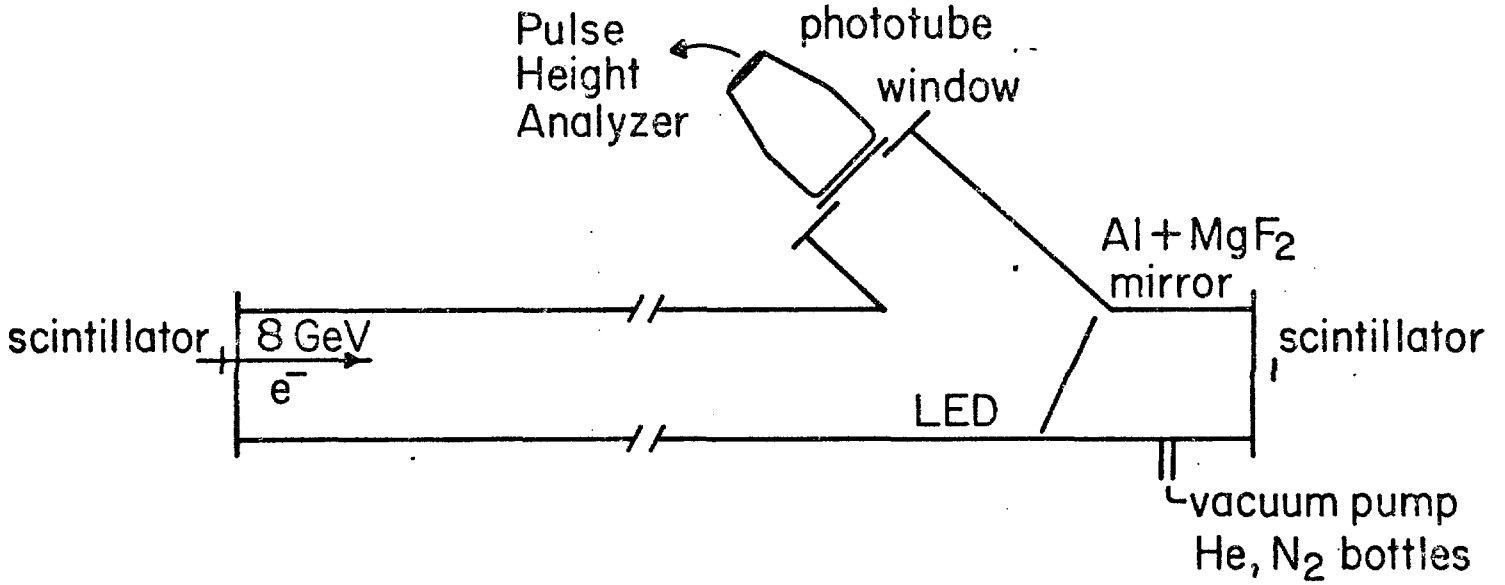


Fig. 1

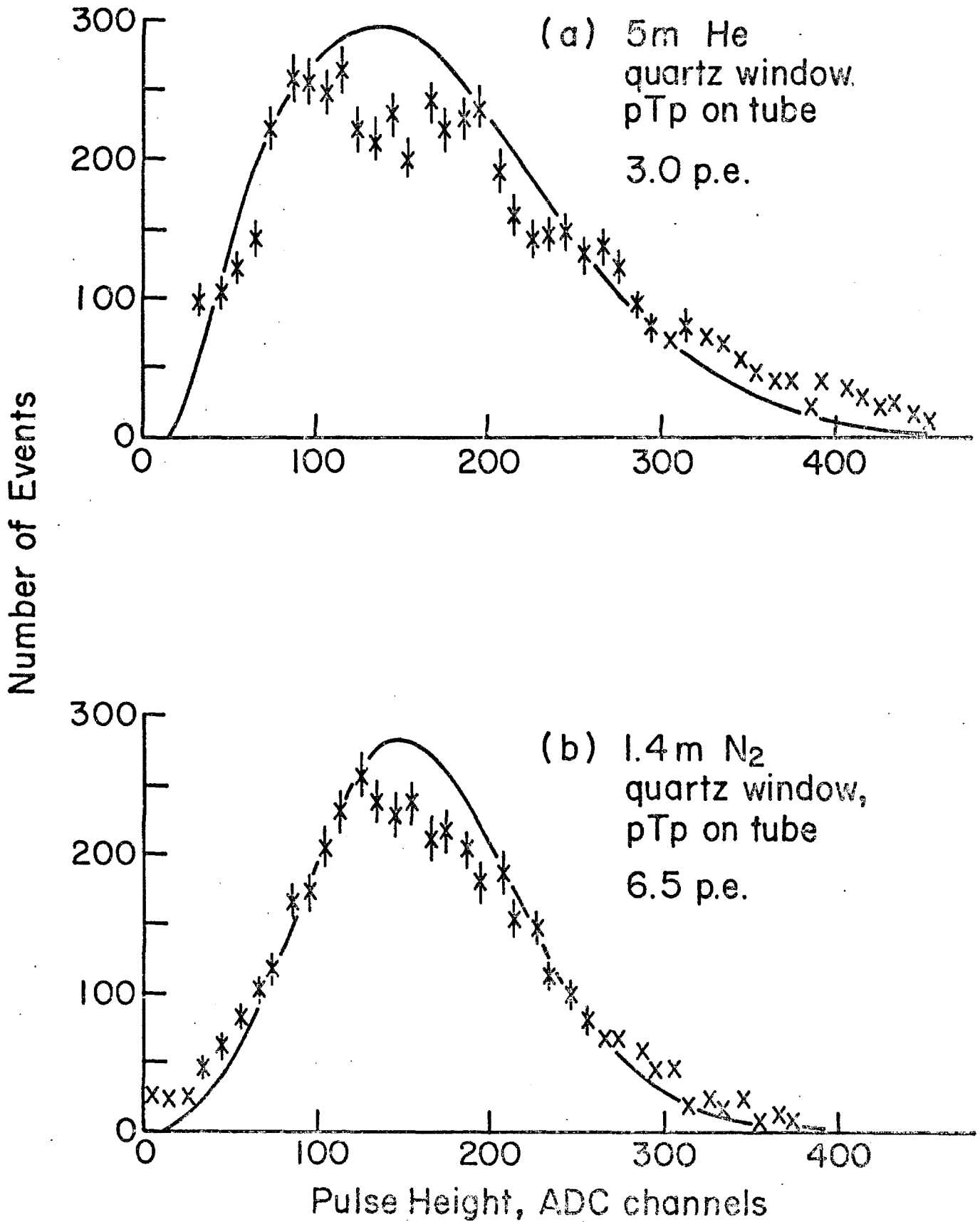


Fig. 2

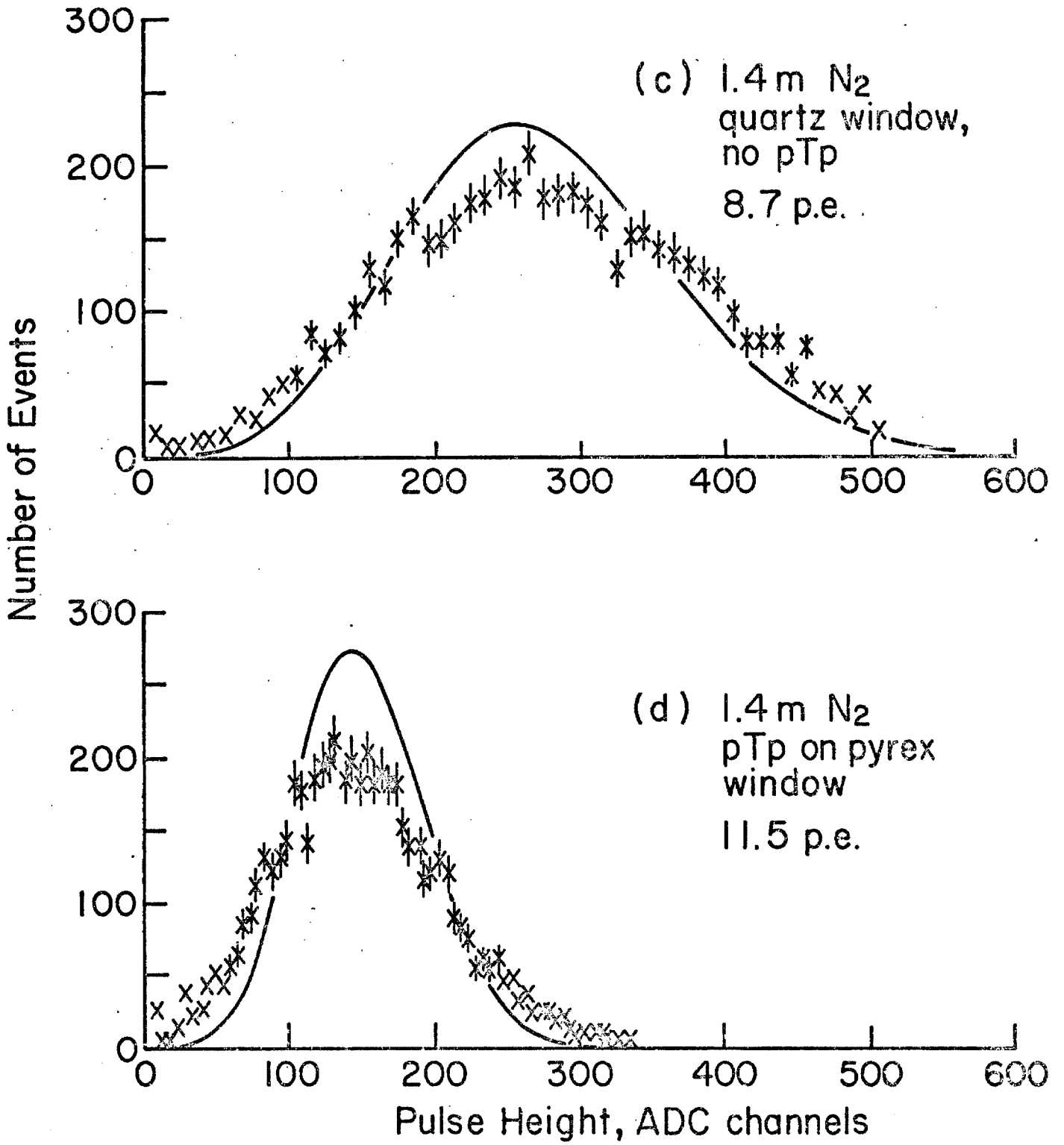


Fig. 2

REVISED  
PROPOSAL FOR A STUDY OF THE INTERACTION OF HIGH  
ENERGY  $\pi^\pm$  WITH GOLD AND MAGNESIUM

to

FERMILAB

W. D. Walker, L. Fortney, P. Lucas, A. T. Goshaw, and  
W. Robertson

Department of Physics  
Duke University  
Durham, North Carolina 27706

12 January 1978

Spokesman - W. D. Walker

(919) 684-8228      FTS 674-8228

(919) 684-8140      FTS 674-8140

PROPOSAL:

To study high energy  $\pi$  interactions in a plate containing a low Z and high Z material (Au) placed in the 30" bubble chamber filled with hydrogen and followed by the D.P.I. counter system. We also propose to use the MWPC system and the hadron calorimeter spectrometer to increase the precision of measurements of the fast forward tracks and  $\gamma$ -rays that are produced.

PURPOSE:1. Incoherent  $\pi$ -A Collisions

By using both  $\pi^+$  and  $\pi^-$  particles incident, it will be possible to make a very detailed study of both  $\pi$ -Mg and  $\pi$ -Au collisions. This means that we can measure the multiplicities and rapidity distributions for  $\pi^\pm$ ,  $K^\pm$ ,  $\pi^0$ ,  $K^0$  as well as the distributions for the knocked on p and n. The determination of the number of knocked on protons makes it possible to make a detailed check of K-N-O scaling for Mg and Au as compared to  $\pi$ -p collisions.

## 2. Diffractive and Coulomb Studies

We should be able to measure inclusively the coherent events from Mg and Au. We expect the order of 10% of all events to be coherent (these are the 3-5-7 prongs). Of these coherent events, about 1/3 of the events in Au should be Coulomb induced.

### 3. $\alpha$ -Centauri Events

We propose to look for this process in which large charged multiplicities are encountered with very few  $\pi^0$ 's produced. We propose to study the high multiplicity events in some detail. With the sample size available ( $\sim 60,000$  high A events) we can look at the high multiplicity events and see if there are any indications of basically new phenomenon such as events with very few  $\pi^0$ 's.

4. A study of direct pair production in condensed matter.
5. A study of high  $p_T$  phenomena in heavy nuclei.

This will be a byproduct of our comprehensive studies of interactions in a heavy nucleus.

6. An exploratory study of multiplicities at the highest possible  $\pi^-$  energy in the heavy nuclei to look for possible new physics.

### METHOD:

We propose to use the 30" FNAL chamber filled with hydrogen and with thin plates of Au and Mg on the upstream side. We also propose to use the PHC consortiums PWC's and the MSU calorimeter and Cerenkov counter downstream to enhance our ability to measure high energy secondaries. By using both  $\pi^+$  and  $\pi^-$  bombarding particles, we will be able to determine the nucleon momentum spectrum emerging from the incoherent interactions.

MOTIVATION:

The purpose of this experiment is several fold. The first purpose is to study the incoherent  $\pi$ -Au (or Pb) interactions. Au is 7.2 nucleons thick which is over twice as thick as a Neon nucleus. We will measure the multiplicity of pions, K's and nucleons in the heavy nucleus. We would also measure the rapidity spectrum of  $\pi$ 's from the heavy nucleus. The importance of measurements of the rapidity distribution in distinguishing between different models of particle production has been stressed in recent papers by Koplik and Mueller.<sup>1</sup> Recent results of studies of 10 GeV  $\pi$ -Ne interactions are shown in Fig. 1. It is clearly necessary to extend these results both to higher energy -- to allow for a wider range of rapidity and to a heavier nucleus. We show in Fig. 2 the KNO multiplicity scaling curve for Neon and hydrogen. It is obviously important to see whether this scaling law holds for a heavy nucleus where the multiplicity will be nearly 2 times as great as in hydrogen. In order to make such a check, it is important to determine the number of protons among the charged shower particles. In a recent publication, the Duke group has shown that one can measure the

---

<sup>1</sup>High Energy Hadron - Nucleus Scattering by J. Koplik, A. E. Mueller (Columbia University preprint).

momentum spectrum and in principle even more information about the nucleon spectrum from these  $\pi$ -nuclear collisions. We will be able to do this for the  $\pi$ -Mg collisions by virtue of the fact that we will have both  $\pi^+$  and  $\pi^-$  collisions to measure. We show the results obtained at 10 GeV in Fig. 3. Any model of these collisions will be constrained in an important way by our results. We should also be able to obtain at least qualitative results on  $\pi$ -Au collisions so far as the nucleon momentum spectrum is concerned.

A comparison of p and  $\bar{p}$ -nuclear collisions with the  $\pi$ -nuclear collisions should be quite interesting. The p or  $\bar{p}$  system has a 30% smaller mean-free path in nuclear matter than  $\pi$ 's.

#### INCLUSIVE DIFFRACTIVE:

In Fig. 4 we show the multiplicity distribution in  $\pi$ -Neon collisions at 200 GeV for cases with zero protons visible. There are prominent peaks visible for cases with 3, 5 and 7 prongs. These results suggest that it is possible to measure diffractive dissociation in an inclusive fashion. By going to a heavier nucleus, it may be possible to do this in a cleaner fashion since the incoherent interactions give rise to a peak in the multiplicity distribution at a higher multiplicity. This means that the background of incoherent events should be less for a heavy nucleus than for the lighter nucleus such as Neon. This is an important point since we would select events on the basis of topology and lack of heavy tracks. This separation is improved by having a higher average multiplicity.

Unfortunately, we had relatively few  $\pi$ -Ne diffractive events that we were able to reconstruct at 200 GeV. The momentum of the fast outgoing tracks were too high to measure with precision. This makes it important for us to have  $\pi$ -Mg diffractive events to compare with  $\pi$ -Au coherent events. The difference between these two classes of events should be attributable to Coulomb interactions. Thus, we should be able to make at least a qualitative comparison of  $\pi$ - $\gamma$  inclusive collisions with  $\pi$ -diffractive inclusive distributions.

The comparison of  $\pi$ -p and  $\pi$ -Mg,  $\pi$ -Au and p-Mg, p-Au should make it possible to determine the cross section and compare  $\pi$   $\rightarrow$  diffractive products and p  $\rightarrow$  diffractive products. We recently found (from the 2-B experiment data) that the  $\pi$  seems to dissociate twice as often as the nucleon. It is important to verify this independently.

#### LARGE MOMENTUM TRANSFER EVENTS:

In the last several years there has been great interest in the study of particles with large transverse momentum. As in any inclusive study, the bubble chamber possesses considerable merit. For interactions in Ne we find about 1 interaction in 5 has a particle with more than 1 BeV/c transverse momentum. The cross section for the production of high  $p_T$  particles is proportional to  $A^{1.1}$  ( $A$  = No. of Nucleons). This means that it might be advantageous to look in Au or U for high  $p_T$  events. We would like to look at high  $p_T$  (1-3 GeV/c) and find the relative frequency of single pions as compared with clusters of particles or resonances produced with

high  $p_T$ . Also it would be very interesting to see whether high  $p_T$  events differ in a qualitative way from the average events. What can be done in a practical way is to look for particles with high  $p_T$  which occur outside of the forward jet of fast particles. This limits the momentum of the particles we look at to  $\sim 10-20$  GeV/c for  $p_T > 1.0$  GeV/c. This means that we can efficiently search about 35% of the available phase space for high  $p_T$  tracks. For this domain we can do an interesting study of the characteristics of the events in which relatively large  $p_T$  tracks occur. With 1000K pictures with one 1-mm thick piece of Au in the chamber, we can extend the search to a  $p_T$  of 3 GeV/c for interactions in the heavy nucleus.

#### $\pi - \gamma$ INTERACTIONS

One of the uses of the high Z target would be as a source of virtual  $\gamma$ -rays. These virtual  $\gamma$ -rays are the target in this part of the proposed experiment. The total  $\pi - \gamma$  cross section should be approximately 50 mb for 100 GeV pions incident on Au. This is to be compared to a total  $\pi$ -Au cross section of 2000 mb and a diffractive cross section of perhaps 200 mb. One of the characteristics of such events might be a diffractive appearing event with an even G parity. The simplest example of such an event would be  $\pi^- + \gamma \rightarrow \rho^- \rightarrow \pi^- + \pi^0$ . Other more interesting (less studied) reactions would be  $\pi^+ + \gamma \rightarrow \pi^+ + \omega^0$  or  $\pi^+ + \gamma \rightarrow \pi^+ + \phi^0$ . Note that both of these reactions can be well studied with the proposed apparatus and, in particular, the downstream particle identifier. The  $\phi^0$  can be detected because the dominant decay  $\phi^0 \rightarrow K^+ + K^-$  will look like an electron pair

but will not register in the calorimeter as an electron pair.

### DIRECT PAIR PRODUCTION

Our group has measured direct pair production by 200 GeV  $\pi^-$  mesons from a hydrogen-neon mixture and found excellent agreement with QED. This result is in contrast to several emulsion experiments where large discrepancies with QED have been reported. The emulsion targets used are about ten times as dense as the hydrogen-neon target we used. If the emulsion experiments are correct, the reason might be that direct pair production is suppressed (because of multiple scattering or other dense medium effects) much more than predicted by theoretical calculations. This seems unlikely, but by measuring direct pair production in lead we can check this possibility. With 1000K pictures (6 tracks/pulse) we would produce over 8000 direct pairs in the Au plates. After all cuts we would have a clean sample of approximately 2000 direct pairs (more than any previous experiment). This would allow us to make a good check of this basic QED process in an unexplored physical domain.

### $\alpha$ -CENTAURI EVENTS

In the last few years (10 or so) strange events have been reported from cosmic radiation investigations. Events in which only electrons and photons are produced, also events of high multiplicities in which essentially no  $\pi^0$ 's are produced. We propose to take a small number (50,000) of pictures at the highest available  $\pi^-$ -energies (360 GeV) to look for indications of such occurrences. The cosmic ray events seem to occur at 10 - 100 TeV

but they must have fairly high cross sections to be seen at all. A 360 GeV  $\pi$  colliding with an Au nucleus will, with modest cross section, collide with 5 nucleons. This type of collision has energy in the  $\pi + 5$  nucleon CM system equivalent to a  $\pi$ -nucleon collision of 1.8 TeV. Such complicated collision may show nothing more than a higher pion multiplicity, but perhaps they might show something qualitatively new like 100's of  $\gamma$ -rays or electrons etc. It's a long shot but it's cheap and should be tried.

#### EXPERIMENTAL DETAILS

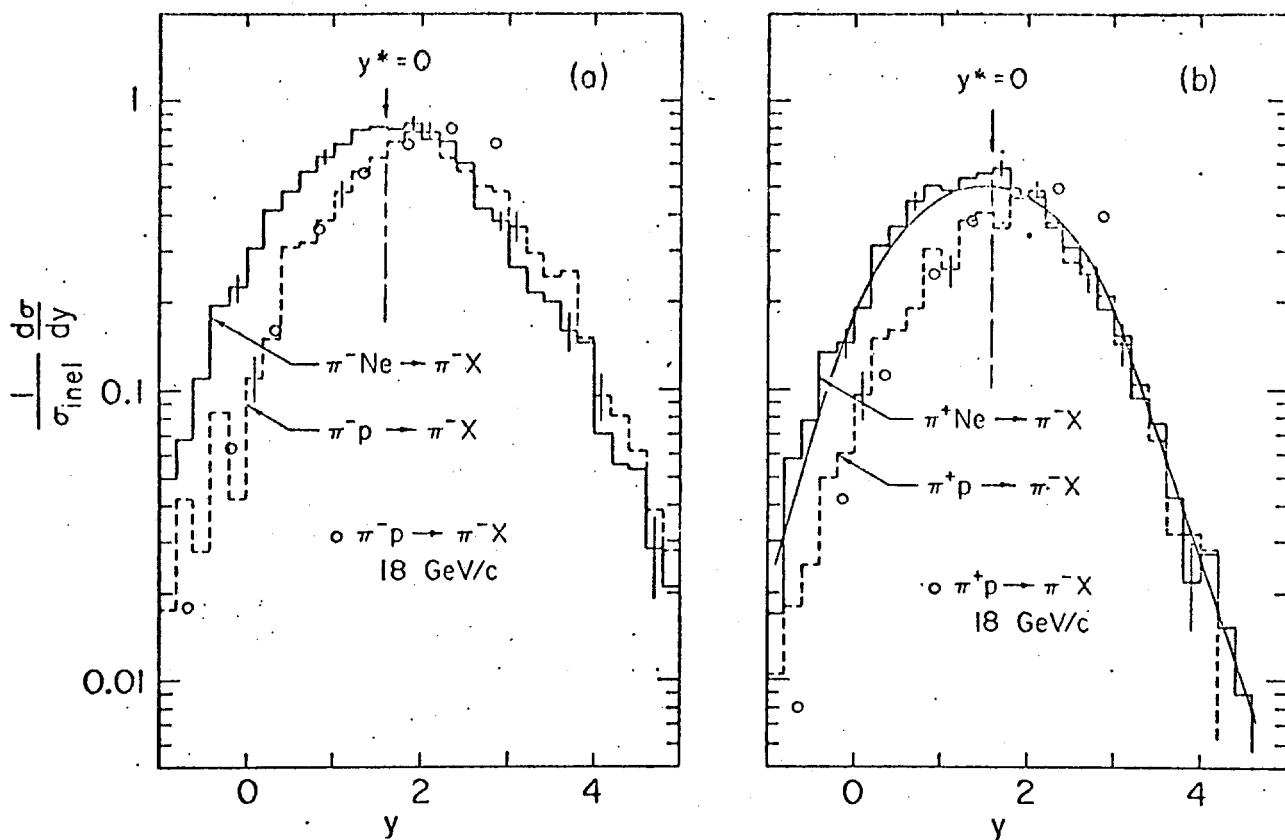
For one-million pictures, we expect about  $6 \times 10^4$  interactions in Au in a target of  $1.6 \text{ g/cm}^2$  thickness ( $\sim 0.75$  mm thickness). Of these interactions we expect about 10% to be coherent. Of the coherent interactions we expect about 20% to be coulombic.

We would then propose to have an additional plate which would be 1/2 of Magnesium and 1/2 thinner Au. The magnesium would be about 1/2% of a mean-free path (about 2.5 mm) and should yield 15,000 interactions. The gold would be thinner than the main plate of the order of  $0.4 \text{ g/cm}^2$  ( $\sim 0.2$  mm thick). The smaller thicknesses are important for estimating the number of  $\gamma$ -rays converting inside the plates and the number of secondary interactions inside the plates.

We propose to use a fourth camera to look edge-on at the plates. The fourth camera would be run with a smaller f-stop (perhaps f 5.6) to make the diffraction spots smaller and thus improve the spatial resolution close to the vertex.

BEAM MOMENTUM

The bulk of the data will be taken with a momentum of 100 GeV/c. At this momentum the capabilities of the chamber plus downstream system are much better matched than if one used a higher momentum. The small exposure at 360 GeV/c will concentrate on higher multiplicity events where the average secondary momentum will be lower.



Inclusive single pion rapidity distributions for  $\pi Ne$  (solid histograms) and  $\pi p$  (dashed histograms) interactions. (a) Favored pions (b) Unfavored pions. The vertical dashed line labeled by  $y^* = 0$  corresponds to the zero of rapidity in the pion-nucleon center-of-mass frame. The curve placed on the unfavored pion spectrum is a prediction of the "coherent tube" model (see text). The circles are representative points from  $\pi^{\pm}p$  interactions at 18 GeV/c (Ref. 35), and are included for comparison.

Fig. 1

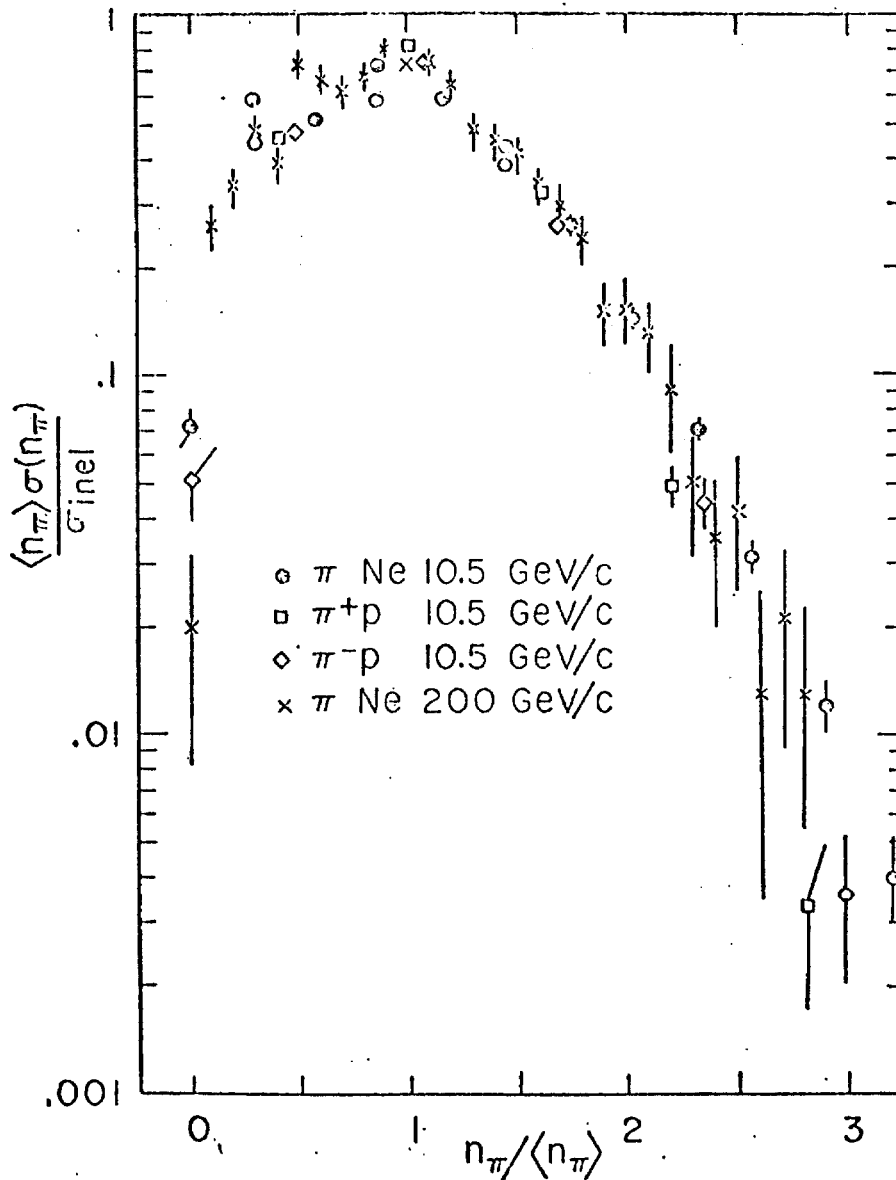
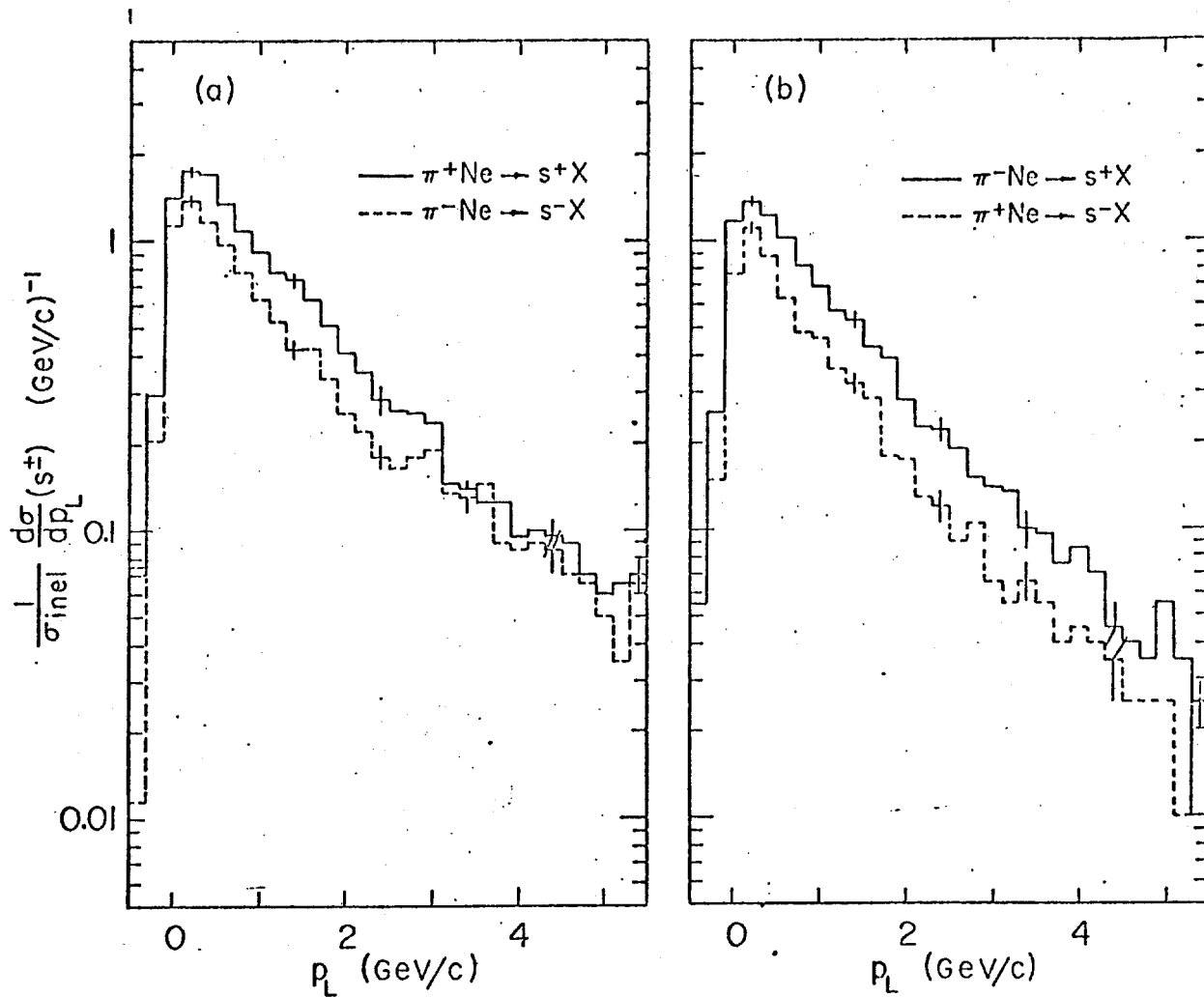


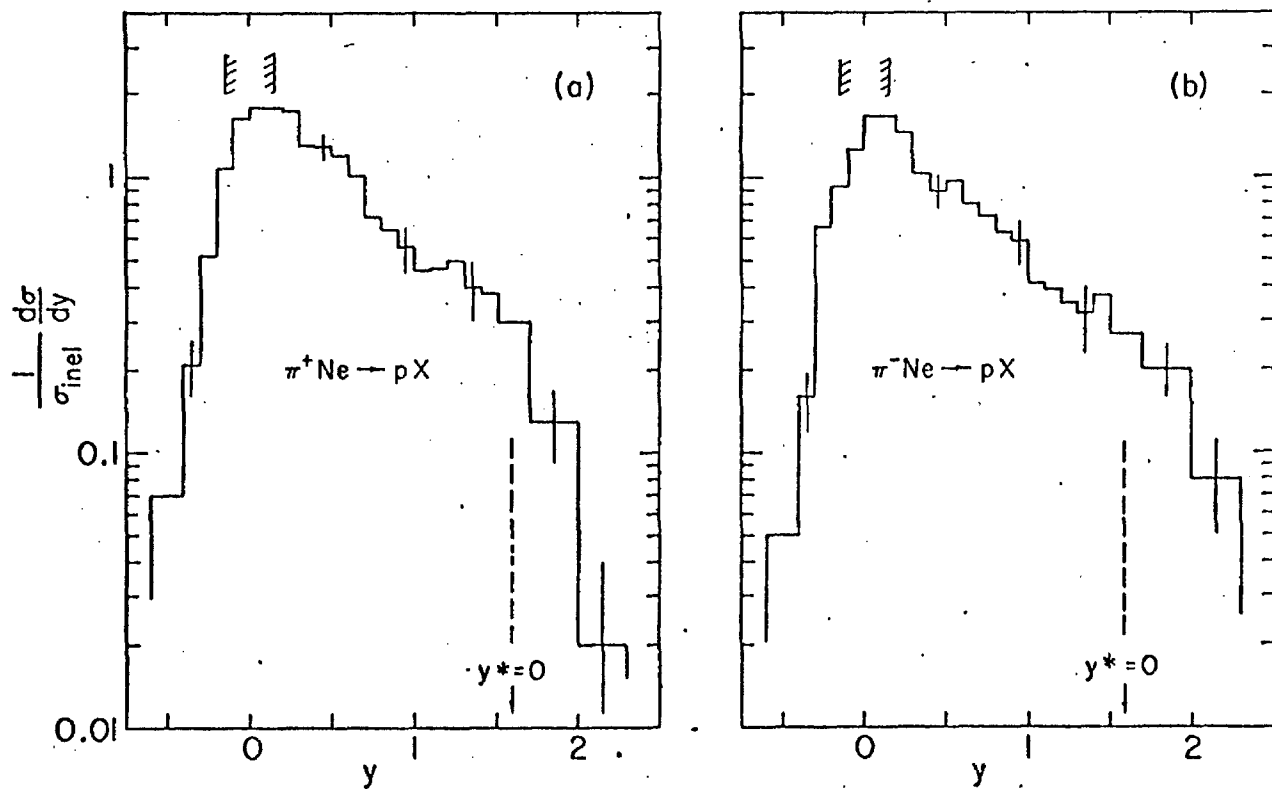
Fig. 2.

Scaled pion multiplicity cross sections for inelastic  $\pi$ Ne interactions ( $\odot$ ) at 10.5 GeV/c. The  $\pi^+$ Ne and  $\pi^-$ Ne results are averaged. Proton tracks have been removed from the  $\pi$ Ne data by the requirements of charge symmetry, as discussed in the text. The open circles result from removing nuclear coherent production in 1, 3, and 5 pronged events. Also plotted for comparison are  $\pi^-$ Ne data at 200 GeV/c (X) from Ref. 11 and  $\pi^+p$  ( $\square$ ) and  $\pi^-p$  ( $\diamond$ ) data interpolated to 10.5 GeV/c. Protons have been removed from the  $\pi p$  data by assuming an average of 0.65 (0.60) protons per inelastic  $\pi^+p$  ( $\pi^-p$ ) interaction.



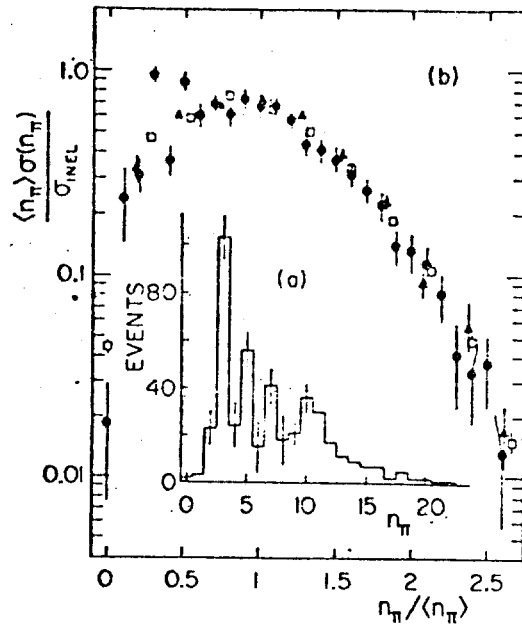
Distributions in longitudinal momentum for (a) favored and (b) unfavored shower particles. The solid (dashed) histograms are for the positively (negatively) charged shower particles, as indicated. The longitudinal momentum distribution for unidentified protons is obtained by the difference (solid minus dashed) between the plotted distributions.

Fig. 3a



Inclusive rapidity spectra for protons produced in (a)  $\pi^+ \text{Ne} \rightarrow pX$  and (b)  $\pi^- \text{Ne} \rightarrow pX$ . The vertical shaded bars enclose a region in which low momentum proton tracks are detected inefficiently. The dashed line marks the zero of  $y^*$ , the rapidity in the  $\pi p$  center-of-mass system.

Fig. 3b



(a) Distribution of charged-pion multiplicities for events having no protons. The error bars include the uncertainties in the removal of  $\pi^-p$  events and in the removal of events with energetic proton tracks. (b) Scaled pion multiplicity cross section for  $\pi^-$ -Ne collisions at 200 GeV/c (solid circles) and 10.5 GeV/c (open squares). Also shown for comparison are the 200-GeV/c  $\pi^-p$  results of Ref. 5 (triangles). The Ne results have been corrected for the presence of energetic proton tracks. The  $\pi^-p$  multiplicities have also been adjusted by assuming that on the average there is 0.6 proton per event.

Fig. 4

DIFFRACTION DISSOCIATIONS OF THE COULOMB FIELD  
BY HIGH ENERGY HADRONS ON HIGH Z TARGETS<sup>+</sup>

W. D. Walker

Department of Physics, Duke University, Durham, North Carolina 27706

We propose a set of experiments to measure the cross section of vector mesons on various projectiles. By using Fermilab energy  $\pi$ 's incident on U cross sections of the order of a millibarn are likely.

---

<sup>+</sup> Work supported in part by the U. S. Atomic Energy Commission under Contract No. AT-(40-1)-3065.

In the last twelve years high energy physicists have become quite used to considering the collisions of high energy particles with virtual pions in the peripheral regions of the nucleon. The use of the concept of the virtual pion has opened up the whole field of pion-pion physics. In this note we point out the possibility of a similar sort of investigation that may be undertaken using the virtual quanta associated with the Coulomb field of a high Z nucleus.<sup>[1]</sup> We know that the photon is intimately coupled to the vector mesons  $\rho^0$ ,  $\omega^0$ ,  $\phi^0$ , the  $\rho^{[2]}$  and the recently discovered  $\psi^{[3]}$  mesons. From a study of the diffraction production of  $\rho^0$ ,  $\omega^0$ ,  $\phi^0$  in  $\gamma + \text{nucleon} \rightarrow \rho^0, \omega^0, \phi^0 + \text{Nucleon}$ , we know approximately the strength of the coupling of these objects to the photon. Thus if we can use the Coulomb field as a virtual source of  $\rho^0, \omega^0, \phi^0$ 's, this would, in principle, be a means of studying the interactions of the vector bosons with elementary particles.

The idea involved in such a process is simple enough. The Coulomb field associated with the nucleus appears as a cloud of photons when viewed from the rest frame of the projectile. By using the idea of vector dominance we know that some of the virtual photons will appear as  $\rho^0, \omega^0, \phi^0$ , etc. There may be either elastic or inelastic collisions between the projectile and the vector meson. The kinematics are fairly simple. Imagine a case of  $\pi$  incident which produces a  $\rho^0$  collinear with itself. In the special case of collinear  $\pi$  and  $\rho^0$  the momentum that must be transferred to the nucleus is

$$\Delta_{\parallel} = \frac{m_{\rho}^2}{2P_{\rho}} + \frac{m_{\pi}^2}{2(P_i - P_{\rho})} - \frac{m_{\pi}^2}{2P_i} .$$

$P_\rho$ ,  $P_i$  are the momentum of the  $\rho^0$  and the momentum of the incident  $\pi$ , respectively. Note that usually  $\Delta_{||} = \frac{m_\rho^2}{2P_\rho}$ . Also note that the mass of the  $\pi$ - $\rho$  system is approximately  $= \sqrt{\frac{P_i}{P}} m_\rho$ .

Let us consider the simplest experiment, namely,  $\pi$ - $\rho$  scattering. A uranium or lead target could be illuminated by pions of 300 or 400 GeV at Fermilab or CERN II; the virtual  $\rho^0$ 's in the Coulomb field can be scattered by the incident  $\pi$ . The lowest momentum  $\rho$  that can be made coherently on uranium is about 12 GeV/c. (This corresponds to having  $\Delta_{||} = \frac{\hbar}{R}$  for a nuclear radius  $R = 1.3 A^{1/3}$ .) For a 300 GeV  $\pi$ , the  $\pi$ - $\rho$  system has a mass 3.8 GeV/c<sup>2</sup>. Thus one can study  $\pi$ - $\rho$  systems of up to 3.8 GeV/c<sup>2</sup> in mass. This means, likewise, that one could study any system of  $\pi$  + vector meson by such an experiment. If, for example, a  $\psi(3100)$  were produced, the minimum momentum of the produced  $\psi$  would be 200 GeV/c.

The potential interest and utility of this sort of experiment is really quite great. One can imagine illuminating a photon target with various projectiles  $\pi$ , K,  $\mu$ ,  $\nu$ ,  $\gamma$ ,  $\Sigma^-$ ,  $\Lambda^0$ . Each projectile listed allows the possibility of an initial state that is unattainable in any other way. What we specifically stress, however, is the possibility of measuring the elastic vector-meson-projectile cross sections. By measuring  $\frac{d\sigma}{dt}$  and extrapolating to  $t=0$  and using the optical theorem, one can estimate (or at least determine an upper bound) for projectile-vector meson cross section. It is interesting to contemplate looking at projectile-vector meson scattering in an inclusive fashion;

this, however, is complicated by the mixture of  $\rho^0$ ,  $\omega^0$ ,  $\phi^0$ , etc. in the target. In the case of a  $\pi$  incident, one could separate the target particles in part by using the G-parity quantum number. A particularly intriguing possibility would be that of doing  $\rho^0 - \rho^0$ ,  $\rho^0 - \omega^0$  scattering by using photons on a high Z target. The competition with electromagnetic processes would limit the target thickness to a few millimeters of the high Z material. Such scatterings would be in two substates of  $m_z = 0, 2$ .

The real possibility of such experiments will ultimately depend on the size of the nuclear induced background. Incoherent interactions between projectile and target will tend to produce rather high multiplicity interactions which should be easy to discriminate against. The coherent interactions of the projectile with the nucleus will be the main source of background. The cross section for such interactions tend to be of the order of 5 per cent of the inelastic projectile-nucleus cross section.<sup>[4]</sup> We are concerned with a special part of that cross section, namely, that part in which a sizeable rapidity gap exists between the vector meson and the projectile, and with the vector meson the slower particle in the laboratory. A hadronic process of this sort has a cross section which is probably between 1 and 10 per cent of the total coherent cross section. Clearly, it will be necessary to study the nuclear background. An additional cut can be made requiring a helicity of  $\pm 1$  for the recoiling vector meson. The coherent nuclear processes which have the same kinematic characteristics are interesting processes in their own right. They might represent elastic diffractive scattering off a  $\rho^0$ ,  $\omega^0$ , etc. in the nuclear field of the nucleus.

One can estimate the cross section for photon processes fairly simply. In Fig. 1 we show the result of a Weiszacker-Williams<sup>[5]</sup> calculation which gives the effective number of photons per GeV/c,  $N(K)$ , in the  $\pi$  rest frame. The overall energy of the  $\pi$ - $\gamma$  system is  $\sqrt{2Km_\pi}$ . The cross section per GeV/c for a given process would be  $(g_{\gamma V})^2 \times \sigma_{V-\pi}(K) N(K)$ .<sup>[6]</sup> The differential cross section for elastic scattering would be given by  $\frac{d\sigma}{dt} = (g_{\gamma V})^2 \times \left(\frac{1}{4\pi}\right)^2 \sigma_{V-\pi}^2 e^{At} \times N(K)$ . In Fig. 1 we also give an estimate for the cross section for  $\pi + U \rightarrow \pi + \rho + U$  from the virtual photons.<sup>[7]</sup>

We believe that if these experiments are feasible (that is, if the nuclear background is low enough) then this type of experiment would add a new dimension to hadronic physics.

These considerations were stimulated by conversations with Professor J. Rosen.

## REFERENCES

[1] The idea of using the Coulomb field as a source of virtual photons is an old one dating back to the original work of E. J. Williams and C. F. von Weizsacker. In this case, we are particularly concerned with the diffractive scattering of these photons on various projectiles rather than the dissociation of projectiles by photons as stressed by M. L. Good and W. D. Walker, Phys. Rev. 120, 1855 (1960).

[2] Vector dominance has been particularly stressed by Sakurai, J. J. Sakurai, Ann. Phys. (New York) 11, 1 (1960).

[3] J. E. Augustin et al., Phys. Rev. Letters 33, 1406, 1453 (1974); J. J. Aubert et al., Phys. Rev. Letters 33, 1404 (1974).

[4] J. Elliott et al., Phys. Rev. Letters 34 (March 1975).

[5] J. D. Jackson, Electrodynamics, (John Wiley, New York, 1962).

We used the formulae as given by this source to calculate  $N(K)$  the effective number of photons.

[6] We used the same notation as in M. Ross and L. Stodolsky, Phys. Rev. 149, 1172 (1966). We have used coupling constants etc. as summarized by G. Wolf in Proc. 1971 Conference on Electron and Photon Interactions at High Energy, Lab of Nuclear Studies, Cornell Univ. p. 190.

[7] The estimate of the  $\pi$ - $\rho$  cross section is estimated on the basis of the elastic  $\pi$ - $\pi$  in the same energy range. The  $A_2$   $\pi$ - $\rho$  scattering is assumed to be 70% elastic in the  $A_2$  region. The fall-off on the high side of the  $A_2$  in addition to the decrease in the resonant  $2^+$  amplitude the falling elastic cross section because of the onset of inelasticity in the scattering process.

FIGURE CAPTION

Fig. 1. The effective number of virtual photons is plotted against the photon energy in the  $\pi$  rest frame with the ordinate on the left side. The cross section for  $\pi + U \rightarrow \pi + \rho + U$  is plotted against photon energy with the ordinate on the right.

